AD-A141 173 ANALYSIS OF ELECTRIC PROPULSION ORBIT TRANSFER VEHICLES 1/2
VS IUS CENTAUR-G A..(U) AIR FORCE INST OF TECH
WRIGHT-PATTERSON AFB OH SCHOOL OF ENGI.. L W MADDOX
UNCLASSIFIED DEC 83 AFIT/GSO/OS/83D-5 F/G 20/3 NL

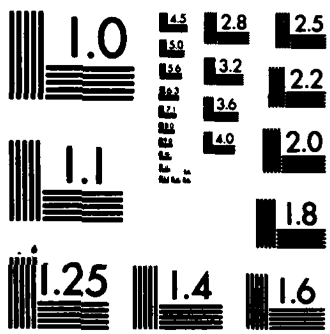

MICROCOPY RESOLUTION TEST CHART
NATIONAL BUREAU OF STANDARDS-1963-A

AFIT/GSO/OS/83

ANALYSIS OF ELECTRIC PROPULSION ORBIT
TRANSFER VEHICLES VS IUS, CENTAUR-G,
AND A REUSEABLE BIPROPELLANT SYSTEM

THESIS

Lee W. Maddox
Captain, USAF

AFIT/GSO/OS/83D-5

Approved for public release; distribution unlimited

AFIT/GSO/OS/83D-5

ANALYSIS OF ELECTRIC PROPULSION ORBIT TRANSFER VEHICLES

VS IUS, CENTAUR-G,

AND A REUSEABLE BIPROPELLANT SYSTEM

THESIS

Presented to the Faculty of the School of Engineering

of the Air Force Institute of Technology

Air University

In Partial Fulfillment of the

Requirements for the Degree of

Master of Science in Space Operations

Lee W. Maddox, B.S., M.S.

Captain, USAF

December 1983

Approved for public release; distribution unlimited

Preface

The intent of this study was to take a fresh look at the viability of using electric thrusters as primary propulsion for near-earth space missions. The Shuttle is a remarkable system and enhancing it with a reuseable upper stage would be very attractive.

Chemical rocket systems, even with SOA LH / LOX engines require enormous amounts of fuel. Without aerobraking, two or more Shuttle refueling flights are required for every one flight bearing GEO payload. Upper atmosphere heat transfer and drag are not yet well modeled, so the technical barriers to aerobraking are not small. Electric propulsion makes far more efficient use of propellant, but has not been used for primary propulsion as yet, and does not have the production base that chemical has. The long transfer times also pose problems for revenue, mission promptness, and Van-Allen degradation. Thus, the decisionmaker has no easy solution. The methodology developed in this thesis should help to provide information as to current capabilities of optimized ion thruster orbit transfer vehicles. It also should permit comparison of performance and cost with baseline chemical rocket systems over a 20 year simulation period.

Originally, I had hoped to include self-field magnetoplasmadynamic (MPD), pulsed inductive, and other promising thruster technologies, but will have to leave those investigations for a later time -- or for future classmates.

I heartily acknowledge the assistance and advice, both technical and paternal, of my thesis committee, LTC (Dr.) Mark Mekaru, Dr.

William Wiesel, and Dr. William Elrod. Their enthusiasm for the project, encouragement, and humor through the long months of computer skirmishes have been greatly appreciated. My wife and 2-yr old son have been extraordinarily patient. In the tradition of saving the best for last, I wish to acknowledge with reverence our faithful Savior, the Lord Jesus, whose wisdom and grace are matchless.

Table of Contents

List of Figures

List of Tables

Notation / Acronyms

1. ACS - Attitude Control System
2. CMG - Control Moment Gyro
3. CNTAR - CENTAUR-G Upper Stage
4. EOTV - Electric (propulsion) Orbit Transfer Vehicle
5. GEO - Geosynchronous Earth Orbit (also Equitorial)
6. IOC - Initial Operational Capability
7. Isp - Specific Impulse
8. IUS - Inertial Upper Stage
9. LEO - Low Earth Orbit
10. LH - Liquid Hydrogen
11. LOX - Liquid Oxygen
12. LSS - Large Space Structure
13. M_{P1} - Propellant Mass used for transfer to destination orbit
14. M_{P2} - Propellant Mass used for return to LEO
15. M_W - Mass of Power Supply (Solar Array for this thesis)
16. OTV - Orbit Transfer Vehicle
17. PAM - Payload Assist Module
18. P/L - Payload
19. PPU - Power Processer Unit
20. RBPV - Reuseable Bi-Propellant Vehicle
21. RCS - Reaction Control System
22. Sats - Satellites
23. SOA - State-of-the-Art
24. UF - User Function in QGERT Programs

25. UI - User Input in QGERT Programs

26. UO - User Output in QGERT Programs

27. W - Power Output of Power supply (KW)

28. X1 - Isp

29. X2 - Power Supply Mass divided by number of thrusters

30. X3 - M_{P_1}

31. X4 - W, Power supply output (KW)

32. X5 - M_{P_2}

ABSTRACT

A flexible methodology has been developed for optimizing electric orbit transfer vehicles (EOTVs) and comparing them with baseline chemical systems. EOTVs have been characterized by the thruster technology and the propellant mass versus power supply mass for standardized NASA BIMOD configurations. Baseline chemical systems are represented by the Inertial Upper Stage (IUS), CENTAUR-G, and a proposed reuseable LOX-LH Centaur derivative.

Five electrostatic propulsion thrusters were chosen for the optimization. These were the baseline NASA / Hughes 30-cm J-Series Mercury Ion Thruster and four derivatives. Each was characterized through linearization of experimental data. Relationships of input power (KW) to the thruster vs specific impulse and input power vs thrust were developed. The first relationship along with equations for power supply mass and propellant mass were input to the Sequential Unconstrained Minimization Technique (SUMT) nonlinear optimization program. The combination of the propellant mass used for transfer to GEO and return and the power supply mass was minimized. SUMT runs were made for the five thrusters carrying representative payloads from 1 to 6 NavStar GPS satellites with associated masses of 908 to 5448 KG. Transfer times were then calculated for each of these payload / optimized EOTV combinations. Of the thrusters chosen, the Ring-Cusp 3-Grid Xenon thruster accomplished the LEO to GEO and return trips with the least mass and the minimum transfer time.

With this thruster as the choice of technology, the

Queueing-Graphical Evaluation Review Technique (QGERT) program was used to simulate a 4-way "fly-off" between EOTV, IUS, CENTAUR-G, and the Reuseable Bi-Propellant Vehicle (RBPV). The results of the 20-year flyoff comparison were used to assign rough Life-Cycle Costs (LCCs) to the operation of each of the vehicles. With a figure of merit of only LCC of each system, the CENTAUR-G appeared best. But, when using a figure of merit of $LCC per KG delivered to orbit, the EOTV was the best.

Besides the initial results, the methodology can be used by those desiring a way to optimize EOTVs with other thruster technologies (eg. self-field magnetoplasmadynamic, pulsed inductive). Other EOTV configurations may be used for the optimizations as well as other payloads. The user may also select other chemical or baseline systems to compare with EOTVs in the QGERT simulation.

ANALYSIS OF ELECTRIC PROPULSION ORBIT TRANSFER VEHICLES

VS IUS, CENTAUR-G,

AND A REUSEABLE BIPROPELLANT SYSTEM

CHAPTER I. Background

Introduction

The United States Space Transportation System (STS) is an impressive feat of engineering and technology. We are now involved in the less spectacular business of practical usage and operation of the Shuttle. It has been made clear to Headquarters Air Force that enhancements to the Shuttle are to have priority when considering future space systems. In keeping with this charter, this thesis examines the improvement of Shuttle capabilities through better transportation in the near-earth space realm. Expendable upper stages may be the most expeditious and the only realizable way to do business now, but will continue to grow unacceptably expensive as more numerous and more massive space systems are launched and placed in operational orbits. Additionally, the capability to visit, refurbish, repair, investigate, or retrieve space assets in higher orbits is non-existant as of this writing.

Very briefly, the applicability of electric propulsion to orbit transfer missions on a routine basis is to be examined during mission simulations of 20 years. Optimal parametric trade-off studies will

first be accomplished to define the electric propulsion vehicle technologies used in the simulation. The performance of these electric OTVs (Orbit Transfer Vehicles) will then be compared with current baselines--the operational IUS (Inertial Upper Stage), the Centaur-G, and a proposed high-energy liquid bipropellant OTV--in simulated missions.

The results of the trade-off studies and the simulations will be examined in light of enhanced capability for the Space Transportation System (STS) and for reduction in the number of Shuttle launches to place given satellite constellations and space structures in orbit.

History

Situation. The U.S. Air Force has been "operational" in space for a number of years, but is facing a new era with the advent of the Space Shuttle. A recognized weak link in the Space Transportation System (STS) is the "upper stage" or a vehicle to place satellites in higher orbits than the Shuttle orbiter can achieve. Smaller satellites sometimes do have their own perigee insertion stage and apogee kick motor (AKM) for orbit transfer. But satellites are growing larger and plans are being made for Large Space Structures (LSS) in the late 1980's, 1990's and beyond. A separate Orbit Transfer Vehicle (OTV) is needed not only for these larger payloads, but also for the operational capability to retrieve, replace, repair, or refurbish (R4) satellites. For orbit transfer, the Air Force-funded Inertial Upper Stage (IUS) is a current answer, but is

expensive and is not reuseable. The entire vehicle, including costly 3-axis guidance system, is discarded after one mission when the solid rocket motors are spent.

Much more efficient would be a vehicle which can be parked in LEO and be available to transport Shuttle payloads to (typically) Geosynchronous Equitorial Orbit.

Importance. The need for a reuseable Orbit Transfer Vehicle has been highlighted in several studies (e.g., 6, 9, 10, 16, 18, 19, 23, 34, 35, 50, 51). Current solid-fuel and liquid-fuel rocket technologies, though highly advanced, and though repeatedly proven in space, require a significant mass-fraction of propellant. Solid fuel motors operate typically in specific impulse ranges of approximately 210-320 seconds (24) and liquid-fuel in specific impulse ranges of 300 to 455 seconds (numerous Refs). Hence, the mass of fuel expended to achieve a given required orbital characteristic velocity increment, Δv, is large. The "rocket equation" shown below illustrates that the relationship between exhaust velocity and fuel mass is exponential.

$$\frac{\text{Final Mass}}{\text{Initial Mass}} = \text{Exp}\left[-\frac{\text{Mission Velocity}}{\text{Propellant Velocity}}\right] \tag{1}$$

$$\text{Initial Mass} - \text{Final Mass} = \text{Propellant Mass}$$

Electric propulsion is attractive in space because it makes very efficient use of fuel which allows a much larger payload mass to be transported. Also, electric propulsion (EP) typically does not generate the extremes of pressure and temperature found in chemical

propulsion. (Temperature is an exception for certain types of EP). Specific impulses may range from 1000 to 10,000+ seconds for EP (numerous Refs). Electric propulsion also has advantages of restartability and variation of thrust level, which are more difficult with chemical propulsion. Nuclear propulsion (i.e. heating of H_2 and expanding through a nozzle) still has some of the limitations of chemical rockets but with some improvement in specific impulse--to 800 seconds.

Thus, electric propulsion has the edge in greatly reduced fuel mass required. And added to this inherent advantage is that of having a significant amount of develoment--especially for ion-bombardment (e.g., 12). NASA-Lewis Research Center has developed a rather complete modular design which includes the engineering detail to submit to contractors. But the problem remains that an EP OTV or vehicle with similar capability has not yet been produced. Nor has the issue of an appropriate propulsion system been resolved.

Problem Statement

The problem is to pick the best propulsion technology for a reuseable, modular OTV. Studies to date have concentrated on trade-offs to see which technology fits each mission category best. Typically these studies have generated a single data set for transfer time or a graph showing technology parameters vs v or payload mass to orbit. The issue of whether electric propulsion can do the orbit transfer mission has been well studied (nearly all references), but from the decision-maker's standpoint, the question of which EP

thruster and power supply for specific missions needs more clarification. Several optimum parametric OTV designs (EP) need to be determined for both general missions and for specific satellite constellation emplacements to better view their capability from the operational standpoint.

Thus, the problem is to find optimum electric propulsion technology and power supply technology parameters for given missions and run the optimal designs in 10 to 40 year simulations to examine long-haul performance.

Brief Approach

Orbital parameters and payload mass for projected DOD and NASA missions will be inputs for both a non-linear optimization program (SUMT), and a simulation program (QGERT). The SUMT program will determine optimum design strategies for the electric OTVs by trading various technical and performance parameters. The simulation runs will in essence provide a parametric "fly-off" of the optimal electric OTV and the IUS, Centaur, and a reuseable bipropellant system (projected). Output of the simulation provides number of satellites ferried in a given number of years, average wait time for an electric OTV in LEO, transfer times, and optimum number of vehicles to do the mission. This will form a basis for cost comparison between OTVs and stages. The results should give the decision-maker a good handle on technologies to invest in and how such systems should perform over the long haul.

CHAPTER II. Literature Review

Scope of the Literature Search and Data Base

The literature search has been quite extensive and it will, hopefully, prove to be a significant and valuable reference for the serious reader. However, it cannot presume to be exhaustive as there are, undoubtedly, many fine reports and studies which have not come to the attention of this author. Another factor which affects comprehensiveness is the on-going electric propulsion research at various laboratories, universities, and aerospace firms. Besides basic research, this author is aware of continuing studies and mission analyses nearing completion, eg., Ref. 34. Though necessitating caveats, such continuing work tends to show the validity of this research area. The sheer number of contract reports and academic/professional papers show electric propulsion to be a viable area of space propulsion. It is difficult to ignore such efficient use of propellant mass.

The following list delineates areas specifically not treated in the thesis and the literature search:

1. Detailed derivation of the theoretical basis for electric propulsion techniques.
2. Detailed design aspects of cryogenic/solid/nuclear/photon propulsion systems.
3. Interplanetary/interstellar missions.
4. Every concept and technique of electric propulsion, only

those applicable to the given mission are treated.

5. Detailed analytical derivation of orbit transfers.
6. Data on materials science experiments with electric propulsion components.
7. Complex, stochastic cost estimation techniques.
8. Detailed reliability forecasting.
9. Intricate design trade-offs for power supplies--solar, nuclear, thermionic, fuel cell, battery, etc.

Solar shadowing, Beginning Of Life (BOL) and End Of Life (EOL) tradeoffs for solar panels are also left to other studies, althougn sensitivity to these effects has been investigated in Appendix V.

Additionally, the OTV "designs" are not rigorous engineering designs ready for the draftsman, but are conceptual. They exist in terms of the parameters of the system (such as overall weight, specific impulse, propellant characteristics, power plant efficiency, propulsion efficiency, thrust, and lifetime).

Method of Treatment and Organization

All 58 of the bibliographical entries for this review have been grouped under six headings. Within these headings are sub-headings which roughly follow the development of the thesis. Not every one of the 58 entries will be reviewed, since several are general references, such as textbooks, since others are ancillary with regard to the main thrust of the thesis, and since several references, though very relevant, were received just prior to publication. Also, conciseness

is a courtesy to the reader as well as a stated requirement.

Therefore, to help guide you in the literature discussion, the following outline is given <references in brackets are the ones not discussed>:

1. Background Sources <22, 23, 47, 48, 56>.

   History (26)

   Advantages of Electric Propulsion (24)

2. Generic Electric Propulsion (EP) Sources <3,52,14, 17,31,32,36,38,46>.

   Electric Propulsion--A Mature Technology (51)

3. Studies of Electric Propulsion as Applied to Orbit Transfer <7,8,15,27,28,43,44,54>.

   Chronological Presentation (18,9,6,35,16,19,50,34)

4. Data Base Sources <5,11,13,21,30,39,40,41,42,45,49,55>.

   Overall Design Approach Data (10)

   Input for the Trade-Off Studies (12)

   Input for the Simulation (29)

5. Sources for Analytical Techniques -- Multi-Criteria Trade-Offs, Non-Linear Optimizations, (SUMT), and Simulation (QGERT) <4,58,37,20,33,57>.

6. Orbital Dynamics Considerations <2,25,53>.

   Low Thrust Transfer is Workable (1)

Please note that the references are not locked in to these headings. For instance, reference 51 also contains excellent background material. Thus, these headings serve only as a convenient means for organizing the entries and are not titles for thesis chapters.

Background Sources

There must be a genuine need or an established requirement to justify the proposal of a new vehicle or system. To lay a foundation for the thesis, the fundamental advantages of electric propulsion for space missions must first be made clear.

History. Dr. Harold Kaufman describes the "Origin of the Electron-Bombardment Ion Thruster" (26) during the late 1950's. This particular thruster is relevant to this thesis in that it has become the most developed form of electric propulsion. This type thruster now bears his name in most current reports. His article is a historical development of the very first operable electron-bombardment ion thruster which he invented or developed along with William Kerslake and other colleagues while at NASA-Lewis Research Center in the late 1950s and early 1960s. The thruster was first test-fired in 1960. The article gives an appreciation for the ingenuity exercised in its crude beginnings, and gives an appreciation for the degree of maturation since then in this technology. The 30-cm electron bombardment thruster (12) and its derivatives are considered state-of-the-art (SOA) as of this writing.

Advantages of Electric Propulsion. Dr. Robert G. Jahn, in his textbook used at Princeton, "Physics of Electric Propulsion," (24) provides a more extensive discussion of the advantages of electric propulsion. The text provides the theoretical physics background for

electric propulsion and the electrical acceleration of gases. It also provides a good review of the types of thrusters and their techniques of acceleration. Chapter 1 is referenced as background for this thesis because it specifically shows the "province of electric propulsion" to be "high impulse space missions." It explains that the primary advantage enjoyed by EP is a much higher specific impulse than is possible with standard chemical propulsion. This directly impacts the amount of propellant necessary to carry out a given space mission. Another very important part of this chapter for this thesis is its discussion of the power supply penalty. That is, the tradeoff of power supply weight for higher thrust and also for higher specific impulse. It introduces the parameters of specific power-plant mass, conversion efficiency, and characteristic velocity increment, Δv. Also discussed are some specific types of missions where electric propulsion is the logical choice over chemical rockets.

Generic Electric Propulsion Sources

The majority of the bibliographical entries for this thesis contains information regarding types and classes of EP. Of interest to this thesis are those classes and specific thruster designs which are most promising in the near term for accomplishing space missions.

Electric Propulsion--A Mature Technology. In his article, "Electric Propulsion Ready for Space Missions", (51), Dr. Stuhlinger gives an excellent overview of the mature state of many EP systems and includes many details of performance. Areas discussed included, "overview of EP programs" and details of work in Japan, West Germany,

Great Britain, and the USSR, as well as U.S. programs. Organizations and companies with EP programs included: US Air Force, NASA, Fairchild, Phrasor Technology, Technion, Hughes, Lockheed, and several universities. Other areas discussed were, "Spacecraft Systems," "Propulsion Concepts," "Thruster Design and Analysis," "Thruster Performance and Qualification," "Endurance Tests," "Component R&D," etc., all of which point directly to the maturity of the technology.

Perhaps the most applicable part of Stuhlinger's article is the extensive treatment and discussion of the 30-cm Kaufman thruster because it is the most developed and is closest to being ready for orbit transfer missions.

Studies of EP as Applied to Orbit Transfer

Chronological Presentation. Because each of these studies is rich in material and data for the thesis, and because each is a rather complete analysis in itself, the following discussion will primarily address their conclusions. For the reader's benefit, attempt has been made to stick to the essentials.

D.G. Fearn (18) found that two uses of EP were especially attractive. For satellites under 1000 kg, the EP system could be an integral part of the spacecraft owing to the small fractional mass of fuel required. The other use was a separate OTV or tug with solar arrays for power. He pointed out the possible problem of solar panel degradation in the Van Allen Belts, but still found the application valid.

D.C. Byers, et al, (9) presented a general methodology for predicting the overall EP system properties, such as input power and mass, when mission parameters and propellant type were given. This provides information for the trade studies portion of this thesis. It aids in the selection of the right vehicle parameters.

D.C. Byers, in a subsequent study (6), specifically addressed the major theme of this thesis, "Upper Stages Utilizing Electric Propulsion." He used the methodology established previously (9) to define the electric thrust system and its power requirements in detail. With that he presented the payload capabilities of upper stages using EP for LEO to GEO orbit transfer missions. This thesis draws upon the payload data from this paper and, additionally, accomplishes the simulation of an operational OTV system for a 20 year period, which was not part of Byers' paper.

William Pipes headed the Martin Marietta Corp. team which finished an extensive contract study (35) for the AF Rocket Propulsion Laboratory in July, 1980. Unlike the 3 studies discussed so far, this one considered liquid propellant (both storable and cryogenic), and solid propellant as well as electric propulsion systems for orbit transfer. It presented the results in terms of the relative advantages of each system for certain weight classes of satellites. Highlighted was the economic benefit of Magnetoplasmadynamic (MPD) propulsion over ion-bombardment, although significant technical difficulties (e.g.,electrode erosion) remain with MPD systems.

The second technical report by D.G. Fearn (16) tends to parallel the Martin Marietta study in its extensive treatment of types of

electric propulsion to be considered for orbit transfer missions. The clear conclusion is that the high specific impulse offered by EP provides an enormous economic advantage over chemical rocket systems for the movement of non-priority cargo. Non-priority is specified because the transfer times are typically 100 days or more. For projecting performance for larger diameter ion thrusters, the tables on page 16 (16) should be helpful.

Robert Finke (19) has edited a volume of collected papers on EP from the 1979 AIAA International Electric Propulsion Conference. This represents one of the most complete and current collections available on EP, as of this writing. Its comprehensiveness is probably the most valuable contribution to this thesis. Several papers dealt with application of EP to orbit transfer missions and especially useful were two papers dealing with cost-effectiveness.

Capt Jess Sponable (50) has shown through computer modeling techniques that the Space Transportation System (STS) can be enhanced and optimized for NASA/DOD missions through the employment of a LEO space station and OTV. Although not the primary issue in his thesis, he also demonstrated significant reductions in launch rates if a space station <u>and</u> an EP OTV are both used. My thesis will not include a space station as part of the scenario and will attempt to answer whether similar reductions in Shuttle launch rates are possible with the EP OTV alone. Also useful from his thesis was the NASA/DOD mission model---a starting point for developing my simulation input.

Capt David Perkins is in the process of having his report printed which is entitled, "Preliminary Analysis and Comparison of Recoverable

Space Based Orbit Transfer Vehicles for LEO to GEO Missions." (34) Publication is forthcoming in late 1983 and should be available to certain DOD users at that time. Needless to say, this report is one of the most current. It offers a look at some very new technologies in the realms of power supplies and thruster concepts rivaling EP in efficiency. While this report does not perform a simulation as in this thesis, it provides some excellent data with which to compare trade studies.

Data Base Sources

Sources to this point have certainly contained pertinent data, but the following sources have especially useful data as outlined below.

Overall Design Approach Data. Cake, et al, (10) presented a modular approach to designing an EP space vehicle which used solar arrays for power. The study was not limited to an orbit transfer vehicle but was flexible enough to include interplanetary missions. Data useful for this thesis includes the component and subsystem arrangements necessary for an operational vehicle. The report emphasized the structural and thermal integration of modular subsystems. Three approaches to a Solar Electric Propulsion (SEP) module were compared on the basis of mass, cost, testing, interfaces with spacecraft, simplicity, maintainability, and reliability. All portions of the generated data have relevence to my data base.

Input for Trade Studies. The "30-Centimeter Ion Thrust Subsystem Design Manual" (12) contains specific details of thrust output, wattage input, specific impulses achieved, and total

efficiency. Because this manual was prepared with the goal of producing a working vehicle with necessary specifications for contract, it has data for several levels of detail. Drawings, mass data, configuration layouts, and engineering details are used directly in this thesis to characterize the Electric Orbit Transfer vehicle (EOTV). As stated earlier, this is the most highly developed of the EP thrusters and, hence, one of the most likely candidates for the first generation EOTV.

Input for the Simulation. Kerslake (29) has covered performance and durability of an ion thruster system which has been in orbit and operating for 11 years until it ran out of fuel in 1981. This experiment was called SERT II (Space Electric Rocket Test - II). This report serves as a major indicator for thruster / EP system lifetimes in the simulation portion of the thesis. Eleven years is a long time to endure the extremes of space and this test provides empirical evidence and credibility for the concept of an electric propulsion OTV in addition to valuable data for modeling.

Orbital Dynamics Considerations

Low Thrust Orbit is Workable. Capt Salvatore Alfano (1) has shown in his recent analytical thesis that the low thrust orbit transfer spiral can be solved in closed form. He has verified the resulting equations using numerical computer techniques. Also, the results were compared with the standard Hohmann transfer ellipse. His conclusion was that the resulting spiral transfer is optimal for low

thrust, continuous thrusting and thus accomplishes the mission in minimum time using minimum fuel. This is the type of orbit transfer that must be used with electric propulsion.

Literature Review Conclusion

The literature review began with the early Kaufman thruster and discussed the advantages of higher specific impulse available with Electric Propulsion (EP) over chemical rockets. Then, Stuhlinger's article was reviewed, pointing out that EP is ready for implementation in space vehicles. Many studies applying EP to the orbit transfer mission were then discussed in chronological order (1978 to 1983). Data base sources were discussed last. For each report reviewed, some indication of its content and scope was given as well as its applicability to this present thesis.

In conclusion, the reader should realize by now that electric propulsion has received a significant amount of attention in the scientific community. The reasons center around its potential for space missions requiring high specific impulse and/or long duration use. Finally, the information and data represented in this bibliography provide a firm foundation for the thesis.

CHAPTER III. Approach / Methodology

Research Questions

The two most general questions to be answered are, "Which electric propulsion technology is the best choice for a reuseable OTV," and "How does this electric system compare with baseline chemical systems in mission performance and cost?" The more specific questions to be answered are as follows:

1. Which electric thruster technology among several lab demonstration prototypes would optimize an OTV in terms of reduced fuel mass and reduced power supply mass for given missions?

2. Given specific missions, what are the transfer times and round-trip mission times for the optimized electric OTVs?

3. Does one electric thruster technology clearly outperform all others for each mission?

4. Using a comparison "fly-off" simulation between Electric OTVs (EOTVs) and baseline chemical systems (IUS, Centaur, Reuseable Bi-propellant), is a reduction in shuttle launch rate possible using EOTVs?

5. Using the same fly-off, is any reduction in cost over present operations suggested?

6. What would an optimal number of EOTVs and Re-useable chemical OTVs be -- i.e., fleet size?

7. Are Shuttle enhancements, expanded near-earth operations, or new DOD missions suggested by the performance of optimized EOTVs?

In answering these questions, the algorithms and methodology which are to be developed should prove helpful to decision-makers and to staff/committees considering the best way to exploit near-earth space on a limited budget. A set of research objectives has been established to further define and specify how these questions are to be answered.

Research Objectives

The following research objectives clarify what this thesis effort is to accomplish in answering the questions posed in the previous section. This should also help to narrow the scope and further define the problem.

1. Choose at least 4 electric thruster technologies that have been operated for lab testing and represent developable systems in the near term (5-15 years), then optimize input power (Kw) and specific impulse (sec) to minimize both propellant mass and power supply mass for EOTVs using these thrusters to accomplish given missions.

2. Develop an algorithm / program to find optimal specific impulses and then use the results to calculate the transfer times out to an orbit, back to the original or another orbit, and the combined round-trip time. This should be flexible enough to use for other missions besides deployment of satellites.

3. Examine the results of the optimization in trading-off different thrusters, overall EOTV masses, and transfer times for all given missions to determine if one technology clearly is best.

4. Develop a QGERT simulation program for each type of Upper

Stage / OTV and use it to find the number of Shuttle launches required to place given missions in their final orbits.

5. Using the simulation program, determine an optimum fleet size for both the EOTV and the Reuseable Bi-Propellant Vehicle (RBPV). "Optimum" is that minimum number which will preclude satellites / payloads from queuing in low earth orbit while waiting for transfer, and provide some vehicle redundancy for reliability.

6. Using the simulation "fly-off" results, attach rough cost estimates to Shuttle launches, Upper Stage & EOTV vehicle purchases, and payload delivery operations. Compare coarse life-cycle costs between non-reuseable and reuseable systems.

7. Use the overall optimization / methodology to investigate other missions such as on-orbit spare placement and recall, spent satellite retrieval and refurbishment, and satellite visitation for refueling RCS, battery / sensor replacement, or intelligence gathering on unfriendly systems.

These represent the specific objectives of the research effort. In the next section, the approach chosen to meet these objectives and justification for the approach are presented.

Approach and Justification

The approach and rationale for the optimization / trade-off studies for different electric thruster technologies will be discussed first. Then the approach and rationale for the simulation will be discussed. The reason for choosing to do both an

optimization/trade-study and a "fly-off" is that none of the references which this author has studied have done both. Yet, decision-makers would like to compare not only thruster technologies, but also examine operational performance and costs over the long term, say, 20 years. That is, when considering how to make better use of the Shuttle for delivering payloads, and when considering the benefits of reuseability, one would like to first compare alternatives and then take an optimized system and "fly" it, even if only in a simulation, against the baseline upper stages.

Electric propulsion, as mentioned before, offers much more efficient use of propellant than chemical combustion or nuclear heating/isentropic expansion. It imparts significantly more energy to each particle of propellant and greatly reduces the propellant mass needed to accomplish a given mission. This higher exhaust velocity provides mission capabilities not possible before, such as retrieval of satellites from geosynchronous orbit, or delivering several satellites to destination orbits without refueling. The trade-off is in power supply size/mass and in very low thrust (hence long transfer times between orbits). The long transfer time could perhaps be tolerated by planning the launch date earlier and/or by hardening the satellite and vehicle against Van Allen radiation. But in all cases for EP, it is possible and desirable to shorten the transfer time through choice of thruster and through vehicle optimization.

The approach chosen for the optimization can be summed up very broadly in two words, "minimize mass." In doing this, cost generally decreases both for earth launch ($/kg to LEO), and also in materials

and manufacturing (many references express costs in terms of \$/kg of the finished vehicle). If the total vehicle mass is fixed, then finding the minimum for propellant and power supply mass means more of the total can be payload. If all other things were constant, transfer time would also be least for minimum mass. But the salient mass trade-off (between propellant consumed and power supply mass) is a function of the exhaust velocity or specific impulse of the thruster which is governed by design and by input electrical power. As ISP increases, total propellant used for a given mission decreases, power supply mass increases, and thrust increases, all of which means that transfer time continues to decrease with increasing input power (and resulting thrust increase)(39,40,41). This relationship of input power to thrust and exhaust velocity is true for electron bombardment ion thrusters but not necessarily for other types of EP. For instance, a Martin Marietta study (44) indicates that increased input power is accompanied by decreased ISP and by increased thrust for the self-field magnetoplasmadynamic (MPD) thruster. As long as a mathematical relationship can be drawn, though, between relevant parameters, the potential exists for optimization.

Because many of the mathematical relationships are non-linear, the optimization technique chosen is the Sequential Unconstrained Minimization Technique (SUMT) for nonlinear programming. It was recommended by faculty having extensive experience with its flexibility in handling a wide range of problems. At first the approach was going to follow Stuhlinger's optimization equations (52) and maximize payload ratio, maximize terminal velocity, and minimize transfer time simultaneously. But after initial formulation,

de-bugging and examination of the results, the output parameters were for a purely mathematical model and did not represent any existing thruster. To rectify this would require extensive modifications to the equations by adding thruster efficiencies and actual thruster relationships of input power, exhaust velocity and thrust.

The approach finally decided upon was inspired by Jahn's text (24). He suggested that as ISP increases, power supply mass increases and propellant mass decreases for a given specific power of the power supply. Rather than aiming for the highest ISP in a design, theoretically an optimum ISP should exist for which the major components of mass which vary (propellant and power supply) would sum to a minimum. However, no method of finding this optimum was given in the text. This relationship is also mentioned in the NASA-Lewis literature (42).

With the idea of minimizing mass, it was then necessary to find the relationship of input power to ISP and thrust. Experiments performed at NASA-Lewis Research Center (LeRC) provided data points from actual operating electron bombardment ion thrusters of different configurations (39,40,41,45). These thrusters are derivatives of the highly developed baseline 30-cm Kaufman ion thruster, J-series. This thruster represents the closest to flight-ready of any primary propulsion EP design.

The data points were first plotted and it was noted that the curves were somewhat linear. A linear curve-fit was applied and relationships for input power vs ISP (& exhaust velocity) and input power vs thrust were developed. The first became an input equation for SUMT. The important added benefit of these relationships is that

all the efficiencies (mass utilization, electric to beam power, etc) are included / accounted for, since the data is measured or derived from actual hardware performance. With other standard relationships from the rocket equation and a relationship for specific power (characterizing the solar arrays) included, the SUMT program was formulated and de-bugged. Further details on equations, outputs, and the program itself are found in chapter 4.

The approach to the simulation stemmed from an earlier study by this author demonstrating the benefits of reuseability of upper stages / tugs in a QGERT simulation model. In this thesis, similar models are developed for each of the candidate vehicles: Electric Orbit Transfer Vehicle (EOTV), Inertial Upper Stage (IUS), Centaur-G (CNTAR), and a representative Reuseable Bi-Propellant Vehicle (RBPV). The EOTV is optimized in SUMT for the payload or mission model and is reuseable. The IUS and CNTAR represent our current upper stage capability for heavier satellites. For lighter satellites, Payload Assist Modules (PAMs) and kick motors are used. The RBPV is a Centaur derivative using LH, LOX in the RL-10 engine. Its general characteristics are combined from a Boeing study (15) and a Systems Engineering study performed at AFIT (49). The proposed RBPV does not, however, include a ballute or use aero-braking as in the case of the the Boeing OTV. It is assumed to be a space-based vehicle requiring a special refueling pallet and astronaut / specialist team for the refueling operation.

Although the SLAM simulation program was first considered due to its flexibility, it was determined that QGERT (37) would be sufficient

for this study. Also, this author was more familiar with QGERT and had used it for a similar modeling problem. QGERT allows modeling of performance over selected periods (eg. 10, 20, 30 years) and allows the modeling of uncertainty to reflect real world operations. Uncertainty can be included in reliability factors, in Shuttle launch schedule, and any other contingencies desired by the decision-maker. Modeling these uncertainties as well as variations in schedules, changes to payload manifest, OTV refurbishment, etc., would normally be difficult to accomplish analytically.

The simulation "fly-offs" between each vehicle are run over a 20 year period. The number of shuttle launches required and the mass delivered to orbit are determined. For the EOTV, the average transfer time is obtained. Inputs to the program are the mission payload mass, velocity increment representing the final orbit, and for the EOTV, the equations characterizing the thruster and vehicle. The outputs of Shuttle launches, numbers of vehicles (each type) needed, and other considerations are then used as a basis for assigning coarse costs and comparing alternative operations during the "fly-off."

Methodology

This section will deal first with a broad picture of the methodology and then show a more detailed view of the tasks, assumptions, and information flow that are involved in doing analysis with this methodology.

It can be seen in Figure 1 that the mission determines the needs

and provides inputs for the SUMT and QGERT programs. Each mission is characterized by three major parameters: mass, orbit altitude, and orbit inclination. The desired orbit altitude and inclination are used to determine the required velocity increment, Δv, through use of the Alfano-Wiesel curves (1). These curves give the minimum energy transfer in the case of low thrust (ie. - the EOTV). Use of these curves is also covered in Appendix II. The Δv for the other vehicles, IUS, CNTAR, RBPV, is a straight-forward Hohmann transfer and because these transfers take place in less than a day, no detailed calculations are required by this methodology. Therefore, for QGERT "fly-off" purposes, chemical systems are assumed to make the transfer in 0.5 day.

The methodology is set up so that the user may specify a mission or a mission set and run the algorithms with this input. The algorithm is designed primarily for a deployment scenario in which payloads are transported from LEO to some higher orbit and inclination. Other scenarios can be envisioned and these are treated in Appendix V. For discussion purposes, the NavStar GPS has been selected as a representative mission payload for use through the entire methodology. Chapters 4 and 5 will discuss the specific inputs and outputs in some detail, but the emphasis is on the overall picture in this chapter.

Referring to Figure 1 again, the lower left block depicts the optimization of an electric propulsion Orbit Transfer Vehicle (EOTV). Components chosen for the propulsion and power systems come mostly from the 30-cm Ion Thruster Design Handbook (12) plus a compilation of data from numerous other sources in the bibliography. The user may

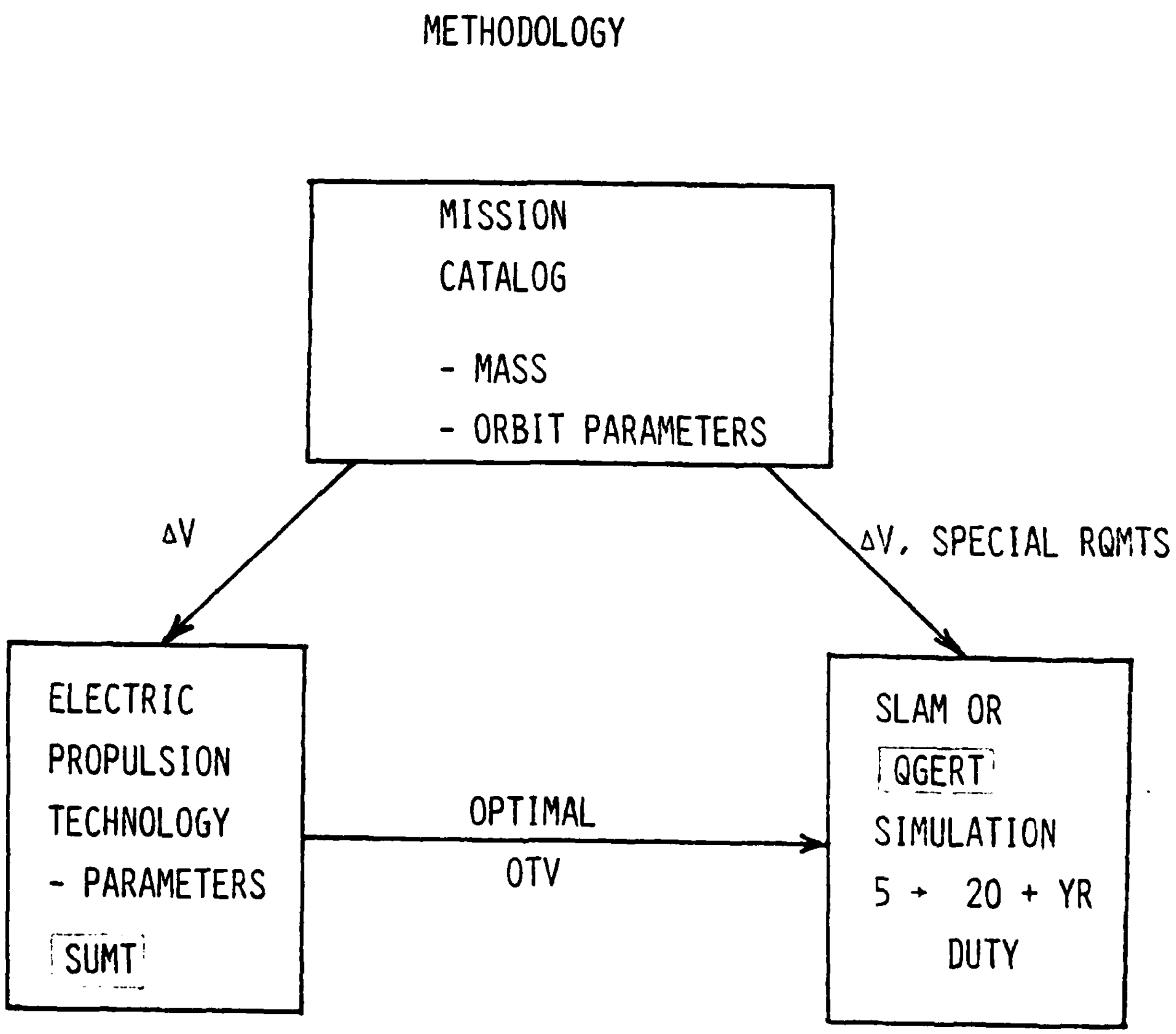

FIGURE 1. METHODOLOGY OVERVIEW

select candidate EP propulsion systems as desired, as long as the relationship between input power and ISP/thrust can be expressed mathematically. If not, the user must modify the SUMT program input more extensively. For the GPS example, five thrusters compatible with the Design Manual were chosen and optimized for 1,2,3,4,5,and 6, GPS satellites aboard. Based on the minimum mass of the system determined by the SUMT optimization and on secondary calculations of the transfer time, an acceptable combination of minimum mass and minimum transfer time are chosen as the desired optimum EOTV. Details will be covered in Chapter 4.

Having chosen an optimal EOTV, this vehicle can then be examined for long term performance in a "fly-off" against our present upper stages and a representative Reuseable Bi-Propellant Vehicle (RBPV) in the QGERT simulation. This phase is shown in the lower right-hand block in Figure 1. Mission characteristics of Δv required, Shuttle integration factors, etc., and vehicle characteristics for EOTV are inputs for the QGERT models. One QGERT model exists for each of the upper stages and OTVs. The user may decide the appropriate time period to run the simulation, but 20 years is used in this thesis. While the simulation may be run using a single type of satellite payload, a mission set can be used. Either may be specified by the user. More details will be covered in chapter 5.

With the results of the simulation, the performance of each vehicle may be examined and costs assigned to the operations. Determining costs has proven to be difficult and elusive for systems not yet in existence, and even for the IUS since it has not had as big a block buy as originally intended. However, coarse cost estimates

can be used for comparison. Other results of interest to the decision-maker are the number of Shuttle launches required in using each upper stage / OTV and the total number of satellites delivered. With these results and a knowledge of the assumptions and inputs comprising the results, the decision-maker should be in a better position to evaluate the merit of operating with one or a mixture of these vehicles.

To grasp more of the details in working with this methodology, refer to Figure 2 for the following discussion. The operational need drives the requirement for a satellite system. Those satellites not deployed in LEO must be delivered to higher orbit by kick stages or Payload Assist Modules (PAMs) for lighter satellites, or IUS, CENTAUR-G for heavier ones. The decision-maker then has a need for a tool or method for evaluating these expendable stages against more fuel-efficient, reuseable electric OTVs and against reuseable chemical OTVs.

For purposes of the optimization, the user may choose a specific payload or a representative mission set. If a specific payload is chosen, the SUMT program will require the mass of the payload to be inserted in the equation tableau. A comment card is included by this author at the appropriate lines in the formulation. If a mission set is chosen, three approaches exist. The first is to run SUMT and optimize an EOTV for every different payload in the set. A single optimum EOTV is then chosen to favor the payload with the highest frequency of launch, or a weighting technique can be devised with weighting factors determined by the decision-maker. The second

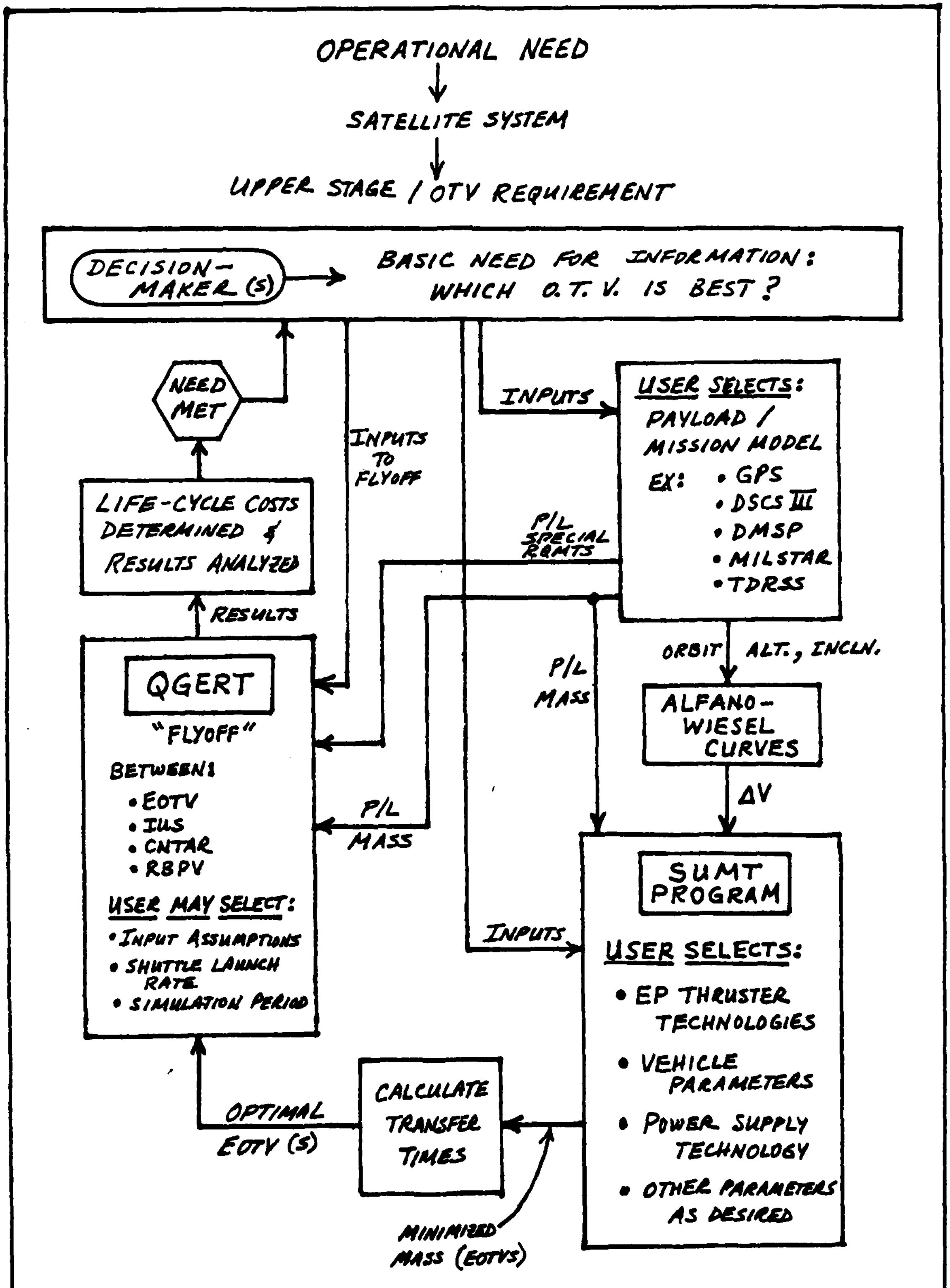

FIGURE 2. DETAILED METHODOLOGY

approach is to categorize the whole set by a single representitive payload and optimize the EOTV for that nominal payload. The third approach is to group the set into similar mass and orbit requirements and optimize a fleet of EOTVs, one for each group.

The orbit altitude and inclination for the payload must be used in the Alfano-Wiesel transfer to obtain the Δv required. This Δv, in KM/sec, is an input for SUMT and for subsequent transfer time calculations. It appears in two equations in the SUMT formulation and is readily edited. With Δv, payload mass, and general EOTV characteristics as inputs, the SUMT formulation allows the user to choose an appropriate thruster technology and optimize the EOTV. For initial runs, the general EOTV parameters were masses from the Design Manual (12). The selected thrusters were all derivatives of the 30-cm electron-bombardment Kaufman thruster. The user may optimize given payloads with these parameters or select other EOTV configurations and thrusters. SUMT is primarily minimizing the combined masses of the required propellant and required power supply. In the optimization, the parameters that are being determined by SUMT are the throttling level for the set of thrusters (input power for given exhaust velocity, thrust, and mass flow) and the resulting trade-off between fuel mass consumed and power supply mass required to do the mission. The mission is two-way, deploy and return with most of the fuel consumed. Note that electric propulsion systems have the potential for accomplishing several "out-and-backs" without refueling, whereas chemical propulsion systems are hard-pressed to make one "out-and-back." The optimization results provide the required input power to the thruster in order to simultaneously minimize the fuel

mass and power supply mass. Since the structure, housekeeping, and payload masses have been specified, the major drivers are propellant and power supply. The optimum EOTV has been found by SUMT as long as the associated transfer time is acceptable.

The equation to determine round-trip transfer time for the optimum EOTV deploying its associated payload is given by:

$$\tau = \frac{(M_{P1} + M_{P2})\, g_c\, (I_{sp})}{N\,(Th)} \qquad (2)$$

τ is round-trip transfer in seconds, M_{P1} is mass of propellant out to orbit, M_{P2} is mass of propellant return, N is number of thrusters, and Th is thrust per thruster. All units are MKS. This is a standard relationship based on a rearrangement of: thrust = mass flow x exhaust velocity. Masses for the equation are obtained from derivatives of the rocket equation, eq. 1. If the transfer time is not acceptable, more thrusters can be added and the EOTV optimized again, or more input power can be supplied (away from the minimum mass) until the transfer time is within an acceptable range. [It should be mentioned here that a program was formulated which minimized both mass and weighted transfer time. However, the solution from SUMT would not converge within central processor time limits. That effort is recommended for further study.]

Once the transfer time is acceptable, the methodology flows to the "fly-off" simulation. The characteristics of the optimal EOTV, the payload mass(es) and Δv(s), and any special mission constraints, such as Shuttle compatibility / integration, transfer time restrictions, etc. are input to the QGERT models. One model for each upper stage / transfer vehicle was developed. This allows a clearer comparison

between them as each delivers the same representative payload or mission model. The characteristics for IUS, CNTAR, and RBPV which were previously determined are incorporated in each model.

Each of the four vehicle QGERT models is directly influenced by the Shuttle launch rate. Because the RBPV is requiring extra Shuttle flights to bring up fuel and because valuable payload bay space is taken by the upper stage in the case of expendable systems, there is potential for reducing the Shuttle launch rate with an EOTV. Requisite for each simulation model is the turn-around for the Shuttle -- how many trips to LEO are possible in a year? Given the difficult tasks of refurbishment, ET and SRB mating, payload integration, refueling, and system checkouts for Shuttle, the turn-around with 3 or 4 Orbiters will probably not be under 20 days very often. So, a realistic figure of 18 launches per year is chosen for late 1980s, early 1990s, even if it is a bit conservative compared to many literature sources. Several studies assume very high launch rates commensurate with greatly increased space activity in the 1990's and beyond. But Federal and industry budget constraints are likely to persist in the next 20 years, and that will undoubtedly curtail both customers and operators of the Shuttle. The lower assumed launch rate may tend to favor the expendable systems, and therefore the study results should be conservative in that regard, too. Examining total number of satellites delivered in the 20 year (selectable by user) period and comparing to the number required by the mission model can suggest what reduction in Shuttle launch rate, if any, is possible.

QGERT readily allows for introduction of uncertainty. While a decision-maker may want to model uncertainty throughout the "fly-off",

this author chose 3 areas that in reality should have uncertainty associated with them. The first is the input Shuttle launch rate. A normal distribution is chosen with standard deviation of +/- 10 days. An earlier modeling had incorporated an uneven interval between launches with an exponential interarrival distribution. But the inherently large variance was not needed in this "fly-off."

The second area of uncertainty is failure of the upper stage or transfer vehicle. For the EOTV, a reliability of .990 is assumed because if one or even several thrusters fail, the mission is not aborted. The transfer will simply take longer as the remaining thrusters are gimballed to compensate for the lost thrusters and the mission continued. At low thrust levels this is possible, whereas all chemical vehicles being compared here would be totally lost upon failure of one engine (the <u>only</u> engine in the case of IUS kick stages). Also, the EOTV has at least two PPUs per BIMOD unit, two interface modules per vehicle and at least two solar panels. It is assumed that the malfunctioning unit could then be replaced upon return to Shuttle orbit and arrival of the next Orbiter with parts. Assumptions for other model reliabilities are: .965 for IUS, .985 for Centaur (weighted by previous performance) and .975 for the RBPV. The decision-maker is free to make alternate assumptions for reliabilities.

The third area of uncertainty is in Shuttle payload manifest, since changes will undoubtedly occur to the schedule. Also, some payloads will not require transfer to higher orbits. To account for this, a node is included where 65% of the time the arriving payload is not transferred by any of the four vehicles. Reasons for this might

include, Spacelab mission, PAM deployed payload, LEO experiment package, and LEO satellites. More will be discussed in Chapter 5. It is important to note that although uncertainty is included, each of the four QGERT models will be subjected to the same random number stream so that variance between compared runs is controlled. That is, uncertainty affects outcomes of the four models, but is applied consistently to each model.

With all of these results of reduced Shuttle launch rates, OTV fleet sizes, number of satellites delivered to final orbits, and effects of uncertainties, the methodology proceeds to the determination of coarse Life Cycle Costs (LCC) for acquisition and operation of each alternative vehicle. More will be discussed as to assignment of costs in Chapter 6. With the performance of each OTV / Stage and a rough comparison of LCCs, the decision-maker now has a tool with certain flexibilities that allow comparison and evaluation. With more information, the decision-maker can assess a decision to continue present operations with IUS and later the Centaur-G or to acquire either electric or chemical reuseable transfer vehicles.

CHAPTER IV. Optimizations Using SUMT

SUMT Non-Linear Program

The Sequential Unconstrained Minimization Technique (SUMT) program, has been chosen to optimize EOTVs for given payloads. SUMT has the flexibility to use more than one available technique to find the minimum of a multivariable, nonlinear function subject to nonlinear inequality and equality constraints.

The general mathematical programming formulation of the problem is:

$$\text{Minimize:} \quad F(X_1, X_2, \ldots, X_N)$$

$$\text{Subject to:} \quad G_k(X_1, X_2, \ldots, X_N) > 0, \quad k = 1, 2, \ldots, M$$

$$H_k(X_1, X_2, \ldots, X_N) = 0, \quad k = M+1, M+2, \ldots, M+M2$$

The procedure for solving this non-linear programming (NLP) problem was developed by Fiacco and McCormick as detailed in references 20, 33 and 57. The inequality and equality constraints are attached to the original objective function to make use of penalty function techniques. The resulting unconstrained function is minimized using one of several appropriate multivariable, unconstrained techniques.

The following quote and diagram (Figure 3) from reference 20 describe the procedure followed by the algorithm in finding the minimum.

"The algorithm proceeds as follows:

1) A modified objective function is formulated consisting of the

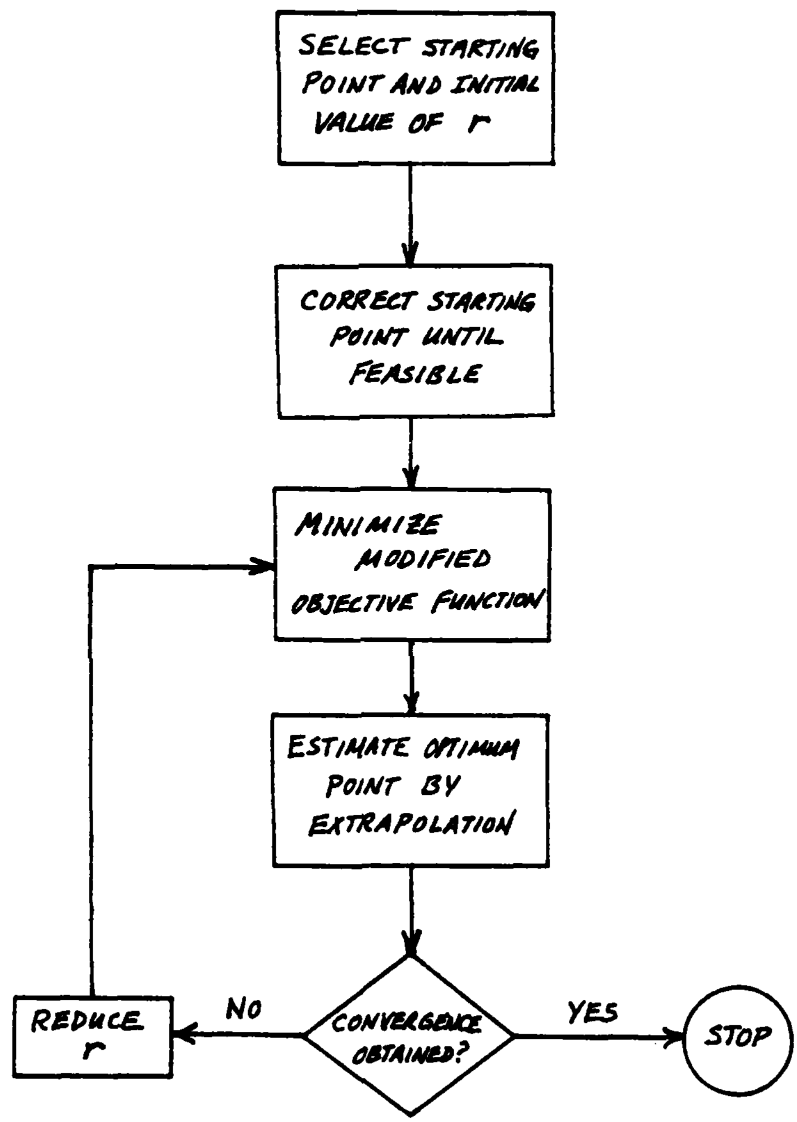

FIGURE 3. FIACCO AND McCORMICK LOGIC DIAGRAM (SUMT ALGORITHM) (20)

original function and penalty functions with the form:

$$P = F - r \sum_{k=1}^{M} \ln G_k + \sum_{k=M+1}^{M+MZ} H_k^2/r \qquad (3)$$

where r is a positive constant. As the algorithm progresses, r is reevaluated to form a monotonically decreasing sequence $r_1 > r_2 > \ldots > 0$. As r becomes small, under suitable conditions P approaches F and the problem is solved.

2) Select a starting point (feasible or nonfeasible) and an initial value for r.

3) Determine the minimum of the modified objective function for the current value of r using an appropriate technique (several options available).

4) Estimate the optimal solution using extrapolation formulas (33).

5) Select a new value for r and repeat the procedure until the convergence criterion is satisfied." (20)

The developers of the code consider it to be a research tool rather than a production code for NLP (33). This is because it allows experimentation with various techniques for solving NLPs, since no existing technique handles all types of problem formulations. It is this flexibility that has made it a choice for optimizing EOTVs.

Preliminary Mission Model

It should be made clear that the user of this methodology is able to choose a single payload or several payloads comprising a mission model and then have the EOTV optimized for that payload or model.

For purposes of demonstrating and verifying this portion of the methodology, the NavStar GPS satellite constellation has been selected as a mission model. This allows preliminary results to be obtained for thesis sponsors at USAF Space Division. Also, other payloads may be represented by the mass categories arising from deploying 1 - 6 GPS satellites at the same time with one OTV. For instance, one FLTSATCOM satellite would be similar in weight to 2 next-generation GPS satellites.

The following table shows the mission model in terms of number of GPS satellites (SATS), mass in KG, weight in LB, and Δv for LEO to GEO orbit change. Current GPS satellites are in sub-synchronous orbits, but GEO is a possibility in the future. So, this "worst case" scenario of deploying from a 200 Km orbit to GEO has been used during initial optimization runs.

****

TABLE 1

# of SATS	MASS (KG)	WT (LB)	Δv to GEO (KM/SEC)
1	908	2002	5.8382
2	1816	4004	5.8382
3	2724	6005	5.8382
4	3632	8007	5.8382
5	4540	10009	5.8382
6	5448	12011	5.8382

****

The Δv in Table 1 was obtained from the Alfano-Wiesel Optimal Many-Orbit Transfer Curves for low thrust. The weight figures resulted from rounding the mass of the 2000 lb planned-growth GPS to 908 Kg.

Multiples of 908 were used for the runs and comprise the KG column. When converted back to lbs. for comparison, the weights are not "nice and round." MKS units are used throughout this methodology for all calculations. "Planned-growth" refers to the fact that other sensors and hardening are planned for future GPS satellites. These satellites should be ready for deployment in the time frame that EOTVs could reach Initial Operational Capability (IOC).

Characterizing the EOTV

In order to make initial runs, assumptions have been made regarding Electric Propulsion Orbit Transfer Vehicle masses and these assumptions will be discussed first. Next, the method for characterizing the thrusters for the SUMT program will be discussed. For more information on the proposed vehicle configuration, the reader is referred to Appendix I.

The 30-cm Design Manual (12) contains tables of masses for the components of the thruster subsystem called BIMOD. As the name implies this BIMOD unit is modular and includes: two thrusters and their associated Power Processing Units (PPUs), thermal control for PPUs, and thruster gimbals. When fastened together, 4 BIMOD units containing 8 thrusters form the basic propulsion configuration assumed for the preliminary optimization runs. On top of the 4 BIMOD units is an interface module which contains propellant tanks, gimbal electronics, thruster controller, power distribution, truss structure, harness, and more thermal control. The given mass of each BIMOD unit is 137.1 Kg and thus 4 units total 548.4 Kg. The single interface module for these

4 BIMODs is 158.7 Kg, less propellant. The total propulsion subsystem is 707.1 Kg. Telemetry, guidance and control, and other avionics plus Control Moment Gyros (CMGs) in lieu of a Reaction Control System (RCS), solar panel array steering, autonomous computing, and payload interfaces are assumed to round the vehicle mass to 1000 Kg., total. Follow-on runs will include further assumptions as to vehicle characteristics. Users are, of course, free to make their own assumtions / calculations of the EOTV masses as new data is available.

With an assumed vehicle mass of 1000 Kg., the next task is to determine a way to characterize thruster performance in the SUMT program. This has been accomplished by noting that experimental data on ion thrusters (39,40,41,45) shows an approximately linear relationship between thruster input power and performance characteristics of ISP (& exhaust velocity) and thrust. Figure 4 is a graph showing ISP and thrust plotted against input power for a Ring-Cusp 3-grid ion thruster. As input power is increased, both ordinate values increase. A simple, linear curve fit was performed for each of 5 electron-bombardment ion thrusters. Examples of the experimental data table and ISP and thrust curve fits are in Table 2 and Figure 5, respectively. These data points and the curve fit are for the Ring-Cusp 3-grid ion thruster. Data and curve fits for the other 4 thrusters are found in Appendix I. In follow-on studies it is hoped to include other electric propulsion technologies such as self-field magnetoplasmadynamic, pulsed-inductive, rail-gun, and other promising designs.

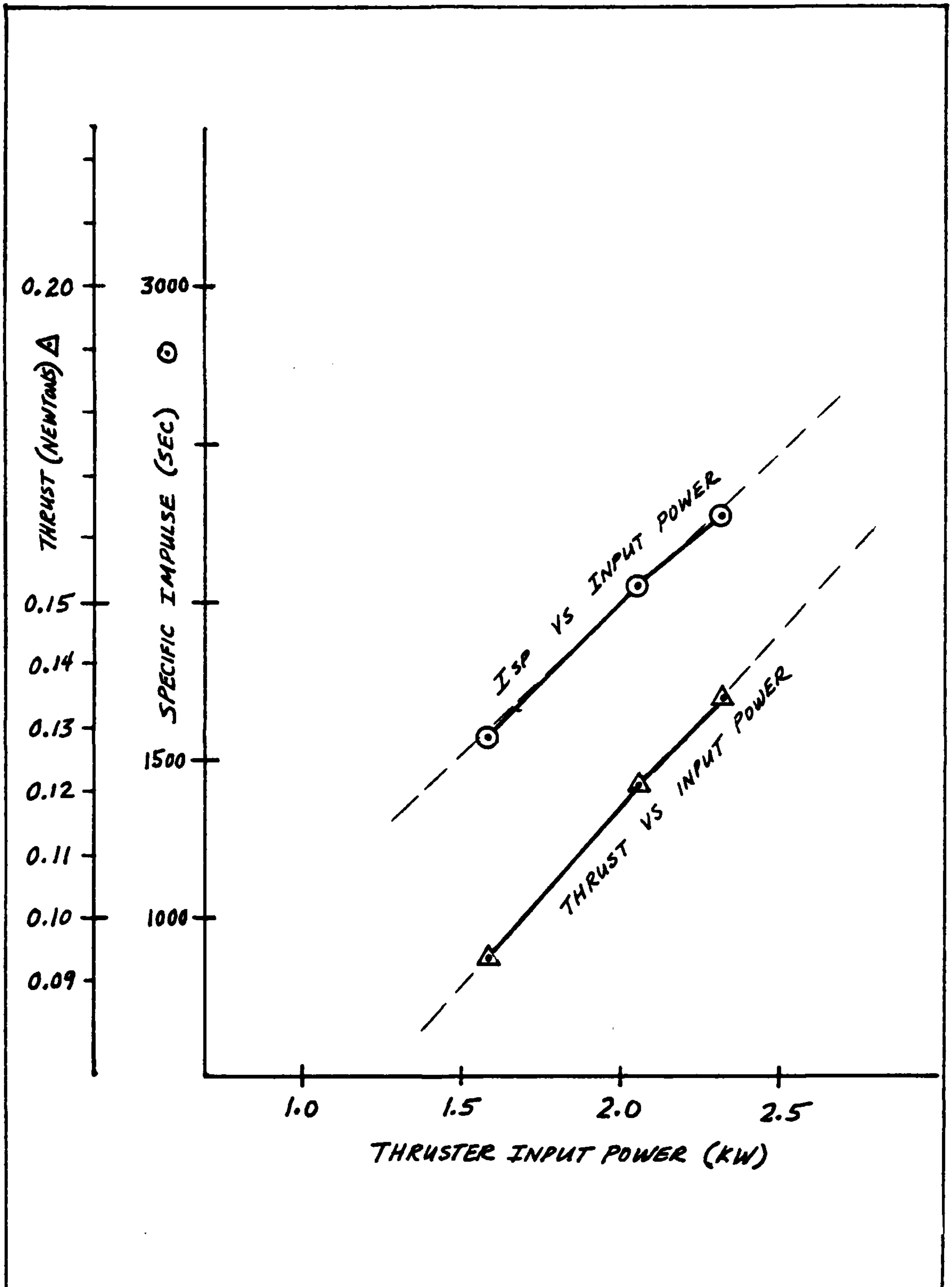

FIGURE 4. INPUT POWER VS ISP, THRUST RING-CUSP 3-GRID XENON THRUSTER

PROJECTED RING-CUSP THRUSTER PERFORMANCE WITH INERT GAS PROPELLANTS USING TWO TYPES OF ION OPTICS

[Assumptions: V_N - 20 V; P_F = 40 W; m_N = 0.10 A; F_I = 0.98 (table (a)); F_T = 0.95 (table (b)).]

Gas	Beam voltage, V_B, V	Beam current, J_B, A	Discharge voltage, V_D, V	Ion beam production ϵ', W/A	Overall propellant nu	Ion mass flowrate correction factor, β	Thrust correction factor, α	Thruster input power, P, W	Thrust, T_A, N	Specific impulse, I_{sp}, sec	T_A/P, mN/kW	Overall thruster efficiency, η_T
(a) Performance with two-grid ion optics												
Ar	1340	5.82	40.8	99.4	0.789	0.990	0.994	8 420	0.188	6270	22.3	0.686
	1440	6.61	46.1	109	.896	.975	.985	10 400	.221	7370	21.2	.767
	1340	6.79	48.3	114	.921	.968	.981	10 050	.220	7340	21.9	.787
Kr	1260	4.24	34.2	105	.861	.974	.985	5 900	.191	4560	32.4	.723
	1320	4.89	39.2	120	1.010	.925	.956	7 180	.219	5300	30.5	.791
	1320	5.40	46.1	143	1.110	.875	.927	8 030	.235	5680	29.3	.815
Xe	1150	3.04	29.4	90.5	.682	.985	.992	3 870	.165	2780	42.7	.581
	1200	3.95	32.8	91.8	.889	.965	.979	5 220	.217	3670	41.6	.746
	1240	4.43	35.6	94.6	.996	.940	.965	6 040	.244	4120	40.4	.814
(b) Projected performance with three-grid ion optics												
Ar	400	5.82	40.8	99.4	0.789	0.990	0.994	3 060	0.100	3330	32.6	0.532
	400	6.61	46.1	109	.896	.975	.985	3 540	.112	3750	31.8	.585
	400	6.79	48.3	114	.921	.968	.992	3 670	.116	3880	31.7	.603
Kr	400	4.24	34.2	105	.861	.974	.985	2 270	.105	2500	46.2	.566
	400	4.89	39.2	120	1.010	.925	9.956	2 680	.117	2840	43.7	.608
	400	5.40	46.1	143	1.110	.875	.927	3 080	.126	3050	40.9	.611
Xe	400	3.04	29.4	90.5	.682	.985	.991	1 590	.094	1580	59.0	.459
	400	3.95	32.8	91.8	.889	.965	.979	2 060	.121	2050	58.7	.589
	400	4.43	35.6	94.6	.996	.940	.965	2 320	.135	2270	58.1	.647

TABLE 2. *RING-CUSP DATA. FROM NASA (45).*

TABLE – Isp

INPUT PWR, W, (KW)	DATA Isp	CURVE FIT	DIFFERENCE	%
1.59 KW	1580	1588.95	5.9508	.004
2.06	2050	2033.29	-16.708	.008
2.32	2270	2280.757	10.7572	.005

Isp STATS: MEAN W: 1.99 $\sigma_{NX} = .3021037$ $S_X = 0.37$
MEAN Isp: 1966.7 $\sigma_{NY} = 287.7885$ $S_Y = 352.4675$

EQN: $Isp = 951.7896\,(W) + 72.6053$

SUMT FORMULATION: 31 $VAL = X(1) - 951.7896\,(W) - 72.6053$

TABLE – THRUST

INPUT PWR, W, (KW)	THRUST (N)	CURVE FIT	DIFFERENCE	%
1.59 KW	.094	.094139	.00013	.001
2.06	.121	.120609	-.000391	.003
2.32	.135	.1352518	.0002518	.002

THRUST STATS: MEAN W: 1.99 $\sigma_{NX} = .3021037$ $S_X = 0.37$
MEAN Th: .1167 $\sigma_{NY} = .0170163$ $S_Y = .0208407$

EQN: $Thrust = .056318\,(W) + .004593$

SUMT FORMULATION: 39 $VAL = X(6) - .056319\,(W) - .004593$

FIGURE 5. THRUST, ISP VS W CALCULATIONS RING-CUSP 3-GRID XE THRUSTER

Program Code Inputs

Several of the available options in the SUMT library were tried against four of the types of thrusters for EOTVs carrying payloads from 2000 lbs. to 12000 lbs. The results of using different options varied from program dump for lack of Central Processor (CP) time to sucessful runs with only slight variations (tenths of seconds) of CP time. Answers varied from exact (>6 decimal places) to erroneous. Thus, a significant amount of time has been devoted to finding a set of options that gives meaningful answers within reasonable CP time limits.

Option keys allow the SUMT user to input different convergence criteria, printout options, and problem linearity, as well as the desired unconstrained minimization technique. The option keys which seemed best for EOTV formulations were:

NT(1)=3 r value option set to RHOIN

NT(2)=1 automatic inclusion of trivial constraints, $X \geq 0$.

NT(3)=1 standard printout

NT(4)=1 final convergence determined on basis of current subproblem solution.

NT(5)=2 final convergence option

NT(6)=1 no extrapolation

NT(7)=1 subproblem convergence option

NT(8)=1 linearity: at least one nonlinear constraint

NEXOP1=1 option for checking derivatives

NEXOP2=1 unconstrained minimization technique -- in this case, the method chosen is the generalized Newton-Raphson method as modified to handle indefinite Hessian matrices.

In some cases where convergence was requiring too much CP time -- such as for the inert gas thruster -- option NT(4) was set to 2 so that final convergence was determined on the basis of first order estimates. This required typically 1/2 the CP time as before, but at the expense of accuracy. Instead of 6 decimal places, this option satisfied equality constraints to within only 3 decimal places of the optimum point. This is not considered significant for the EOTV optimization problem.

Formulation of the set of equations for the SUMT algorithm was straight-forward. Limits had to be set for the feasible region both to insure realistic values and to prevent spending CP time on too wide a search. These formed the inequality constraints. The equality constraints were based on standard relationships derived from the rocket equation for propellant mass used out to orbit (M_{p1}) and return (M_{p2}). Also included are the relationship for input power vs thrust previously developed and a standard relationship for the specific power of the solar power supply.

Figure 6 shows an initial formulation for the Ring-Cusp thruster with 3-Grid ion optics. Limits on specific impulse (X1) were 500 to 10000 sec. Limits on power supply (solar array) mass (X2) were 10 to 10000 Kg. Limits for both propellant masses (X3 out to GEO and X5 return) were 10 to 10000 Kg. Finally, limits r input power (X4) to the thruster were 0.5 to 20 KW. The specific p er equality (X2 vs X4) assumes no cabling resistance losses and assumes 1.0 for PPU efficiency. Thruster efficiencies are inherent in the thruster relationship of input power (X4) vs ISP (X1).

Figure 7 shows a program printout of the completed formulation for

a different thruster -- the Ring-Cusp 3-Grid Xenon Ion thruster. With the exception of input power, the constraints are the same. Line number 31 of the program input is the new thruster relationship.

Figure 8 shows the final results printout for the formulation in Fig.5, and is typical of the output format for the final solution to the minimization problem. The final value of F represents the minimization of the objective function. Recall that this function is the total mass of the power supply (8 $\times$ X2) plus the total propellant mass out to GEO and back (X3 + X5). The X values are just the solution values of the X vector for the minimized function. Constraint values are the equality and inequality constraints solved using the final X vector.

VARIABLE DEFINITIONS:

$X(1) = I_{sp}$ = Specific Impulse (sec)
$X(2) = M_W$ = Mass of Power Supply per thruster (KG)
$X(3) = M_{P1}$ = Mass of Propellant used out to GEO (KG)
$X(4) = W$ = Input Power per thruster (KW)
$X(5) = M_{P2}$ = Mass of Propellant used for return trip (KG)

FORMULATION:

OBJ. FCN, MINIMIZE: $F = 8 * X(2) + X(3) + X(5)$

CONSTRAINTS, SUBJ. TO:

$X(1) \geq 500$
$X(1) \leq 10{,}000$
$X(2) \geq 10$
$X(2) \leq 10{,}000$
$X(3) \geq 10$
$X(3) \leq 10{,}000$
$X(4) \geq 0.1$
$X(4) \leq 20$
$X(5) \geq 10$
$X(5) \leq 10{,}000$
$X(1) = 951.7896 * X(4) + 72.6053$
$X(2) = X(4)/.052$
$X(5) = (1000 + 8 * X(2)) * (\exp(5.8382/.00981 * X(1)) - 1)$
$X(3) = (2000 + 8 * X(2)) + X(5)) * (\exp(5.8382/.00981 * X(1)) - 1)$

SUMT INPUT EQUATIONS:

OBJ. FCN: VAL = $8 * X(2) + X(3) + X(5)$

EXAMPLE CONSTRAINT: VAL = $X(1) - 500.0$

FIGURE 6. PROBLEM FORMULATION FOR SUMT RING-CUSP 3-GRID XENON THRUSTER

FIGURE 7

SUMT Equation Input - Ring Cusp, 1000 Kg

After Program Main:

```
C         RESTRAINT PORTION
          SUBROUTINE RESTNT (IN,VAL)
          COMMON/SHARE/X(100),DEL(100),A(100,100),N(5),
         +M,MN,NP1,NM1
          IF (X(1) .LE. 1.0) X(1)=500.0
          IF (IN) 10,10,20
   10     VAL= 8*X(2)+ X(3) + X(5)
          RETURN
   20     GO TO (21,22,23,24,25,26,27,28,29,30,31,32,33,34),IN
   21     VAL = X(1)-500.0
          RETURN
   22     VAL = 10000.0- X(1)
          RETURN
   23     VAL = X(2) - 10.0
          RETURN
   24     VAL = 10000.0 - X(2)
          RETURN
   25     VAL = X(3) - 10.0
          RETURN
   26     VAL = 10000.0 - X(3)
          RETURN
   27     VAL = X(4) - 0.5
          RETURN
   28     VAL = 20.0 - X(4)
          RETURN
   29     VAL = X(5) - 10.0
          RETURN
   30     VAL = 10000.0 - X(5)
          RETURN
   31     VAL = X(1) - 951.7896*X(4) - 72.6053
          RETURN
   32     VAL = X(2) - (X(4)/(0.052))
          RETURN
   33     VAL = X(5) - (1000 + 8*X(2))*(EXP(5.8382/(0.00981*X(1)))-1)
          RETURN
C         PAYLOAD MASS IS: 1000KG
   34     VAL=X(3)-(2000.0+8*X(2)+X(5))*(EXP(5.8382/(0.00981*X(1)))-1)
          RETURN
          END
*EOR
 $DATA N=5,M=10,MZ=4,
           X=1976.2,38.462,972.437,2.0,459.538,
           NT(2)=1,NT(5)=2,NEXOP2=1 $END
```

FIGURE 8

SUMT Final Output Values - Ring Cusp, 1000 Kg

After the Last Iteration:

```
8950= * * * * * * * * * * * * * * * * * * * * * * * * * * * * * * * *
* * * * * * * * * * * * * * * * * *
8960=  FINAL VALUE OF F =    1.36117001E+03
8970=
8980=
8990=  FINAL X VALUES
9000=
9010=  X(   1) =    3.87917996E+03  X(   2) =    7.69112828E+01  X(   3) =
4.78049119E+02
9020=  X(   4) =    3.99938669E+00  X(   5) =    2.67830631E+02  X(
9030=
9040=  FINAL CONSTRAINT VALUES
9050=
9060=  G(   1) =    3.37917996E+03  G(   2) =    6.12082004E+03  G(   3) =
6.69112828E+01
9070=  G(   4) =    9.92308872E+03  G(   5) =    4.68049119E+02  G(   6) =
9.52195088E+03
9080=  G(   7) =    3.49938669E+00  G(   8) =    1.60006133E+01  G(   9) =
2.57830631E+02
9090=  G(  10) =    9.73216937E+03  G(  11) =   -5.84986992E-09  G(  12) =
2.23737516E-07
9100=  G(  13) =    5.76437742E-09  G(  14) =   -2.48164724E-08  G(
9110=*EOR
9120=1  CSA   NOS/BE L564E       L564  CMR1  1/01/83
9130= 15.38.50.LWMHUM4  FROM    /HU
9140= 15.38.50.IP  00000320 WORDS - FILE INPUT  , DC 04
9150= 15.38.50.LWM,T35,IO100,CM100000.T830229,MADDOX
```

Initial Analysis of Results

The 5 thruster technologies were input to SUMT one by one and optimized against the NavStar GPS mission model. Figures 9 and 10 show a compilation of the results of these 35 runs.

The output of the runs is in terms of a minimized mass. Since basic vehicle mass is not changing as greatly as power supply and propellant mass, these are the only masses minimized by the objective function in initial runs. With the final X values, the transfer times must be calculated. A programmable calculator handled this task well, and it should not be difficult for users to do the same or to write a FORTRAN code for a larger machine. Examples of how this transfer time was calculated appear in Figure 11. Follow-on work may be able to include the entire methodology in a single code which calls on SUMT and QGERT as subroutines, thus eliminating the need for separate calculations.

THRUSTER →	BASELINE J-SERIES THRUSTER						3-GRID Hg						EXTENDED PERF – S. PPU					
P/L MASS →	908	1816	2724	3632	4540	5448	908	1816	2724	3632	4540	5448	908	1816	2724	3632	4540	5448
X1 – I_{sp}	3014	2938	3259	3549	3398	3294	2686	2621	2875	3106	2984	2898	2845	2845	2845	2845	2845	2845
# THRUSTERS	6	8	8	8	10	12	6	8	8	8	10	12	6	6	8	8	8	10
X2 – M_W	49.9	47.1	58.8	69.5	63.9	60.1	89.5	86.1	99.3	111.5	105.1	100.6	38.4	38.4	38.4	38.4	38.4	38.0
X3 – M_{P1}	543.8	786.4	899.5	998.8	1243	1487	700.9	1003	1134	1251	1554	1860	564.2	775.4	1008	1220	1431	1663
X4 – W	2.60	2.45	3.06	3.61	3.32	3.13	4.66	4.48	5.17	5.80	5.47	5.23	2.0	2.0	2.0	2.0	2.0	2.0
X5 – M_{P2}	283.7	309.2	294.7	284.0	313.8	340.9	381.2	430.5	412.8	399.5	452.6	503.1	286.3	286.3	304.2	304.2	304.2	321.0
F – OBJ. FCN.	1127	1472	1665	1838	2196	2550	1619	2122	2342	2542	3058	3570	1081	1292	1620	1832	2043	2364
T – Thrust	.1274	.1206	.1492	.1751	.1616	.1524	.2322	.2266	.2485	.2685	.2580	.2505	.1096	.1096	.1096	.1096	.1096	.1096
τ_1 – TO GEO	243.4	271.8	278.9	248.2	296.7	304.2	153.4	164.7	186.3	205.3	204.2	203.5	277.2	381.0	371.7	449.6	527.4	490.3
τ_2 – Return	127.0	106.9	91.4	81.7	74.9	69.7	83.4	70.7	67.8	65.6	59.4	55.1	140.7	140.7	112.1	112.1	112.1	94.6
τ – Round Trip	370.4	378.7	370.3	369.0	371.6	373.9	236.9	235.4	254.0	270.9	263.6	258.6	417.9	521.7	483.8	561.7	639.5	585.0
RATIO THRUST/PWR	49.1	49.2	48.8	48.5	48.6	48.7	49.9	50.6	48.1	46.3	47.2	47.9	54.8	54.8	54.8	54.8	54.8	54.8

FIGURE 9. SUMT RESULTS

THRUSTER →	30-cm w/ Argon						RING-CUSP						5-THRUSTER COMPARISON SAME INPUT PWR, ALL W/2724 KG				
P/L MASS →	908	1816	2724	3632	4540	5448	908	1816	2724	3632	4540	5448	Baseline	3-GRID	EXT PF	ARGON	R-CUSP
X1 − I_{sp}	4514	4514	4514	4514	4514	4514	3834	4261	4653	5013	5349	5665	3754	2445	3114	4548	3880
# THRUSTERS	6	8	8	8	10	12	8	8	8	8	8	8	8	8	8	8	8
X2 − M_W	38.4	38.4	38.4	38.4	38.4	38.4	76.0	84.6	92.5	99.8	106.6	113.0	76.92	76.92	76.92	76.92	76.92
X3 − M_{P1}	325.8	466.1	594.1	722.1	862.4	1002.7	467.8	561.3	641.6	713.1	778.0	837.8	793.2	1318.2	985.3	638.2	763.7
X4 − W	2.0	2.0	2.0	2.0	2.0	2.0	3.95	4.40	4.81	5.19	5.54	5.88	4.0	4.0	4.0	4.0	4.0
X5 − M_{P2}	173.4	184.2	184.2	184.3	195.1	205.9	270.0	251.4	237.5	226.7	218.1	210.9	277.5	445.1	340.2	225.8	267.8
F − OBJ. FCN.	729.9	957.9	1086	1214	1442	1670	1346	1490	1619	1738	1849	1953	1686	2379	1941	1479	1647
T − Thrust	.0462	.0462	.0462	.0462	.0462	.0462	.2685	.2937	.3169	.3383	.3582	.3768	.1933	.2114	.1849	.0875	.2712
τ_1 − Out to GEO	602.8	646.8	824.4	1001.9	957.3	927.6	94.8	115.6	133.7	150.0	164.9	178.8	218.6	216.5	235.6	470.9	155.1
τ_2 − Return	320.9	255.6	255.6	255.7	216.6	190.5	54.7	51.8	49.5	47.7	46.2	45.0	76.5	73.1	81.3	166.6	54.4
τ − Round Trip	923.7	902.4	1080	1258	1174	1118	149.5	167.3	183.1	197.7	211.1	223.8	295.1	289.5	316.9	637.5	209.5
RATIO THST/PWR	23.09	23.09	23.09	23.09	23.09	23.09	67.94	66.76	65.86	65.17	64.60	64.14	48.33	52.85	46.22	21.87	67.80
													NON-OPTIMIZED CALCULATIONS → 4 KW				

FIGURE 10. SUMT RESULTS. FIVE THRUSTER COMPARISON.

GENERAL EQUATION:

$$\tau = \frac{M_P\,(KG)}{\dot{m}\,(KG/s)} = \frac{M_P V_e}{8 * T} = \frac{M_P\, g_c\, I_{sp}}{8 * T}$$

$$= \frac{(M_{P1} + M_{P2})\, g_c\, I_{sp}}{8 * T}$$

Number of Thrusters

VARIABLES:

τ = transfer time (sec)

M_{P1} = Mass of propellant to higher orbit

M_{P2} = Mass of propellant to return

V_e = exhaust velocity

I_{sp} = Specific Impulse

T = Thrust

g_c = gravitatnl. constant.

$\dot{m}$ = mass flow rate

EXAMPLE: 908 KG Payload, 3-Grid Optics Thrusters.

$$\tau = \frac{(M_{P1} + M_{P2})\, g_c\, I_{sp}}{8 * T} = \frac{(X3 + X5)\, g_c\, (X1)}{8 * T}$$

Next, obtain thrust from linearized relationship

$$T = .0318\,(X4) + .084$$

$$= .2022785 \text{ Newton per thruster}$$

NOW, USING SUMT OPTIMIZED X VALUES FOR M_{P1} & M_{P2}:

$$\tau_{\text{ROUND TRIP}} = \frac{(849.7 + 455)(9.81)(2340)}{8 * (.2022785)}$$

$$= 1.85078 \times 10^{7} \text{ sec} = \boxed{214.21 \text{ days}}$$

Round trip to GEO and back

$$\tau_{OUT} = \frac{(849.7)(9.81)(2340)}{8\,(.2022785)} = 1.20534 \times 10^{7} \text{ sec} = \boxed{139.5 \text{ days}}$$

Trip time out to GEO

$$\tau_{RETURN} = \frac{(455)(9.81)(2340)}{8\,(.2022785)} = 6.4544 \times 10^{6} \text{ sec} = \boxed{74.7 \text{ day}}$$

Return empty from GEO to LEO

FIGURE 11. DETERMINING TRANSFER TIME

Note that the transfer time calculations were made for point designs. That is, when SUMT finished optimizing the EOTV for a given payload mass, the transfer time was calculated based on those final X values. This is irrespective of the reduction in transfer time possible with off-optimum power input and mass change. In all cases it is possible to reduce these transfer times by increasing the thrust or the number of thrusters, even though the mass increases as a result of using more power. This is illustrated in the sensitivity analysis, Figure 12.

Referring back, now, to Figures 9 and 10, it can be seen that transfer times are out of reason for the Extended Performance thruster with simplified PPU and for the Argon thruster. The reason is that minimum mass occurs at the lower limit of input power. As input power is increased above this lower limit, mass of the power supply rises rapidly just as for the other thrusters, but the mass of the propellant does not decrease, but increases slightly to offset the increasing power supply mass. Thus, while a crossover point does occur between curves in the feasible region, the sum of the power supply mass and propellant mass increases monotonically throughout the feasible region. Therefore, the SUMT program is correct in finding the minimum mass at the lower limit of input power, 2.0 KW, but the result is not very useful when considered alone. In this case, the decision-maker must specify a desired minimum transfer time and work back through the set of equations to obtain the input power and other parameters of the EOTV. Minimums within the limits of the feasible region do occur for the other three thrusters and the minimum mass and resulting X vectors are found by SUMT.

BASED ON 30-CM 3-GRID Hg THRUSTER, 1000 KG PAYLOAD FOR EOTV, 8 THRUSTERS.

	BELOW OPTIMUM	BELOW OPTIMUM	SUMT OPTIMUM POINT	MID-LIMIT ABOVE	UPPER LIMIT ABOVE
X1 - I_{SP}	2335.06	2342.42	2369.02	3549.23	8332.32
X2 - M_W	71.154	71.538	72.929	134.615	384.615
X3 - M_{P1}	878.05	875.61	866.93	629.64	397.49
X4 - W	3.700	3.720	3.792	7.00	20.00
X5 - M_{P2}	455.53	454.80	452.20	378.46	301.31
F - MASS OBJ FCN	1902.8	1902.72	1902.56	2085.02	3775.72
THRUST PER ENGINE	.201837	.202473	.204772	.306810	.720340
τ_1 OUT (DAYS)	144.17	143.77	142.35	103.38	65.25
τ_2 Return (DAYS)	74.80	74.68	74.25	62.14	49.47
τ ROUND TRIP (DAYS)	218.97	218.45	216.60	165.51	114.72

NOTE: ABOVE OR BELOW THE OPTIMUM, F (COMBINED MASS) INCREASES.

MAIN IDEA: AS INPUT POWER INCREASES, ISP AND THRUST INCREASE, AND TRANSFER TIME STEADILY DECREASES, DESPITE GREATER MASS OF THE POWER SUPPLY.

FIGURE 12. TRANSFER TIME SENSITIVITY

Concentrating now on the final minimized mass (F), it can be seen that each category of thruster does, in fact, require a different mix of propellant vs power supply mass to deploy the same set of GPS satellites. As discussed in the previous paragraph, without a tradeoff of power supply mass and propellant mass, both Argon and Extended Performance thrusters have minimum mass values at the lower limits of input power. Consequently, they have the smallest objective function mass values (F), respectively. The next lowest is Baseline, followed by Ring-Cusp 3-Grid Xenon and 3-Grid Hg. With its high thrust to power ratio, the Ring-Cusp 3-Grid Xenon has, by far, the shortest trip times. In order to compare the 5 thrusters at the same input power, the last table in Figure 10 shows non-optimized calculations of each thruster operating at 4.0 KW. Each is carrying a 2724 Kg payload representing 3 GPS satellites. Each has the same power supply mass. Each deploys from a 200 KM Shuttle orbit to GEO and returns empty. The 3 GPS satellites are assumed to be deployed in the same orbit plane with each satellite using its ACS/RCS to position itself within the orbit plane. [Follow-on studies may address the possibility of deploying to other orbit planes using the EOTV, as this seems quite feasible for EP]. As the figure shows, the Ring-Cusp Xenon thruster ranks number 1 in shortest transfer time, and number 2 in least mass to accomplish the mission. Its relative position regarding transfer time will hold across the spectrum of payload masses. Its relative position regarding minimized mass will trade, however, with at least one other thruster.

The question arises, "given these outputs as summarized on Figures 9 and 10, how does the user pick an optimal EOTV configuration?" If there were no clear cut choice, as there is in this preliminary set of

runs, a minimum mass within an acceptable transfer time would be chosen. For instance, say 3 GPS satellites form the payload for which an optimim EOTV is desired. Optimized final masses (F) for each category thruster are: Baseline, 1665 Kg; 3-Grid, 2342 Kg; Extd Perf., 1620; Argon, 1086 Kg; and Ring-Cusp, 1619. These represent combined power supply and propellant masses for the optimized EOTV. In the same order, round-trip transfer times are 370, 254, 484, 1080, and 183 days. If the acceptable transfer time cut-off is 300 days, then 2 choices remain: 3-grid Hg and Ring-Cusp Xe. Between these, Ring-Cusp uses less mass. Thus, the final choice for an optimized EOTV to do the mission is a Ring-cusp 3-Grid Xenon Ion Thruster driven at 4.812 KW with a solar array unit of 740.296 Kg and using 641.58 Kg of propellant out to GEO and 237.47 Kg of propellant for the return empty.

In this case, the choice was obvious because Ring-Cusp accomplishes the same mission with significantly less transfer time <u>and</u> with less propellant and power supply mass. This might not be true for other choices of electric thruster technologies which a user might wish to evaluate. Hence the need for examining both mass and transfer time in the methodology.

The third research question posed in Chapter 3 was, "Does one thruster technology clearly outperform all others for each mission?" It appears that the Ring-Cusp design is a clear winner. This is consistent with the fact that it is currently being investigated as a significant improvement to the baseline 30-cm ion thruster. Given these initial results, the first 3 research questions have been answered and the first three objectives of the thesis have now been met.

CHAPTER V. Fly-Off Using QGERT Simulations

Conceptual Model

The following discussion and diagram, Figure 13, of the general conceptual model are to assist in understanding the four QGERT networks. These networks model the four vehicles, EOTV, RBPV, IUS, and CENTAUR, for the "fly-off."

Graphical Evaluation and Review Technique (GERT) with Queueing system capability (Q), or QGERT, is a modularized and easy to formulate simulation language (37). Follow-on users should find QGERT easy to modify and work with when changing the models. As mentioned before in Chapter 3, the strength of the simulation is the capability to introduce uncertainty. Also, the capability to vary inputs to determine long term (length of the simulation) effects is a strength.

In order to show the rationale for each model and the general construction, refer to Figure 14. This general concept applies to all four networks. The Shuttle turn-around and payload integration time are external to the system modeled, but do impact the Shuttle launch rate. The model begins with the arrival of each Shuttle in LEO carrying one or more payloads. The next module, payload manifest, is the mission model. This has been determined previously by the user. For the runs made by this author, payloads were chosen probabilistically by category, realizing that not all payloads needed transporting to higher orbit. The next module represents picking an available OTV and docking prior to transfer. This module does not apply to expendable upper stages (IUS and CENTAUR). The orbit transfer

CONCEPTUAL MODEL

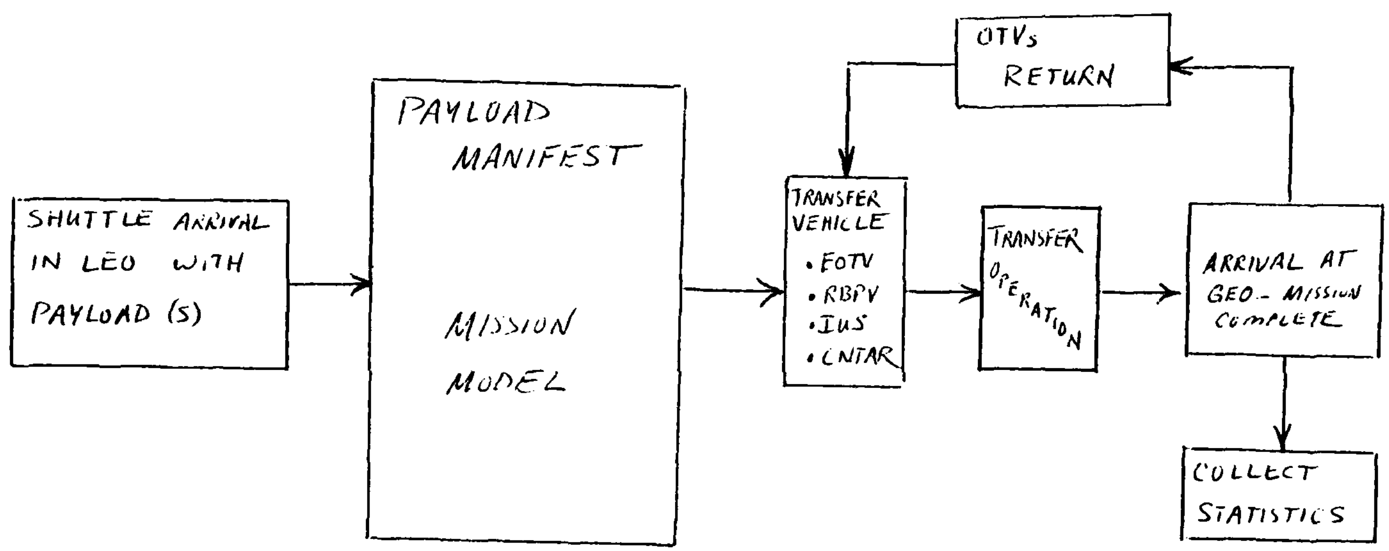

FIGURE 13.

is the next module and is represented primarily by the time delay required for the operation. Next is the arrival at GEO where OTVs separate and return via the OTV return module to a queue in LEO. Statistics are collected on the payloads delivered to GEO and this mission is complete. The process then continues with the arrival of the next Shuttle and cargo. With this general conceptual model in mind, understanding the individualized networks which follow should be easier.

Since it is an important input assumption, the mission model applied to each of the four vehicles will be briefly discussed. For the initial runs, a mission model was devised which used the masses for GPS (Chapter 4) but accounted for the fact that not all payloads will be candidates for orbit transfer using OTVs or IUS or CENTAUR. Based on numerous mission model projections from the literature, the following assumptions are made:

1. 65% of the missions brought to LEO will not be candidates for using the fly-off vehicles. Reasons include: payload is to remain in LEO, Spacelab sortie, PAM is being used.

2. 10% of the missions brought to LEO aboard Shuttle carry some other LEO payload and one GPS (908 KG) or a similar mass satellite needing transport to GEO.

3. 20% of the missions are in the mass category of 3 GPS satellites (2724 KG) or 6000 lbs.(pushing IUS limits).

4. 5% of the missions are heavy, in the category of 6 GPSs (5448 KG), which pushes the limit on an updated CENTAUR.

Again, the user is free to use another appropriate mission model, but this one had the nice feature of "dual representation." That is,

while GPS numbers are used so that results can be evaluated for this system, the mass categories can also represent other satellites just as easily. Examples within the 908 KG range: Landsat, Nimbus, 2 or 3 GOES, Comstar, RCA Satcom, Galaxy, DSCS, DMSP, and SDS. Examples within the 2724 Kg range: Newer FltSatCom, TDRSS, ERBS, and combinations or multiple satellites in the 908 Kg category. The 5448 Kg category might include MILSTAR and multiples of the 908 or 2724 Kg groups. Limitations on the IUS and CENTAUR are one payload and upper stage per launch, currently. Given the masses involved with CENTAUR and potential payloads, this should remain a good assumption. Integration that must take place on the ground and the mass of the IUS also make it likely that no other transportable payloads would also be aboard. More will be said about how each vehicle handles the payload as individual networks are discussed.

Electric OTV Network

Figure 14 shows the QGERT network for the EOTV. The Shuttle arrival rate is normally distributed about 20.27 days for 18 launches per year. The standard deviation of this arrival rate was chosen as 10 days to introduce more variability. This will likely be true for Shuttle launches well into the future, given the large number of variables during turn-around. No delay exists between arrival node 1 and payload determination node 4. As stated previously, 65% of the payloads are not candidates for OTVs/IUS/CENTAUR and go to node 20, where the number of sorties is counted. Then 10%, 20%, and 5% go to nodes 5, 6 and 7, respectively. At this point, the payload has been selected. Its mass is assigned in the appropriate node. This mass is later used to determine the appropriate transfer time in the QGERT User Function (UF). Node 5 is the payload scenario where one GPS or similar mass satellite is to be transported to GEO and the remaining cargo bay space is used for LEO satellites, experiment packages, and the like. The 2724 Kg node in the EOTV case can represent actually two 2724 satellites or 6 satellites (this is not possible with IUS and CENTAUR due to space and mass limitations mentioned previously.) Thus, two activity branches join nodes 6 and 10. Node 10 is the queue for satellites ready to dock with EOTVs. One day delay is built into the model here for this operation. It is intended that Shuttle and crew be present for monitoring and assistance during docking. Node 11 is the assembly node wich selects a payload and an EOTV from respective queues and begins the transfer. At this point the QGERT program calls UF 1 and assigns the appropriate transfer time to this activity. Transfer time has already been calculated for each respective payload and is

input in number of days to the UF as variable T1. Arrival at GEO is signified by node 12 and apropriate statistics are collected by nodes 15, 16, 18, 19. Node 13 is the return path for the EOTV. UF 2 is the return transfer time, also previously determined and input to UF as T2.

Besides the uncertainty modeled in the Shuttle arrival rate and the payload manifest, uncertainty is also included as a reliability figure for the EOTV. The figure assumed, .990, arises from the parallel redundancy of the 8 thrusters and associated PPUs. Reliability for parallel components is given by:

$$Rel(R) = 1 - (1 - R)^n \qquad (4)$$

Rel(R) is the reliability of the parallel system, R is the reliability of the individual, identical components, and n is the number of identical components. Considering just the 8-thruster, 4-BIMOD subunit alone, this would allow a reliability as low as .43 for each thruster-PPU combination, if the subunit were to be .99 overall. However, operation on only one thruster prevents total mission failure, since the vehicle could eventually limp back to LEO. But this would be far from desirable, as is the intent of equation 4. Also, the interface module and avionics, power supply, and housekeeping functions/subunits are in series with the BIMODs, so that this thruster redundancy is mitigated.

The EOTV thruster technology chosen for the initial runs was the optimum picked from SUMT results: the Ring-Cusp 3-Grid Ion thruster operating on Xenon. The optimum vehicle configuration was for the worst case payload, 5448 Kg. Choosing the vehicle optimized for the

heaviest payload means that lighter payloads will be delivered faster than if vehicle mass had been optimized for that lignter payload. Having chosen the optimum vehicle to use for the fly-off, transfer times were calculated for each payload and the return. For the respective payload masses, the transfer times input to the UF Fortran IF Statement were 71.4, 114.4, and 178.8 days. The return time calculated was 45.0 days. This, of course, does not vary between payloads since each vehicle always operates at a constant maximum thrust. Solar occultation and Van Allen degradation have not been modeled in these initial runs. Propellant is assumed to be carried aboard each Shuttle flight which bears payloads requiring EOTV services. Propellant tanks are assumed to be modularized to the extent that they can be exchanged via the Shuttle manipulator arm or with EVA.

Another input assumption is that one Shuttle launch is required for each EOTV to deploy the optimum 11 vehicle fleet. More will be discussed about the optimum fleet in the results section of this chapter. Input card listings are found in Appendix IV for each vehicle model (QGERT network).

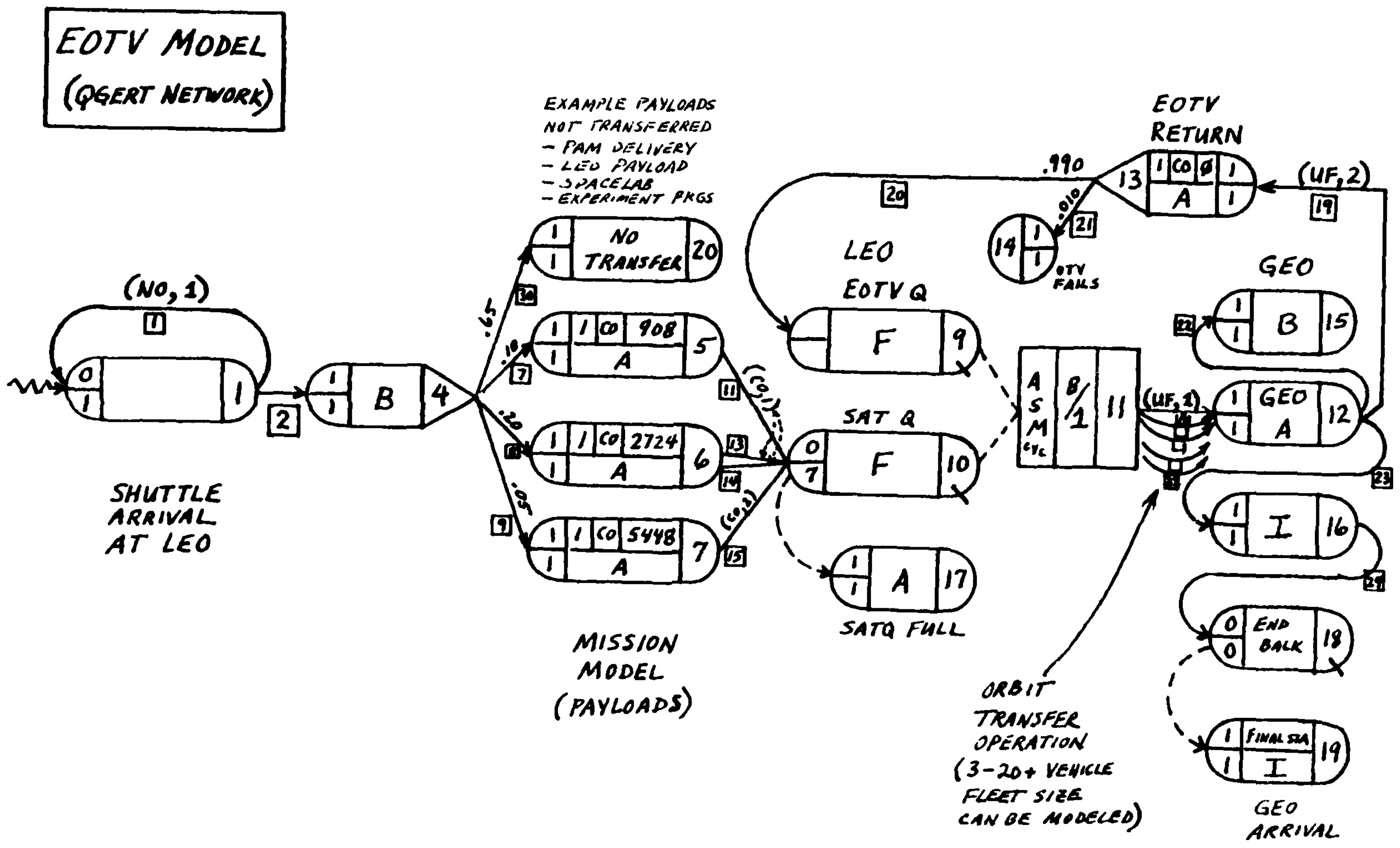

FIGURE 14. *EOTV MODEL — QGERT NETWORK*

RBPV Network

Characteristics of the RBPV have been determined primarily from a Boeing study (15) and from a Systems Engineering study (49), with some input from other references. A table of component masses and more detail as to this chemical OTV will be found in Appendix I. Generally, it is to be a reuseable derivative of the Centaur using upgraded RL-10 engines.

Important to this network is the determination that, without aerobraking, this RBPV must have 2 Shuttle missions dedicated to bringing up fuel each time a 2724 or 5448 payload is to be transported to GEO. Even the 908 Kg mission required an additional Shuttle flight with fuel, which is why the assumption is made that the RBPV would not even be used for such a mission. This is one inflexibility that has been accounted for when comparing against the other 3 vehicles.

Referring now to Figure 15, the network is similar to the EOTV in that the transfer and return portions are essentially the same. However, the payload module or mission model portion of the network must account for the extra Shuttle missions lost to refueling. This has been modeled by nodes 21 and 22. They represent Shuttle launches carrying a specialized refueling pallet with pumps, valving and tanks of LOX and LH. Mission specialist astronauts who are qualified for the touchy refueling mission must also be aboard. Both nodes 20 and 5 do not utilize the RBPV, so connecting activities from 5 and 20 back to node 1 only complete the required QGERT arrival scenario.

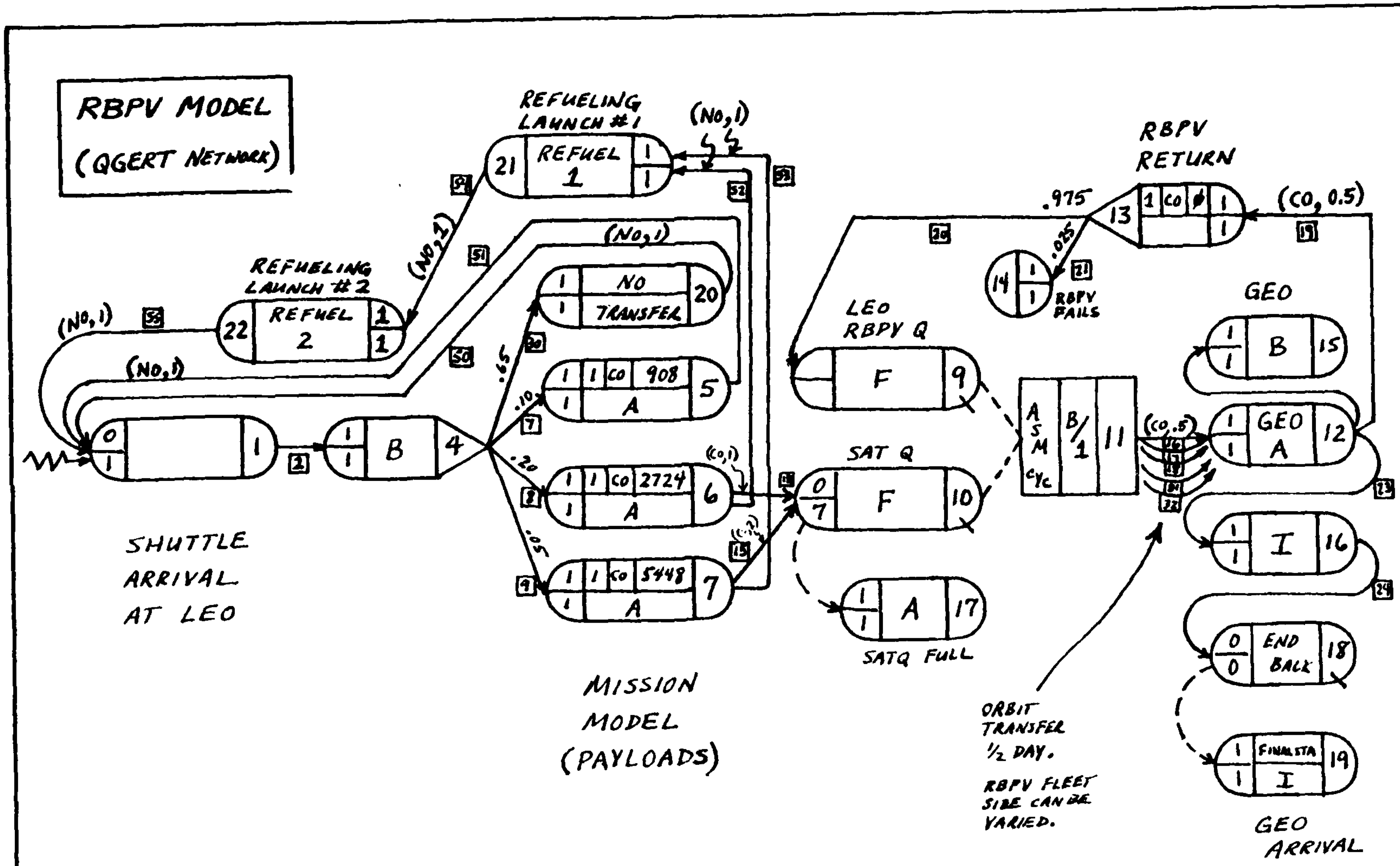

FIGURE 15. RBPV MODEL — QGERT NETWORK

IUS Network

In discussions with personnel in the IUS program, it seems clear that only one combination of payload and mated IUS may fly aboard a given Shuttle mission. Thus, as seen in Figure 16, the two payloads which can be handled by IUS, 908 and 2724 Kg., are taken just one at a time by a single mated IUS. Recall that the EOTV model permitted two 2724 Kg payloads aboard the node 6 mission. IUS is stretched at present to transfer 2724 Kg., or 6000+ lbs. But it is assumed that this category of satellite could be handled, even if not the full 2724 Kg. The 5448 mission is beyond the capability of the IUS as presently operated. A major network difference from the OTV may be noted. There is no return node since the IUS is expendable. The IUS reliability is assumed to be .965 and node 14 serves as a collection node for those which fail in the 20-year simulation. Characteristic of the high thrust chemical Hohmann transfer, the time to GEO is about 1/2 day and is not significant when compared to the large transfer times with EOTV. The remainder of the network is like the previous ones -- ie., primarily for statistics collection.

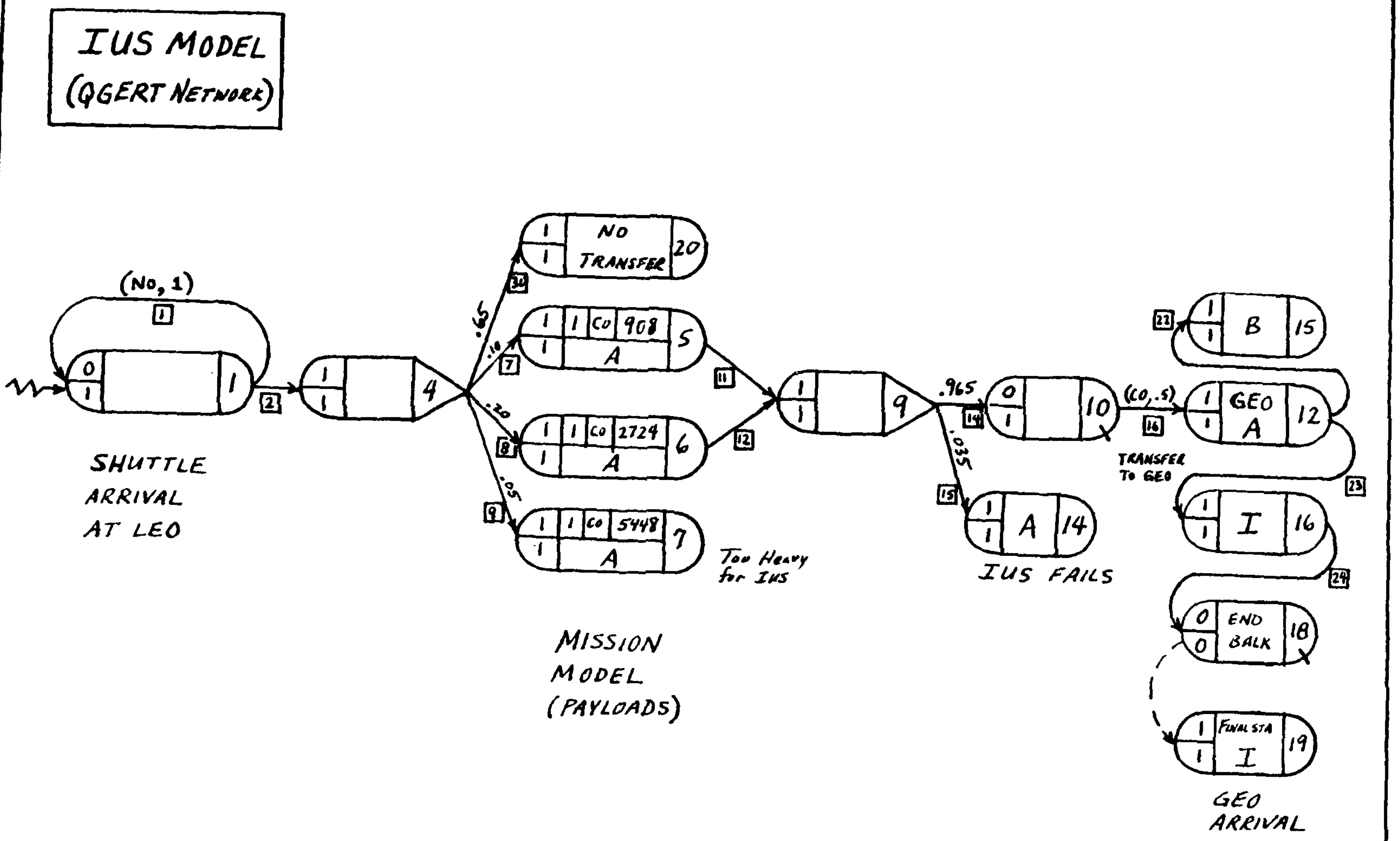

FIGURE 16. IUS MODEL — QGERT NETWORK

CENTAUR-G Network

The CENTAUR-G (CNTAR) network is quite similar to the IUS network in arrival rate, lack of return module, and a transfer time of .5 day. (See Figure 17.) The major difference is that the CNTAR would not likely be mated to as small a satellite as the 908 Kg. mission. Thus, it is assumed CNTAR'S large size is a point of inflexibility when rigidly keeping the same mission set for each of the flyoff vehicles. It is also stretching the current published CNTAR capability (11) of 10,000 lbs. to have it deliver 5448 Kg. to GEO. But it is assumed for these initial runs that the RL-10 engines and the vehicle will incorporate design upgrades by 1990. Reliability is modeled as .985.

Fly-Off Results Summary

Determining the optimal fleet size for the EOTV and RBPV was the first task in using the output from initial runs. Refer to Figure 18 and note that the fleet size for EOTV was varied from 3 to 20. As the number of parallel servers (EOTVs) approached 11, the average number of satellites waiting in LEO (in SATQ, node 10) for transfer dropped to .0278. The average waiting time in the queue dropped to 1.0039 days. As more servers (EOTVs) are added above 11, these values go to 0 and no satellites ever wait for transfer -- an EOTV is always ready in the OTVQ, node 9. Below 11 servers, the wait time and number waiting begins to rise exponentially. Thus, while 10 servers might be acceptable, the sensitivity is too great and the wait time climbs rapidly if one vehicle fails. Thus the optimum number of EOTVs for the [illegible] that empties the satellite queue was 11.

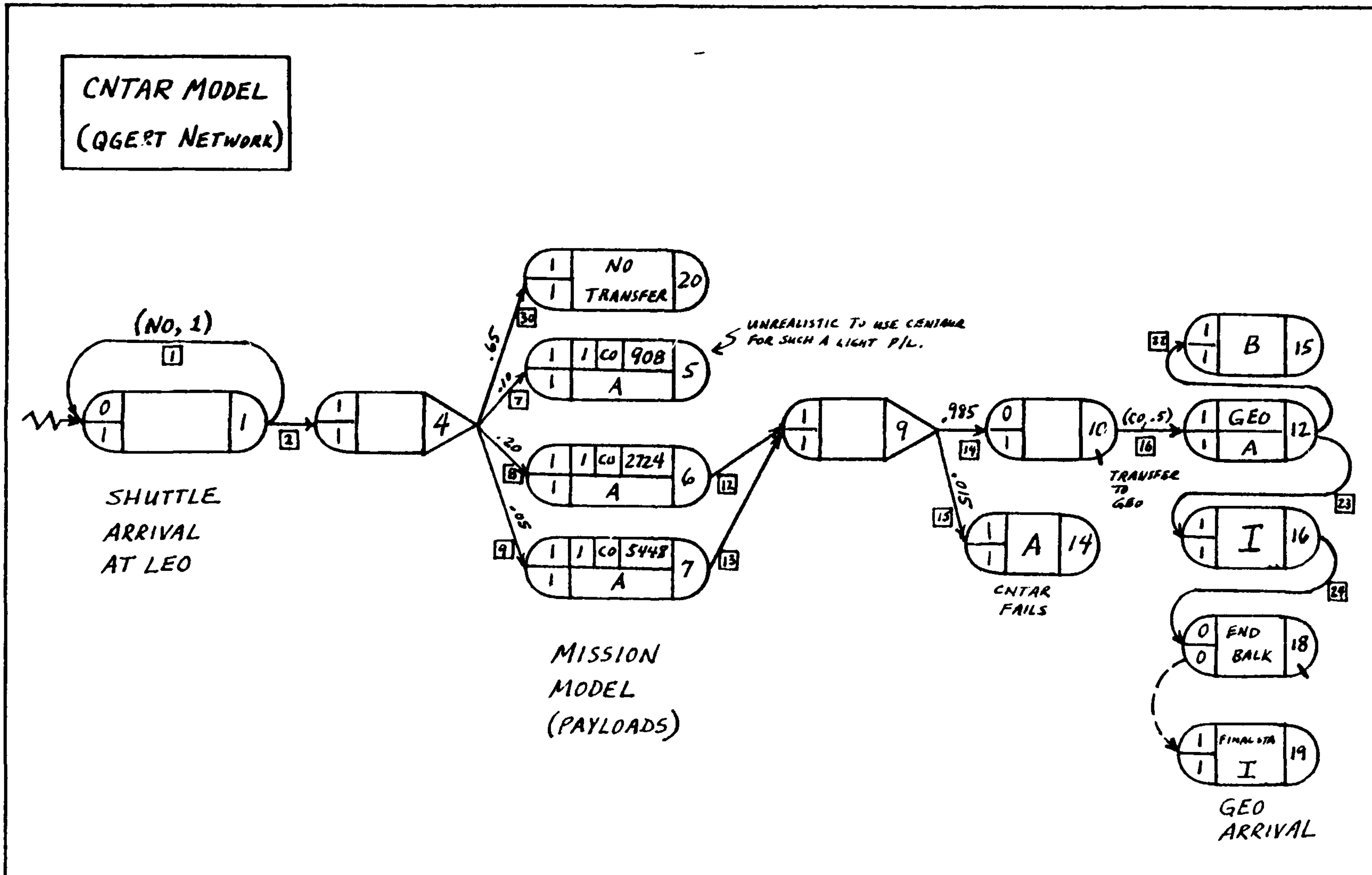

FIGURE 17. CENTAUR-G MODEL — QGERT NETWORK

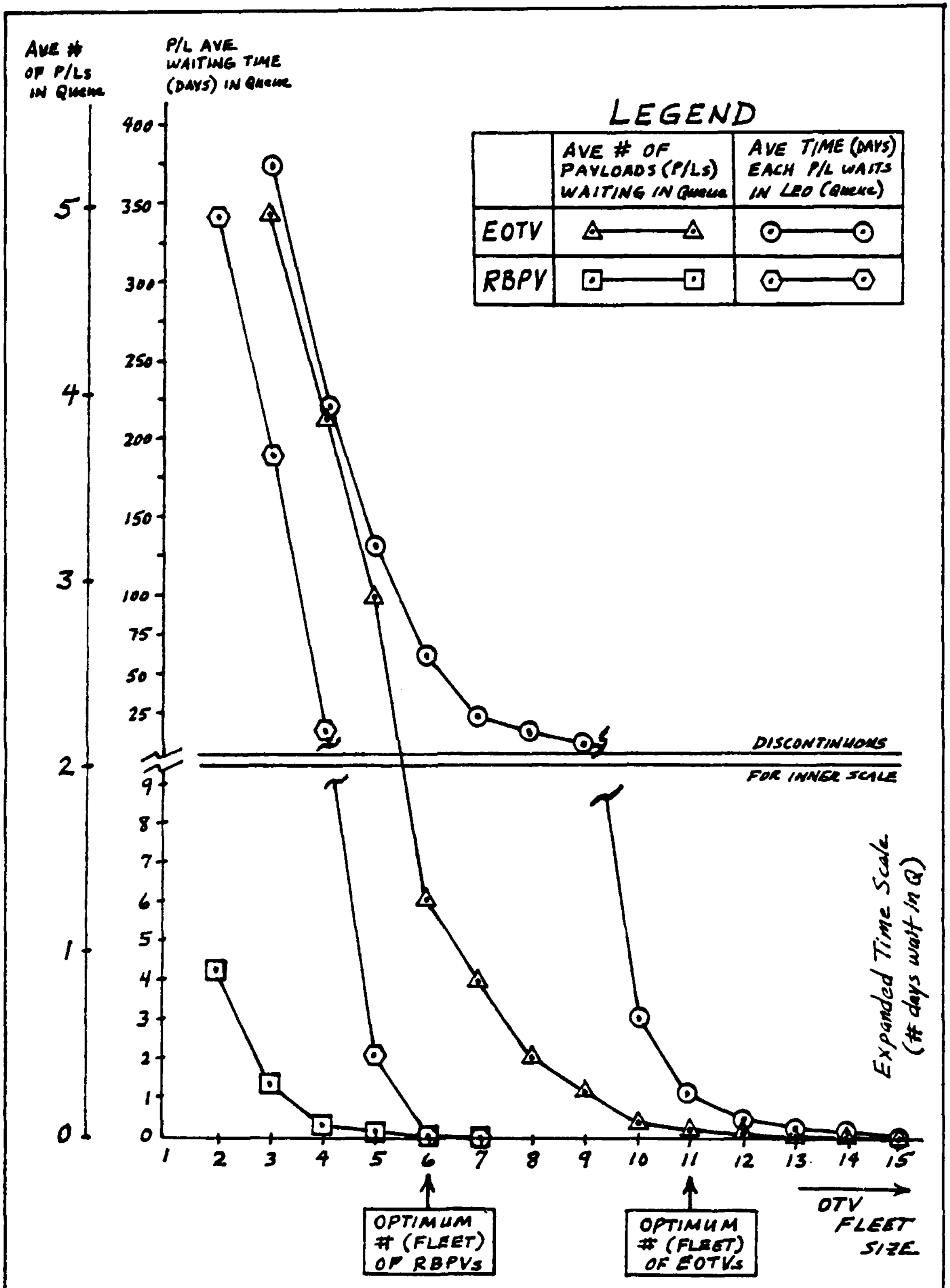

FIGURE 18. *OPTIMUM FLEET SIZE*

Again, referring to Figure 18, it is noted that the RBPV curve for average number of days wait in the queue for transfer is very steep. Thus, while 5 servers (RBPVs) would be acceptable, the sensitivity is too great. That is, if one RBPV fails, the queue builds very rapidly. In fact, since transfer time is not a factor for this chemical system, the reliability figure is the main driver in setting the number of RBPVs for the fleet. If replacement were part of the model, this optimum number of 6 could be reduced. Having determined the optimum fleet sizes of 11 and 6 for EOTV and RBPV, respectively, research question #6 has been answered and research objective #6 has been met.

Table 3 summarizes the results and output analysis of the initial set of runs. Approximately 40 runs were made to determine optimum fleet sizes. But after that determination is made, only one run for each of the 4 vehicles is needed. Each QGERT run simulates 20 years of operating the fleet and also repeats the 20 year simulation 50 times to average the effects of uncertainty and randomness. The number of repititions required had been determined for a previous study using similar models. It should be emphasized that the results were based on given initial input assumptions. These assumptions were explained previously in the vehicle network discussions. It should also be made clear that the results are somewhat sensitive to the input assumptions, particularly the payload mission model assumptions. For instance, if more satellites were assumed to require use of transfer vehicles, the total number of deliveries would go up and more EOTVs would be required, though perhaps not a commensurate increase in RBPVs. If a wider variety of satellites were modeled rather than using the "dual

FROM OUTPUTS OF QGERT RUNS

	IUS	CNTAR	EOTV	RBPV
TOTAL # OF SHUTTLE LAUNCHES IN 20 YEARS, (AVE/20YRS for 50 Reps)	360	360	360	360
AVE # OF LAUNCHES CARRYING P/L FOR TRANSFER	126	126	126	84 (Refueling Impact)
AVE # OF SATELLITES MADE AVAILABLE FOR XFER	126	126	198	108
AVE # OF SATELLITE-P/Ls DELIVERED TO GEO (WT. CATEGORIES AFFECT FINAL #s)	105	88	193	108
			Multiple Payloads possible w/ OTVs	
AVE TOTAL MASS (OF ALL P/Ls, KG) DELIVERED TO GEO IN 20 YRS	222,460 KG	288,744	511,204	326,880
AVE # OF EXTRA SHUTTLE OTV REFUELING LAUNCHES	—	—	Modular tanks carried w/ P/Ls & Replaced	120
INITIAL SHUTTLE LAUNCHES REQUIRED FOR FLEET EMPLACEMENT	—	—	11	6
MAXIMUM POTENTIAL SHUTTLE LAUNCHES SAVED IF EOTVs USED INSTEAD (20 YRS)	67	24	—	139
POTENTIAL SHUTTLE LAUNCHES SAVED / YEAR	3.35/YR	1.2/YR	—	11.58/YR Due mostly to required refueling launches for the RBPV.

TABLE 3. QGERT "FLYOFF" RESULTS SUMMARY

representation" or representative mass assumption, then, again, more EOTVs would be required and perhaps the fact that IUS, CNTAR, and RBPV cannot be used for the whole spectrum of masses would be less noticable. That is, the gap in satellites delivered by EOTV and the other vehicles would be narrowed.

Table 3 indicates that each vehicle had the same average number of Shuttle launches available to the model. A percentage of those launches carried payloads which required transport to GEO. The average requiring transport was 126. One exception is RBPV which had fewer payload-bearing missions due to the requirement for dedicated refueling missions. Recall from the RBPV discussion that a full fuel load could not be carried in one Shuttle flight for either the 2724 or the 5448 missions. These two separate Shuttle launches for refueling each RBPV transfer operation significantly reduces the number of satellites brought to LEO.

Next, note the number of satellites delivered to GEO by each vehicle in 20 years. This is an average number of satellites delivered, since it varies for any given 20-year simulation (based on the current random number stream). The reason fewer are delivered than are made available results from vehicle/payload incompatibilities and from vehicle failures. It can be seen, however, that both OTVs launch more satellites than seemingly are available. This is because node 6 represents one 2724 Kg load for the IUS and CENTAUR, as these must be launched together with the payload. But this payload bay space can used for another satellite or for 3 GPSs if reuseable OTVs are utilized. Thus, node 6 represents actually two times 2724 for both OTVs. Since it is more practical to launch a larger mass with the

RBPV, both 2724 payloads are assumed to be carried on one vehicle, eliminating the need for refueling two RBPVs. This must be accounted for by the user in the analysis since the model does not handle this necessary quirk in the RBPV formulation. Again, the largest difference in average number of satellites delivered stems from input assumptions that IUS, CNTAR, and RBPV have limitations as to the payload category which each can handle, either by design limitation, or by practicality limitation. Example of the latter is using CNTAR or RBPV for small payloads in the 908 range. Number of satellites / payloads does not give a complete picture of capability, since some payloads are much heavier. Therefore, the next entry in Table 3 is the total mass in KG of all payloads delivered in the 20-year period, averaged for 50 repititions of the simulation. Now, CNTAR outranks IUS as would be expected. But EOTV still has the lead.

Launches to refuel the RBPV definitely reduce the capability to deliver as many satellites to orbit. The EOTV requires typically 1000 Kg. of propellant or less. This is carried on the same flight as the payload in a modular tank assembly. The spent tank assembly is returned to earth for filling.

EOTV can be seen to offer potential reductions in Shuttle launches after accounting for the initial 11 launches to place the EOTV fleet in LEO. Also, it potentially can deliver more satellites to GEO in a 20-year period than the other vehicles. Research questions #4 and #6 have been answered, and objectives #4 and #5 have been met.

CHAPTER VI. Overall Results / Analysis

Assigning Life-Cycle Costs

The assignment of Life-Cycle Costs (LCCs) to each of the vehicles being compared is not an easy nor straight-forward task. It is made more difficult in that such information is well guarded by contractors. Often it is just as sensitive with NASA and DOD. Some of the telephone conversations on the subject can not be referenced. But, this is perhaps as it should be when considering the legal aspects of contracting and when considering the sensitivity of program survival to costs.

Good data was available in the literature, however, and forms the primary source for costing the models. Some studies normalized costs and performed sensitivity analyses to determine cost effective directions for technology development. But, the intent here is not to again seek optimums, but to attach a very rough estimate of LCCs and compare totals for each vehicle.

Table 4 contains the life-cycle cost summary for the four vehicles. IUS and CENTAUR cost figures were based on several telephone conversations (not referenced by request) and on several literature sources. Both RBPV and EOTV were based on information from a combination of several references. The EOTV used for cost estimating was the optimized EOTV modeled in the QGERT flyoff. The summary table is fairly self-explanatory. Vehicle costs were figured and/or amortized over 20 years such that the per-vehicle cost could be multiplied by the number of vehicles required during the flyoff. The

TABLE 4.

LIFE CYCLE COST SUMMARY (1983 Millions $)	IUS	CENTAUR	EOTV	RBPV
VEHICLE COST W/ AMORTIZATIONS	$83.0	$30.0	$41.21	$46.95
SHUTTLE PAYLOAD INTEGRATION COSTS	1.0	13.8	2.0	12.0
TOTAL COST PER VEHICLE LAUNCHED	84.0	43.8	43.21	58.95
FROM QGERT RESULTS:				
# VEHICLES REQUIRED	105	88	12	7
# SHUTTLE LAUNCHES TO PLACE FLEET	—	—	11	6
# SHUTTLE LAUNCHES TO LAUNCH PAYLOADS	105	88	126	84
TRIP TIME PENALTY	—	—	$370/20 YR	—
# SHUTTLE LAUNCHES FOR REFUELING (20 YRS)	—	—	INCL W/ P/L	120
PROPELLANT COSTS (20 yrs)	INCL.	INCL.	128.97	108.0
ADDITIONAL GND OPERATIONS COSTS (ABOVE CURRENT)	—	—	$5/YR	$3/YR
TOTAL, 20 YR LCC	$21,000.	$14,062.4	$17,009.5	$24,940.7
FROM QGERT RESULTS:				
KG of MASS DELIVERED TO GEO IN 20 YEARS	222,460	288,744	511,204	326,880
FIGURE OF MERIT FOR COMPARISON:				
$\boxed{\$M\ LCC/KG}$	$\boxed{\$.094399}$	$\boxed{\$.048702}$	$\boxed{\$.033273}$	$\boxed{\$.07630}$

number of Shuttle launches was determined by QGERT for each vehicle / mission set combination. Other operational costs were figured, particularly for the reuseable systems, and a total, 20-year LCC was determined. This LCC is divided by the total Kgs. of payload mass delivered to orbit in 20 years (from QGERT) to obtain a ratio of dollars per Kg delivered to GEO. This cost to benefit ratio is the basis for comparing each vehicle over the life cycle. Based on this analysis the ranking was: EOTV, CNTAR, RBPV, and IUS.

New Missions and Enhancements

New missions and enhancements have been suggested by the results of both the SUMT and QGERT analyses. Because this analysis shows a definite cabability to do orbit transfer, other missions involving more and less mass were examined with SUMT. Results appear in Tables 5 - 9.

The first mission investigated was the Large Space Structure (LSS) component transfer from LEO to GEO. Two masses were chosen approaching the limit of one Shuttle load. (Tables 5 and 6). The first LSS payload mass of 20,000 Kg. required an optimized EOTV with higher specific impulse than previous payloads, as expected. The transfer time out to GEO is nominal, 218 days, and the return is quite fast for EP, 48 days, since 24 thrusters are driving a light load. The second payload mass, 29,480 Kg., also continued the trend, requiring yet higher specific impulse. It had reasonable transfer times of 228 days out and 47.7 days back to LEO for a round trip of approximately 275.7 days.

For lighter missions, a roving intelligence gathering vehicle with

TABLE 5

LSS 2, 20,000 KG Payload, 24 Ring-Cusp XE Thrusters,
12 BIMODs

```
10150= * * * * * * * * * * * * * * * * * * * * * * * * * * * * * * * * *
* * * * * * * * * * * * * * * * * * 
10160=  FINAL VALUE OF F =    6.24838310E+03
10170=
10180=
10190=  FINAL X VALUES
10200=
10210=  X(  1) =   6.06485577E+03  X(  2) =   1.21072537E+02  X(  3) =
2.73374196E+03
10220=  X(  4) =   6.29577216E+00  X(  5) =   6.08900253E+02  X(
10230=
10240=  FINAL CONSTRAINT VALUES
10250=
10260=  G(  1) =   5.56485577E+03  G(  2) =   3.93514423E+03  G(  3) =
1.11072537E+02
10270=  G(  4) =   9.87892746E+03  G(  5) =   2.72374196E+03  G(  6) =
7.26625804E+03
10280=  G(  7) =   5.79577216E+00  G(  8) =   1.37042278E+01  G(  9) =
5.98900253E+02
10290=  G( 10) =   9.39109975E+03  G( 11) =   1.33033609E-07  G( 12) =
-4.57452325E-06
10300=  G( 13) =  -8.93935066E-07  G( 14) =  -5.78521576E-06  G(
10310=*EOR
```

TO GEO = 218.39 DAYS

RETURN = 48.64 DAYS

ROUND
TRIP   = 267.03 DAYS

TABLE 6

LSS 3, 29,480 KG Payload, 32 Ring-Cusp XE Thrusters, 16 BIMODs

```
10300= * * * * * * * * * * * * * * * * * * * * * * * * * * * * * * * *
* * * * * * * * * * * * * * * * * * 
10310=  FINAL VALUE OF F =   8.61602884E+03
10320=
10330=
10340=  FINAL X VALUES
10350=
10360=  X(   1) =    6.28088055E+03  X(   2) =    1.25437291E+02  X(   3) =
3.80555340E+03
10370=  X(   4) =    6.52273911E+00  X(   5) =    7.96482131E+02  X(
10380=
10390=  FINAL CONSTRAINT VALUES
10400=
10410=  G(   1) =    5.78088055E+03  G(   2) =    3.71911945E+03  G(   3) =
1.15437291E+02
10420=  G(   4) =    9.87456271E+03  G(   5) =    3.79555340E+03  G(   6) =
6.19444660E+03
10430=  G(   7) =    6.02273911E+00  G(   8) =    1.34772609E+01  G(   9) =
7.86482131E+02
10440=  G(  10) =    9.20351787E+03  G(  11) =    1.68802217E-09  G(  12) =
1.71096417E-07
10450=  G(  13) =   -3.55357770E-08  G(  14) =   -2.93657649E-07  G(
10460=*EOR
```

TO GEO = 228.01 DAYS

RETURN = 47.72 DAYS

ROUND
TRIP = 275.73 DAYS

TABLE 7

Rover Vehicle, 8 Ring-Cusp XE Thrusters,
Interchangeable Sensors, 500 KG

```
9220= × × × × × × × × × × × × × × × × × × × × × × × × × × × × × × × × ×
× × × × × × × × × × × × × × × × × ×
9230=  FINAL VALUE OF F =   1.37461359E+03
9240=
9250=
9260=  FINAL X VALUES
9270=
9280=  X(  1) =   3.95768990E+03  X(  2) =   7.84975642E+01  X(  3) =
4.01332023E+02
9290=  X(  4) =   4.08187334E+00  X(  5) =   3.45301052E+02  X(
9300=
9310=  FINAL CONSTRAINT VALUES
9320=
9330=  G(  1) =   3.45768990E+03  G(  2) =   6.04231010E+03  G(  3) =
6.84975642E+01
9340=  G(  4) =   9.92150244E+03  G(  5) =   3.91332023E+02  G(  6) =
9.59866798E+03
9350=  G(  7) =   3.58187334E+00  G(  8) =   1.59131267E+01  G(  9) =
3.35301052E+02
9360=  G( 10) =   9.65469895E+03  G( 11) =  -2.61934474E-10  G( 12) =
-4.79021764E-08
9370=  G( 13) =  -6.05959940E-08  G( 14) =  -8.06412572E-08  G(
9380=×EOR
```

TO GEO = 96.14 DAYS

RETURN = 82.72 DAYS

ROUND
TRIP   = 178.86 DAYS

TABLE 7

Rover Vehicle, 8 Ring-Cusp XE Thrusters,
Interchangeable Sensors, 500 KG

```
9220= * * * * * * * * * * * * * * * * * * * * * * * * * * * * * * * *
* * * * * * * * * * * * * * * * * * *
9230=  FINAL VALUE OF F =   1.37461359E+03
9240=
9250=
9260=  FINAL X VALUES
9270=
9280=  X(  1) =   3.95768990E+03  X(  2) =   7.84975642E+01  X(  3) =
4.01332023E+02
9290=  X(  4) =   4.08187334E+00  X(  5) =   3.45301052E+02  X(
9300=
9310=  FINAL CONSTRAINT VALUES
9320=
9330=  G(  1) =   3.45768990E+03  G(  2) =   6.04231010E+03  G(  3) =
6.84975642E+01
9340=  G(  4) =   9.92150244E+03  G(  5) =   3.91332023E+02  G(  6) =
9.59866798E+03
9350=  G(  7) =   3.58187334E+00  G(  8) =   1.57181267E+01  G(  9) =
3.35301052E+02
9360=  G( 10) =   9.65469895E+03  G( 11) =  -2.61934474E-10  G( 12) =
-4.79021764E-08
9370=  G( 13) =  -6.05959940E-08  G( 14) =  -8.06412572E-08  G(
9380=*EOR
```

TO GEO = 96.14 DAYS

RETURN = 82.72 DAYS

ROUND
TRIP   = 178.86 DAYS

AD-A141 173 ANALYSIS OF ELECTRIC PROPULSION ORBIT TRANSFER VEHICLES 2/2
VS IUS CENTAUR-G A..(U) AIR FORCE INST OF TECH
WRIGHT-PATTERSON AFB OH SCHOOL OF ENGI.. L W MADDOX
UNCLASSIFIED DEC 83 AFIT/GSO/OS/83D-5 F/G 20/3 NL

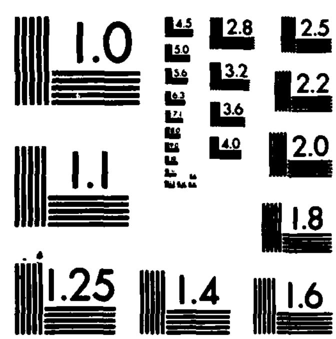

MICROCOPY RESOLUTION TEST CHART
NATIONAL BUREAU OF STANDARDS-1963-A

TABLE 8

Repair/Refurbish Vehicle, 8 Ring-Cusp XE Thrusters,
Interchangeable Repair Modules, 1000 KG

```
9550= * * * * * * * * * * * * * * * * * * * * * * * * * * * * * * * * *
* * * * * * * * * * * * * * * * * * 
9560=  FINAL VALUE OF F =   1.53783936E+03
9570=
9580=
9590=  FINAL X VALUES
9600=
9610=  X(  1) =    4.46852564E+03  X(  2) =    8.88189255E+01  X(  3) =
4.41148314E+02
9620=  X(  4) =    4.61858412E+00  X(  5) =    3.86139645E+02  X(
9630=
9640=  FINAL CONSTRAINT VALUES
9650=
9660=  G(  1) =    3.96852564E+03  G(  2) =    5.53147436E+03  G(  3) =
7.88189255E+01
9670=  G(  4) =    9.91118107E+03  G(  5) =    4.31148314E+02  G(  6) =
9.55885169E+03
9680=  G(  7) =    4.11858412E+00  G(  8) =    1.53814159E+01  G(  9) =
3.76139645E+02
9690=  G( 10) =    9.61386035E+03  G( 11) =    4.33647074E-09  G( 12) =
6.66668711E-08
9700=  G( 13) =   -1.62508513E-08  G( 14) =   -2.47455318E-08  G(
9710=*EOR
```

TO GEO = 105.69 DAYS

RETURN = 92.51 DAYS

ROUND
TRIP   = 198.21 DAYS

TABLE 9

Free Rover, 500 KG Payload, 8 Ring-Cusp XE Thrusters,
Interchangeable Sensors/Modules,
1600 KG Extra Propellant

```
9130= * * * * * * * * * * * * * * * * * * * * * * * * * * * * * * * *
* * * * * * * * * * * * * * * * * * *
9140=  FINAL VALUE OF F =   1.61174152E+03
9150=
9160=
9170=  FINAL X VALUES
9180=
9190=  X(  1) =   4.65776684E+03  X(  2) =   9.26425162E+01  X(  3) =
5.65150266E+02
9200=  X(  4) =   4.81741084E+00  X(  5) =   3.05451120E+02  X(
9210=
9220=  FINAL CONSTRAINT VALUES
9230=
9240=  G(  1) =   4.15776684E+03  G(  2) =   5.34223316E+03  G(  3) =
8.26425162E+01
9250=  G(  4) =   9.90735748E+03  G(  5) =   5.55150266E+02  G(  6) =
9.43484973E+03
9260=  G(  7) =   4.31741084E+00  G(  8) =   1.51825892E+01  G(  9) =
2.95451120E+02
9270=  G( 10) =   9.69454888E+03  G( 11) =   2.03726813E-08  G( 12) =
3.20460458E-09
9280=  G( 13) =  -2.83522240E-07  G( 14) =  -6.70475856E-07  G(
9290=*EOR
```

TO GEO = 135.41 DAYS

RETURN = 73.19 DAYS

ROUND
TRIP = 208.60 DAYS

interchangeable sensors was investigated. It is seen from Table 7 that this vehicle would be able to travel to GEO in 96 days and return in 83 days, although most missions would probably involve closer orbits. The next mission investigated (Table 8) was the repair / visit / refurbish mission. Again, the lighter payload allowed more propellant to be carried and the vehicle accomplished transits between orbits faster than when used for deploying satellites. The last mission considered (See Table 9) involved carrying extra fuel for several LEO - GEO - Return trips. Thus, it would be more autonomous and posess multi-mission capability. The first leg, carrying the most propellant mass, still only required 135 days transfer time.

It was not necessary to use QGERT for these missions since the IUS and CENTAUR were not competitors. The RBPV has such a large fuel requirement that it also does not appear to be a contender in its present parametric form.

Overview Analysis

It appears that although the EOTV can offer potentially fewer $/Kg for delivering payloads to orbit, the transfer time and Van Allen exposure for the payload owners may still be unacceptable in some cases. An all-EOTV fleet might not be wise. The EOTV is a strong contender for LSS and free rover type missions, since chemical vehicles use enormous amounts of fuel in the former case and have a greatly reduced payload fraction in the latter case. For those payloads compatible with EOTV transfer times, dollar benefits are to be had. Mixed fleets were not specifically addressed by the methodology, but

could be modeled by combining vehicles and missions in one QGERT network. From the results of both SUMT and QGERT analyses, and considering the low cost of PAM-D, the best mix of upper stages / OTVs / rovers appears to be:

1. PAM-D for spinable satellites.
2. CENTAUR-G for heavier rapid transfer payloads.
3. EOTV for all other payloads, using several for rovers -- intelligence, sensing, refurbishment, repair.

CHAPTER VII. Summary / Conclusions / Recommendations

Summary

The need which gave rise to this thesis is the need to enhance or make better use of the Space Transportation System with a reuseable upper stage or orbit transfer vehicle. In examining the mass of fuel required to operate a chemical OTV, it quickly becomes apparent that higher specific impulses are a necessity. Liquid bi-propellant engines have pushed the theoretical limits of specific impulse as exemplified by the Space Shuttle Main Engines. But, the specific impulse needed for practical reuseability in near-earth space should be well above that which is possible with chemical combustion and expansion.

After a personal visit to NASA-Lewis Research Center in summer, 1983, it was clear that a great many refinements have taken place in electric propulsion technology -- especially electron-bombardment ion thrusters. These thrusters have a specific impulse normally in the 2000 to 4000 sec range which allows mission accomplishment with greatly reduced propellant mass over that required for chemical propulsion systems. The supporting propulsion module with avionics, thermal control, propellant tanks and power processing has been developed to an advanced state, as well as the electric thrusters. This system, developed by NASA, is envisioned to be modular with two to ten or more thrusters as needed to cover a wide range of thrust requirements. Given these advantages, it seemed a good candidate for Shuttle enhancements, whether as an upper stage or as a repair/ refurbish/ retrieval vehicle. But, several issues needed to be addressed: Which

of several thruster technologies would be best for certain missions? What size power supply would be required? How much propellant would be required? Numerous studies had addressed these issues in one fashion or another, but none had performed an optimization of actual thrusters / prototype technologies followed by a comparison "fly-off" against baseline chemical systems.

The decision-maker investigating Shuttle enhancements and increased near-earth capability would probably like to find the optimal electric system for a required mission or mission set and "fly" it against the current upper stages, IUS and CENTAUR-G, for comparison of performance and cost. Also desirable would be a comparison with a projected reuseable chemical system.

Providing the decision-maker with this type of information has been the subject of this thesis. The approach has been to first develop a method for parametrically characterizing existing prototype thrusters and an existing prototype solar array power supply. It was desired to characterize existing, experimental thrusters rather than ideal, mathematical projections in order to provide the decision-mader with more realistic, conservative data. This was done by linearizing relationships of input power to the thruster vs ISP and vs thrust as obtained from measured data from NASA-Lewis Research Center and Hughes Research Laboratories. A very key point in this thesis is that these relationships then included and accounted for all thruster losses and efficiencies! The rest of the propulsion subsystem has been patterned closely after the NASA BIMOD configuration. The primary parameters then input to an optimization program (SUMT) were: power supply specific power; thruster input power vs ISP relationship for the given

thruster technology; and vehicle mass. Relationships from the rocket equation were also incorporated to specify propellant mass used for the mission. The mission / payload was characterized by two parameters, Δv, or velocity change required for the orbit transfer, and payload mass.

The specific thrusters chosen for the optimizations were the baseline NASA-Hughes 30-cm J-Series Hg thruster, the 30-cm with Argon propellant, the 30-cm with 3-grid ion optics, the extended performance 30-cm with simplified PPU, and finally the Ring-Cusp 3-Grid 30-cm configuration using Xenon propellant. This was felt to offer a good spectrum of thruster technologies. (Follow-on users may select additional ones). The specific power supply was the NASA-Lockheed experimental solar array with a total system specific power of .052 KW/KG. The mission set chosen for the optimization was the NavStar GPS with 1-6 satellites transported at a time. Carrying six satellites simultaneously would mean deploying 1/3 of the GPS constellation to an orbit plane and using either the OTV or the satellite RCS to achieve the desired position in the orbit plane.

The optimization program found the minimum mass to accomplish the given set of missions for each thruster technology. Minimizing mass impacted vehicle cost, launch costs, payload capability, and transfer time. In the program, mission performance was a constraint that the vehicle had to meet -- it had to provide the necessary Δv. Since the EOTVs were optimized for specific payloads, several runs had to be made. But, a key point in the analysis is that the masses in the mission model could correspond not only to GPS satellites, but could represent other categories of payloads as well. This dual

representation reduced the number of computer runs and allowed the analysis to indicate EOTV performance over a wide spectrum of potential payloads. Once outputs from the 35 runs were obtained, transfer times had to be calculated. Then, with both optimized mass and transfer time as criteria, the vehicle offering the best combination was picked. Out of the thruster technologies analyzed for this thesis, the clear winner (most optimum) was the Ring-Cusp 3-Grid Ion thruster operating on Xenon propellant.

The "fly-off" simulated operation of this optimized EOTV for a 20 year (user selected) period. Also simulated were the IUS, CENTAUR-G, and a Reuseable Bi-Propellant vehicle based on CENTAUR technologies with the RL-10 engine. Long-term (20-year) operation and performance was then examined without having to build and launch the system. The outputs of the QGERT "fly-off" simulation were examined and analyzed for these results: the total number of satellites launched over the 20-year period; the potential number of Shuttle launches saved; the total mass (KG) of payload placed in final orbit; and the number of refueling missions required for the RBPV.

Using these results from the fly-off, the assignment of rough Life-Cycle Costs (LCCs) for each orbit transfer vehicle system was made. These costs represented R.D.T.& E. not yet accomplished, acquisition / production costs, and operation costs. Given the coarse assumptions made for this part of the analysis, the results of LCC analysis were as follows. The CENTAUR-G upper stage had the lowest LCC followed by, in order: EOTV; RBPV; and IUS. A more applicable figure of merit, however, was the ratio of dollars, LCC, per KG of payload mass delivered to final orbit. This could be regarded as a

cost to benefit ratio. For this figure of merit, $LCC/KG payload delivered, the ranking was: EOTV; CENTAUR; RBPV; and IUS. CENTAUR and EOTV had exchanged first place ranking because EOTV is more flexible in delivering a wider range of payload mass.

This example of the methodology should be regarded as an initial analysis comparing each of the existing and proposed vehicles. The methodology is flexible enough that different mission models and accompanying assumptions may be incorporated by follow-on users. Other electric propulsion technologies may be examined, with this initial analysis as a baseline. Other orbit transfer vehicles may be compared. Thus, besides the initial results obtained showing the viability of EOTVs, the methodology and algorithms developed should prove useful to other users, planners, and decision-makers.

Conclusions

The results have been presented in some detail in the Summary, and it should be helpful to the reader to now relate these results to the original research questions and objectives which were delineated in Chapter 3 of the thesis.

The first research question posed in the thesis was, "Which electric thruster technology among several lab prototypes would optimize an OTV in terms of reduced propellant mass and reduced power supply mass for a given mission?" Objective #1, choosing thruster technologies and optimizing them, as well as objectives #2 and #3, were accomplished using SUMT formulations. Using SUMT results, the answer

to the first research question was the Ring-Cusp 3-Grid Xenon thruster. Round trip transfer times were calculated for each thruster and mission combination. Questions #2 and #3 dealt with transfer times and with determinimg a single best thruster technology for all missions. These were answered as well. Since it clearly outperformed all others in this initial study, the Ring-Cusp thruster was consistently the optimum choice.

The next three questions and objectives were answered and fulfilled when the QGERT models were developed and run to simulate a 20-year "flyoff." A definite reduction in Shuttle launch rate was possible when using resueable EOTVs, and mitigated for the chemical OTV due to extra fuel launches. The optimal fleet size determined for the EOTV fleet operating without IUS or CENTAUR was 11. The optimal chemical RBPV fleet size was 6. The rough estimates of LCCs revealed that the vehicles ranked best in this order for $/KG delivered to GEO: EOTV, CENTAUR-G, RBPV, and IUS.

The last research question and objective, dealing with new mission possibilities, both were accomplished as other potential missions were examined. The SUMT optimization was the applicable part of the methodology. This was because QGERT comparison runs were only needed when competition existed between the chemical propulsion vehicles and the EOTV. EOTV payload ratios were clearly superior for the following cases. Two missions delivering LSS components to GEO were input for EOTV optimization. Also, a free-flying rover for intelligence gathering, remote sensing, and satellite repair / refurbishment was optimized. The results fell within the feasible region and show that the EOTV, when not being used for deployment of satellites, could be

used for carrying sensor packages over "hot-spots", replenishing modular satellites or any of a number of such missions. The EOTV has been shown to be able to carry the propellant and payload for repeated trips at the velocity changes required by these missions.

For an EOTV, the acceptability of the long transfer times and radiation exposure in the Van Allen belts must still be assessed by the payload owner. Though this preliminary study indicates cost effectiveness for an all-EOTV fleet, a mixed fleet of CENTAURs and EOTVs might be more effective, given that perhaps a significant fraction of satellites could not linger in the Van-Allen belts. It should be noted, though, that a shielded capsule for the payload might alleviate some of the radiation and would be feasible given the results of this analysis. It was shown that EOTVs are less sensitive to increases in payload mass than are chemical propulsion vehicles. In a mixed fleet, the EOTVs could be used for numerous missions when not being used for deployment. As mentioned above, orbiting sensor packages over "hot-spots" and return, repair and return, and retrieval are capabilities not possible with expendable stages. Such vehicles would definitely enhance our present capabilities in near-earth space as well as create new capabilities for NASA, private industry, and DOD operations.

Recommendations

Given the results of the extensive analyses and given the breadth of the literature reviewed for this thesis, three sets of recommendations have arisen. The first set has come from seeing the potential uses of electric primary propulsion for expanding U.S. capability in near-earth space. The second set has arisen from noting areas of the methodology that can be improved with follow-on work. The third recommends how actual implementation of an EOTV capability should begin.

With this introduction, the following three sets of recommendations are made as a result of the studies performed in this thesis:

1. A phased approach should be adopted to bring electric primary propulsion vehicles into general usage.

Phase I -- Develop and launch an on-orbit prototype 8-thruster BIMOD unit with the following specific missions:

(1) Demonstrate concept, test vehicle.

(2) Use as roving sensor platform for DOD. Also use to inspect malfunctioning satellites.

(3) Measure actual Van-Allen radiation dosage during several trips to GEO and back.

Phase II -- Place two more vehicles in orbit which have appropriate improvements incorporated. Primary missions should involve intelligence and sensing.

Phase III -- Place a small fleet of vehicles in LEO to complement the current upper stages in use. Specific missions should include:

(1) Deployment of hardened DOD satellites, including on-orbit spares above GEO.

(2) Deployment of satellite constellations using one EOTV.

(3) Exchange DOD satellites with spares on an irregular basis to extend satellite lifetime and to thwart unfriendly ASAT planning and preplanning.

(4) Demonstrate feasibility of disposing of nuclear waste capsules on a sun intercept.

(5) Retrieve satellites for inspection or refurbishment.

(6) Visit NASA multi-mission modular satellites for module replacement or exchange.

(7) Retrieve spent stages for possible refurbishment (CENTAUR) or avionics retrieval (IUS). Retrieve dangerous space debris.

2. These follow-on studies are recommended and may be regarded as potential thesis topics:

a. A more complete cost study using the QGERT results.

b. Develop an optimization scheme for Beginning-of-Life (BOL) vs End-of-Life (EOL) sizing of solar arrays.

c. Take the entire methodology and incorporate it into a single executive computer program, thus eliminating hand calculations and the many separate runs. Develop into a management information system.

d. Develop a more sophisticated QGERT model with more flexibility for handling differing mission models -- ie., more modular such that mission changes do not cause

major changes to the model network.

e. Continue working with SUMT to simultaneously minimize mass and transfer time based on a user's weighting of the importance of each.

3. Given the potential benefits to each, both NASA and DOD should jointly fund the first phase suggested above.

This third suggestion is made with the knowledge that any new system is going to be expensive, especially if it is a viable space system. However, building a prototype demonstrator and launching it should be very cost-effective. If program funding for Phase 2 or Phase 3 is slipped or delayed, the prototype vehicle could still be used as a platform for testing other concepts in addition to its Phase I missions. Additional missions might include demonstrating modular repair of satellites, retrieval of spent satellites or space debris, or, in fact, any of the missions suggested for the other two phases.

These recommendations are made with the knowledge that electric propulsion is serving very well at this writing on the Navy NOVA satellite program. Pulsed electric thrusters are providing secondary propulsion for stationkeeping / drag make-up for this highly accurate navigation satellite system (56). These micropound Pulsed Plasma Thrusters, though not envisioned for use in primary orbit transfer propulsion, are providing greatly improved accuracy for the NOVA and the Ballistic Missle Submarine Fleet it serves. An improvement in in-track position error from 70 meters in a 0.8 day period to less than 70 meters in a 6 day period has been achieved, meaning more autonomy

and less ephemeris updating (56).

The results of this thesis show that besides potential economic advantages to employing an EOTV fleet, the increased operational capabilities suggested by this system would be the greater payoff. Instead of a "push-the-button-and-watch-it-go" mode of operation, the U.S. could move toward more flexible and responsive modes of operation in near-earth space. Return and retrieve features, high payload ratios, and large velocity change increments of EOTVs would certainly enhance the present capabilities of the Space Transportation System.

APPENDIX I. Proposed Vehicle Configurations / Thruster Data

The following drawings, tables, and figures are from the references in parantheses on each. A few show calculations by this author. Figures 19 - 23 show vehicle configurations for all but IUS. Tables 10 and 11 show masses for the EOTV propulsion subsystem. Figures 24 and 25 and Tables 12 - 16 show the thruster data provided by NASA-Lewis and the resulting linearized relationships. The ring-Cusp data was already presented in Chapter 4.

The vehicle configuration for the Centaur-G, as shown in Figure 19 from (11), provides an idea of its dimensions, masses, and a few subsystems. The IUS is not included because it is operational and its configuration generally known. Figure 20 shows the Boeing Space-Based OTV (15). While their study included a ballute for aerobraking, note that this mass is deleted for the present configuration. Upper atmospheric heating and drag are not yet well modeled and nearer term technology is assumed. Eventually, aerobraking technology must be developed though, if manned operations are to be realized for OTVs. The masses shown were used as a rough estimate for the RBPV and as a basis for fuel requirements

Figure 21 shows the [illegible] layout of the 30-cm Kaufman electron-bombardment thrust[illegible] diagram of the Ring-Cusp thruster. The iron filing map shows the magnetic field line enhancements. Figure 22 shows the BIMOD unit with two 30-cm thrusters. This was assumed to be the basic thrust subunit for the EOTV. The vehicle structure above the BIMOD and Interface module would contain solar array steering,

avionics, housekeeping, and payload interface mechanisms. Details of the thruster subunit are found in the Design Manual (12). Tables 11 and 12 contain the mass breakdowns which were used as a baseline for eacn of the five thrusters analyzed with SUMT. Figure 23 shows the modularity of the BIMOD engine system and the Interface module. Both the EOTV and the RBPV have been represented parametrically for the analysis, and these configurations are primarily used for overall mass estimates, not as final designs for a proposed vehicle.

Tables 12 - 16 and Figures 24 and 25 contain remaining data for the four thrusters besides the Ring-Cusp. The Tables of data from NASA-Lewis tests precede the linearization calculations in each case.

Centaur G weight summary.

Item	Centaur G Weight (lb)
Total Centaur cargo element weight	54,431
Total airborne support equipment	7,462
Spacecraft airborne support equipment	0
Centaur airborne support equipment	7,462
Total vehicle weight	46,969
Spacecraft gross weight*	10,288
Centaur tanked weight	36,681
Centaur jettison weight	6,720
Centaur dry weight	6,163
Centaur residuals	557
Centaur expendables	29,961
Propellants (LH_2 & LO_2)	29,707
Engine burns	29,105
Start, shutdown & vent	602
Hydrazine	250
Helium	4

*Spacecraft system weight-capability

2089-2C

FIGURE 19.

CENTAUR-G

SPECIFICATIONS AND DRAWINGS FROM REFERENCE (1).

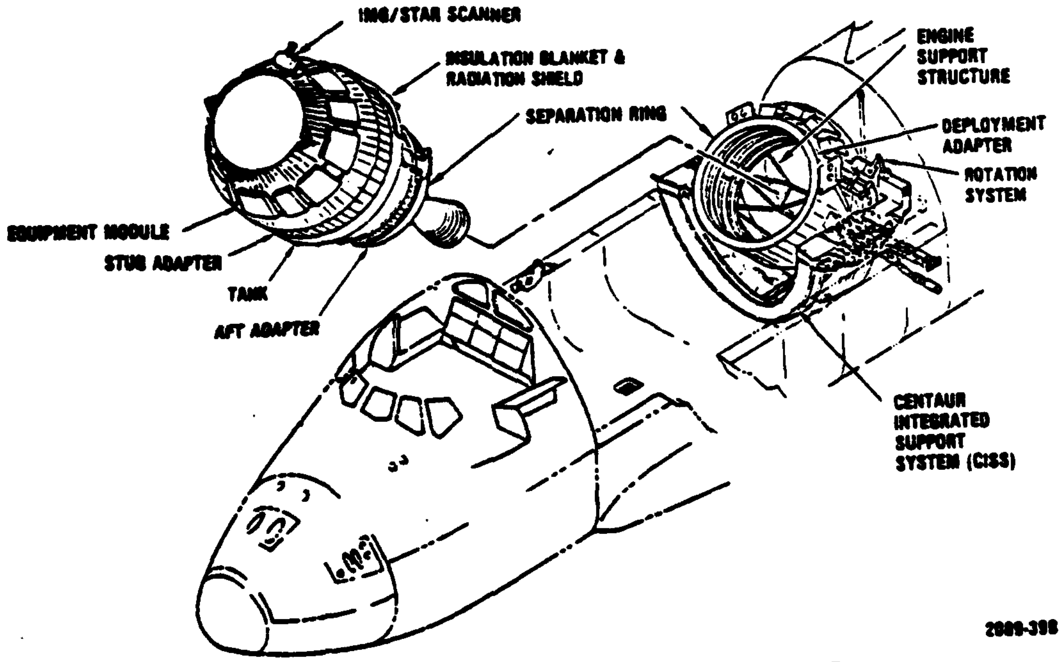

Shuttle/Centaur System for Centaur G.

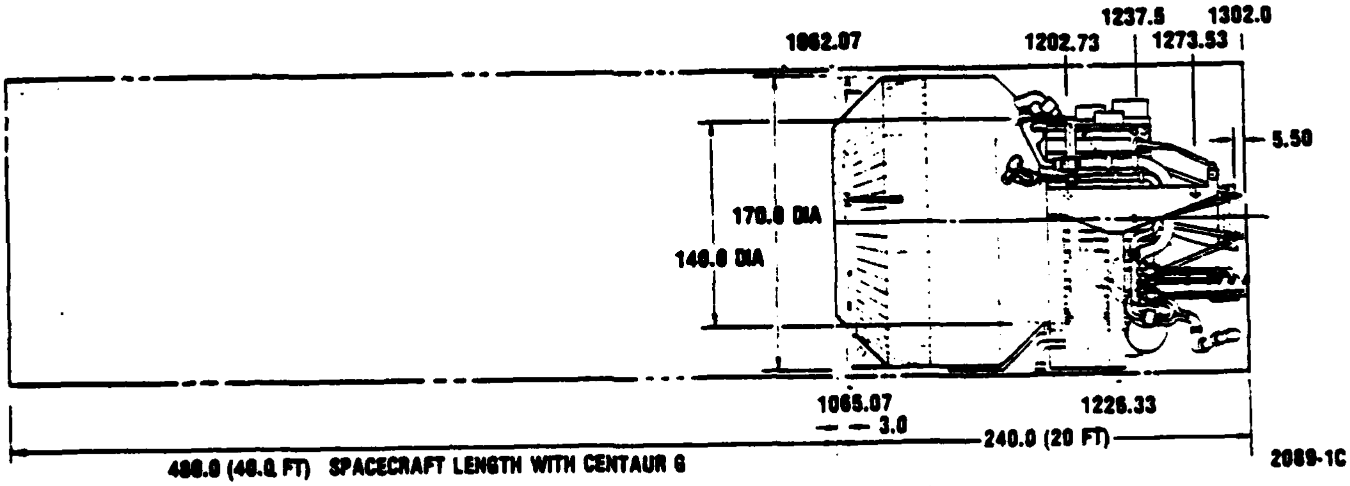

Centaur G and spacecraft length capability.

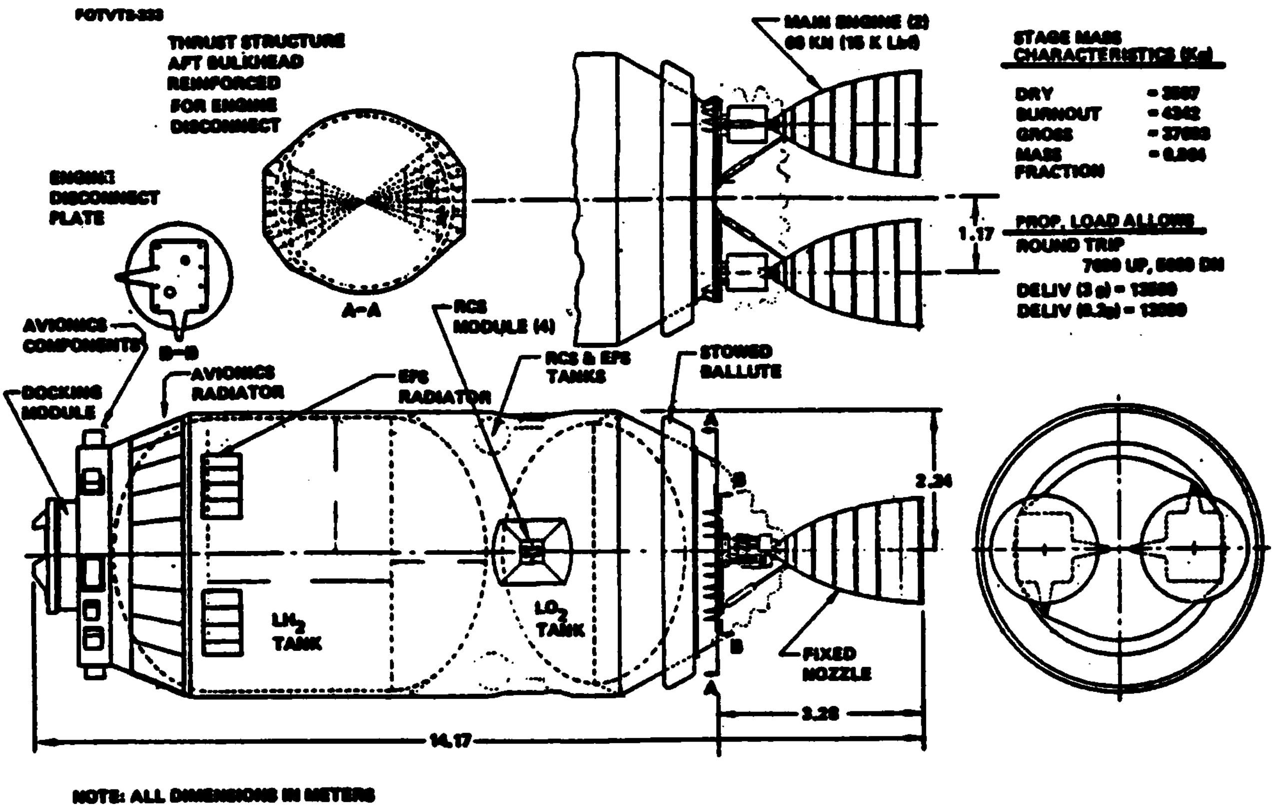

Space-Based OTV Configuration

SB OTV Design Reference Mission Summary Mass Statement

ITEM	MASS (kg)
STRUCTURE	1447
THERMAL CONTROL	124
AVIONICS	292
ELECTRICAL POWER SYSTEM (EPS)	234
MAIN PROPULSION SYSTEM (MPS)	691
ATTITUDE CONTROL SYSTEM (ACS)	125
SPACE MAINTENANCE PROVISIONS	216
WEIGHT GROWTH MARGIN	468
(DRY WEIGHT - LESS BALLUTE)	(3597)
RESIDUALS	413
RESERVES	332
(BURNOUT WEIGHT)	(4342)
BALLUTE	308
INFLIGHT LOSSES	382
FUEL CELL REACTANT	46
ATTITUDE CONTROL PROPELLANT	326
MAIN IMPULSE PROPELLANT	32,289
(OTV GROSS WEIGHT)	(37,693)
PAYLOAD	7687
(OTV + P/L WEIGHT	(45,380)
OTV MASS FRACTION	0.8638

FIGURE 20.

RBPV INPUTS - FROM BOEING STUDY (15)

Note: Ballute was excluded from proposed RBPV.

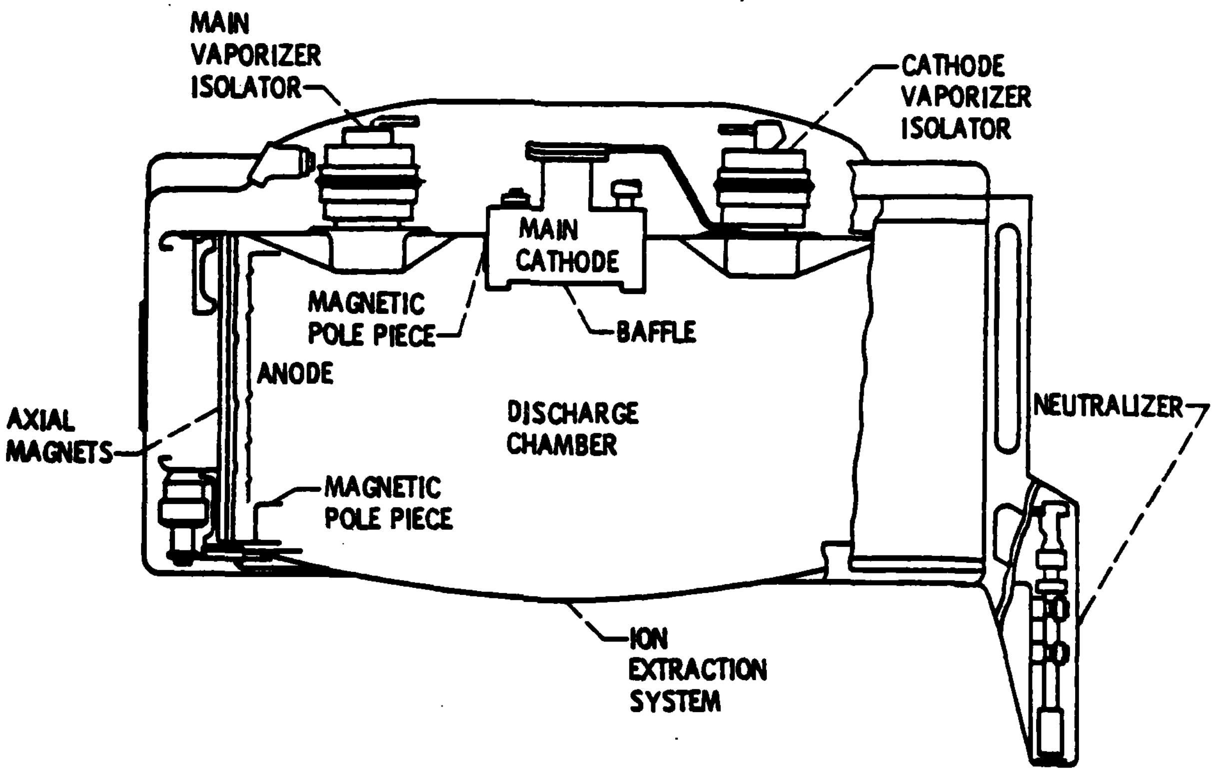

Thruster section

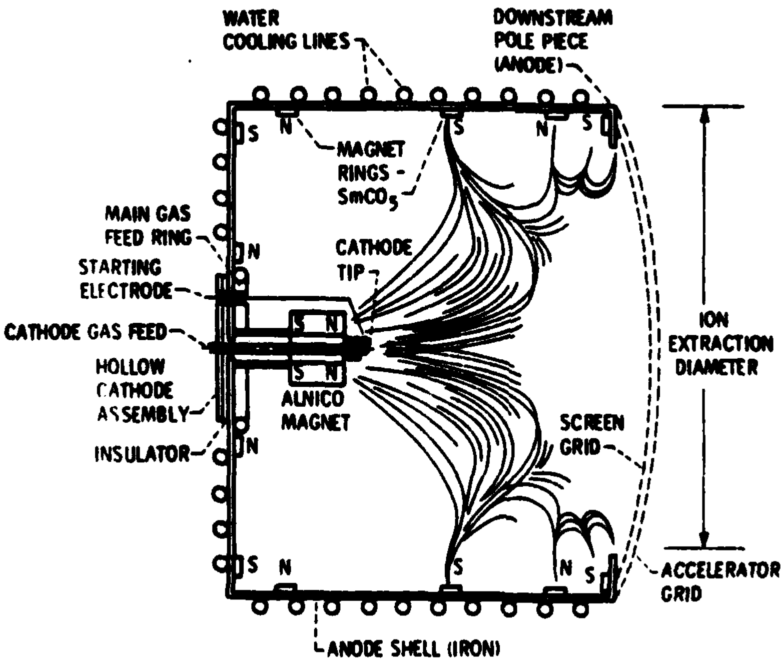

Ring-cusp discharge chamber (RC3) with a sketch of an iron filing map.

FIGURE 21.

30-CM ION THRUSTER CROSS-SECTION -- DETAILED IN (12).

RING-CUSP THRUSTER DIAGRAM -- FROM NASA-LEWIS REPORT (45).

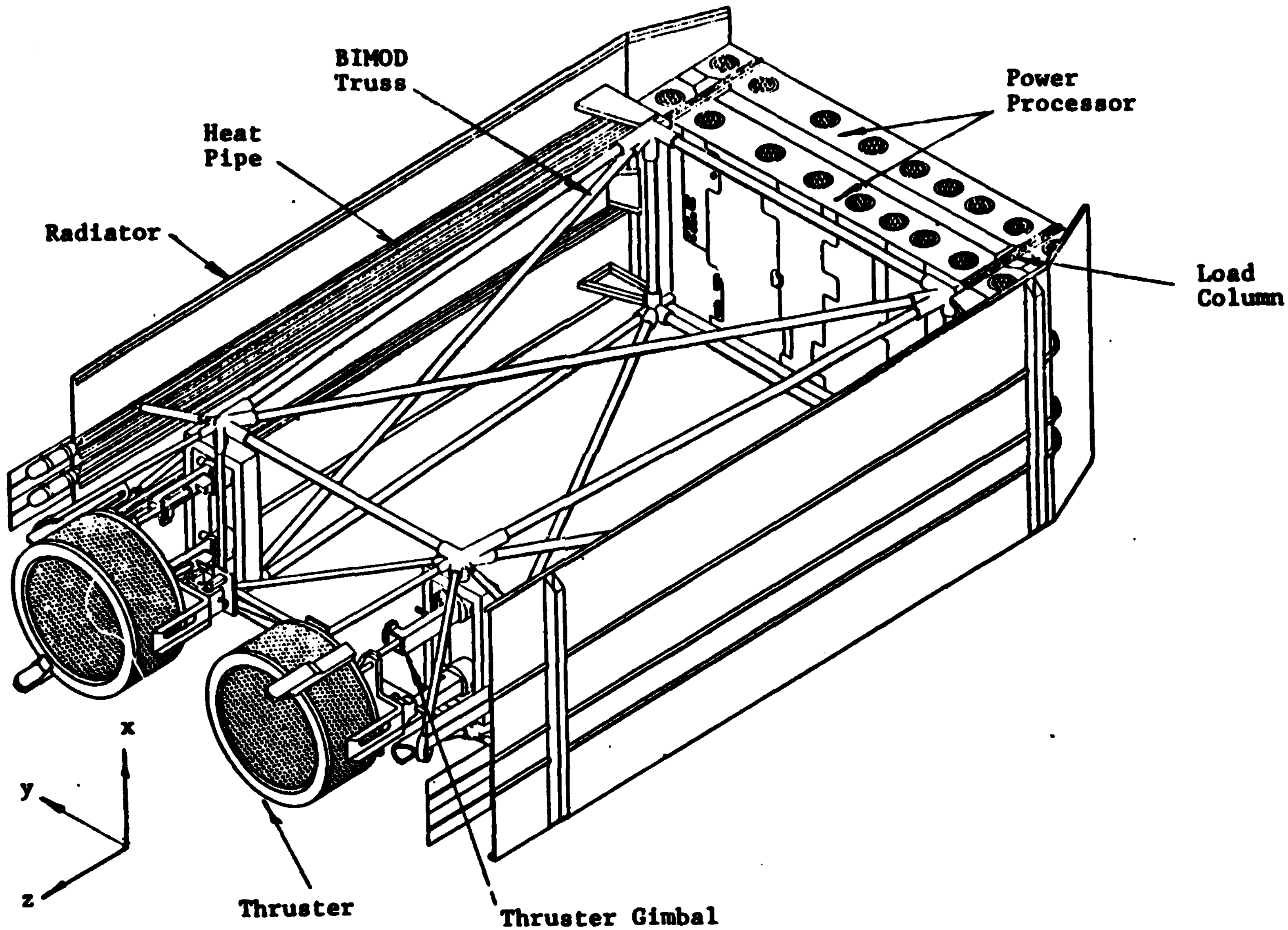

Figure 22. BIMOD Engine System (12)

Table 10. BIMOD Engine System Mass Breakdown(12)

Item	Mass, Kg	Comments
BIMOD Total	137.1	
Power Processors (2)	74.7	Functional Model
Thermal Control	21.0	
Thrusters (2)	20.7	J-Series Includes Mass of Harness to PPU
Thruster Gimbals (2)	6.8	
Truss and Struts	10.1	
Propellant Distribution	0.7	Valves, Field Joints, Lines
Miscellaneous	3.1	

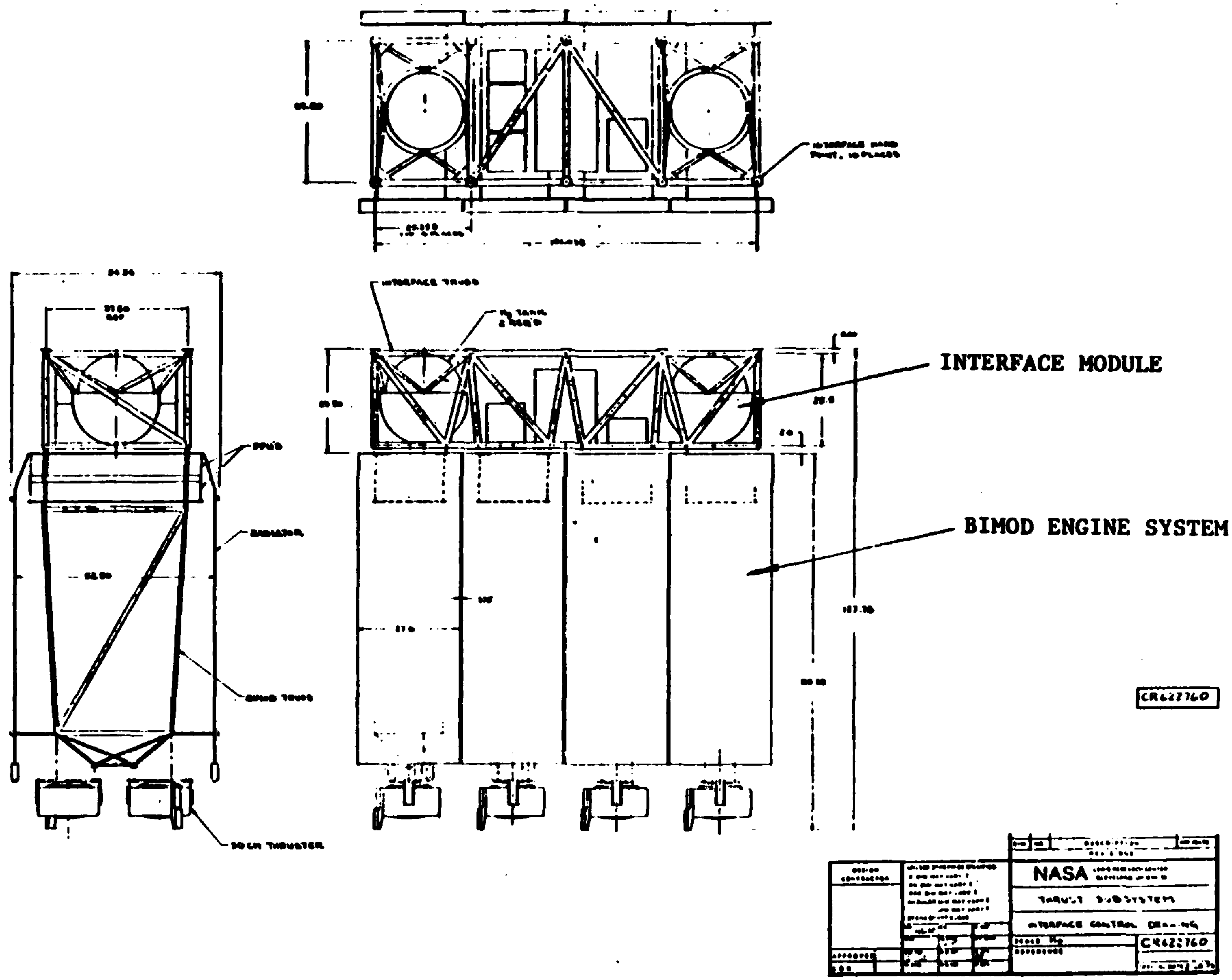

Figure 23. Thrust Subsystem Configuration (12)

Table 11. Interface Module Mass Breakdown (12)

Entry	Mass, kg
Interface Module Total	158.7
Truss Structure	24.8
Propellant Storage and Distribution	28.2
Thermal Control	9.9
Power Distribution Unit	54.4
Thruster Controller	6.8
Gimbal Electronics	8.0
Harness	26.6

TABLE 12. POWER PROCESSOR CHARACTERISTICS (39.)

	Component mass, kg	Parts count	Electrical efficiency, percent
Functional Model Power Processor (FMPP)	17.2	4000	87.2
Modification	Percent change due to modification		
Reduced number of power supplies	-14	-37	+1.6
Fixed point or 4:1 throttle	-13	-31	+1.3
New circuit design[10]	-6	-19	+0.4
Minimum total change	-19	-50	-1.7

TABLE 13. THRUSTER PERFORMANCE – BASELINE THROTTLE RANGE (39.)

Thruster	Beam current, amp	Beam voltage, V	Accelerator voltage, V	Discharge voltage, V	Discharge losses per beam ampere, W/A	Measured propellant utilization efficiency	Thrust loss factor[a]	Thruster input power, W	Thrust, N	Specific impulse, sec	Thruster efficiency
J-Series (J-4, 6 LeRC)	2.0	1100	317	32	192	0.940	0.955	2660	0.1293	2980	0.709
	1.6	940	313		200	.923	.955	1890	.0955	2705	.670
	1.3	820	311		209	.893	.961	1400	.0729	2459	.627
	1.0	700	307		224	.857	.967	965	.0522	2194	.570
	.75	600	300		245	.803	.974	691	.0365	1917	.496
Experimental thruster without magnetic baffle	2.0	1100	297	32	192	0.920	0.960	2663	.1303	2942	.705
	1.4	860	297	32	206	.880	.964	1549	.0807	2490	.636
	.75	600	300	30	245	.775	.974	667	.0365	1850	.462

[a]Estimated values from Ref. 1 and spectroscopic measurements.

TABLE 14. THRUSTER PERFORMANCE – EXTENDED THROTTLE RANGE (39.)

Beam current, amp	Beam voltage, V	Accelerator voltage, V	Discharge voltage, V	Discharge losses per beam ampere, W/A	Measured propellant utilization efficiency	Thrust loss factor[a]	Thruster input power, W	Thrust, N	Specific impulse, sec	Thruster efficiency
2.0	1100	300	32	192	0.920	0.960	2663	0.1303	2942	0.705
3.0	1300	400	28	224	.920	.971	4651	.213	3207	.726
4.0	1450	450	28	220	.958	.952	6773	.294	3457	.743
5.0	1570	600	28	232	1.04	.927	9133	.374	3823	.767

[a]Estimated values from Ref. 26 and spectroscopic measurements.

BASELINE J-SERIES THRUSTER

Input Pwr (KW)	Isp Data	Curve Fit	Thrust Data	Curve Fit
0.691	1917	2012	.0365	.03814
0.985	2194	2167	.0522	.05193
1.400	2459	2385	.0729	.07139
1.890	2705	2643	.0955	.09437
2.660	2980	3048	.1292	.13047

$$Isp = 526.4602\,(X4) + 1648.0429$$

$$Thrust = .04689\,(X4) + .005738$$

EXTENDED PERFORMANCE (THROTTLE RANGE) w/ SIMPLIFIED PPU

Input Pwr (kW)	Isp Data	Curve Fit	Thrust Data	Curve Fit
2.663	2942	2934	.1303	.13453
4.651	3207	3202	.2130	.20938
6.773	3457	3488	.2940	.28927
9.133	3823	3805	.3740	.37812

$$Isp = 134.5887\,(X4) + 2575.9623$$

$$Thrust = .037648\,(X4) + .034277$$

FIGURE 24. Isp and Thrust vs Input Power Relationships — Baseline & Extd. Perf.

TABLE 15. THRUSTER PERFORMANCE (GRID SET B) (41)

Beam current, amp	Beam voltage, V	Accelerator voltage, V	Discharge voltage, V	Discharge losses per beam ampere, W/A	Measured propellant utilization efficiency	Thrust loss factor[a]	Ratio of net to total accelerating voltage	Thruster input power, W	Thrust, N	Specific impulse, sec	Thruster efficiency
1.0	785	100	32	224	0.880	0.964	0.87	1094	0.055	2378	0.586
	585	300	↓	↓	↓	↓	.65	894	.048	2053	.540
	385	500					.43	694	.039	1666	.459
	185	700					.21	494	.027	1155	.309
2.0	1185	200	32	192	.911	.955	.85	2854	.134	2997	.689
	885	500	↓	↓	↓	↓	.63	2254	.116	2590	.653
	585	800					.42	1654	.094	2106	.586
	285	1100					.20	1054	.066	1470	.451
3.0	1485	300	28	197	.920	.956	.83	5161	.225	3392	.725
	1185	600	↓	↓	↓	↓	.66	4261	.201	3030	.700
	885	900					.49	3361	.174	2619	.664
	585	1200					.33	2461	.141	2129	.598
	385	1400					.21	1861	.115	1727	.523
4.0	1485	400	28	198	.943	.948	.78	6862	.298	3448	.734
	1185	700	↓	↓	↓	↓	.62	5662	.266	3080	.709
	985	900					.52	4862	.243	2808	.688
	785	1100					.41	4062	.217	2507	.656
	485	1400					.26	2862	.170	1970	.573

[a]Estimated values from Refs. 17 and 18.

TABLE 16. THRUSTER PERFORMANCE ARGON PROPELLANT (40.)

Beam voltage, V	Beam current, A	Discharge voltage, V	Discharge power per beam ampere, W/A	Measured propellant efficiency	Thrust loss factor	Thruster input power, W	Thrust, N	Specific impulse, sec	Thruster efficiency
1230	3.11	47	166	0.608	0.979	4400	0.098	4680	0.508
1230	3.47	47	184	.678	.976	4970	.108	5200	.554
1230	3.59	46	203	.701	.975	5200	.112	5370	.567
1230	3.64	47	238	.711	.935	5400	.109	5220	.517
1060	3.20	47	188	.692	.976	4040	.093	4920	.553
1260	3.43	41	182	.542	.980	5000	.109	4220	.451
1390	4.76	45	223	.673	.976	6920	.141	5480	.549
1380	4.70	47	154	.687	.975	7260	.155	5570	.583
1380	4.97	47	160	.726	.974	7710	.164	5880	.613
1380	5.15	46	149	.641	.978	7940	.171	5210	.551
1380	5.36	45	160	.668	.976	8320	.177	5420	.566
1380	5.92	49	145	.681	.975	8980	.194	5550	.588

[a]Assumes neutralizer flow rate of 0.1 eq.amp.
[b]Assumes neutralizer power of 40 watts

3-GRID OPTICS – Hg

INPUT POWER (kw) -- X4	Isp Data	Curve Fit	Thrust Data	Curve Fit
2.862	1970	2026.74	.170	.1752
4.062	2507	2468.26	.217	.2134
4.862	2808	2762.60	.243	.2388
5.662	3080	3056.94	.266	.2642
6.862	3448	3498.46	.298	.3024

$$I_{sp} = 367.931\,(X4) + 973.7193$$

$$\text{Thrust} = .03181\,(X4) + .084138$$

J-SERIES THRUSTER W/ ARGON PROPELLANT

Input Power (kw)	Isp Data	Thrust Data	Input PWR cont.	Isp Data	Thrust Data
4.40	4680	.098	7.26	5570	.155
4.97	5200	.108	7.71	5880	.164
5.20	5370	.112	7.94	5210	.171
5.40	5220	.109	8.32	5420	.177
6.92	5480	.141	8.98	5550	.194

continuation

$$I_{sp} = 17.005748\,(X4) + 4480.0865$$

$$\text{Thrust} = .0206547\,(X4) + .0048624$$

FIGURE 25. Isp and Thrust vs Input Power (X4) Relationships – 3-GRID Hg & Argon Thrusters

APPENDIX II. Use of Transfer Curves

Alfano and Wiesel (1) explicitly solved the slow timescale optimal control problem for low thrust, minimum time, minimum energy orbit transfer. Edelbaum had previously solved the optimal one-orbit control problem for the first time.

Figure 27 represents a global mapping of the solution space for this transfer. The mapping is in semimajor axis -- inclination space and provides explicit total velocity change requirements for any desired transfer.

Figure 26 provides an example calculation of the required velocity change, Δv for 200 km LEO to GEO transfer with 28.5° inclination change. Note that the dynamics are independent of vehicle specifics such as thrust, payload / vehicle mass, and specific impulse.

EXAMPLE CALCULATION

Given: Any low thrust electric propulsion OTV
$R_\oplus = 6378.145$ km
LEO = 200 km
GEO = 6.610521 $R_\oplus$
$\Delta i = 28.5°$, inclination change = .4974188 radians
FIGURE 27

Find: Velocity Increment, ΔV, required for the transfer

Solution: Finding change in semimajor axis, a (DU_*):

$a_{lower} = R_\oplus + 200\text{ km} = 6578.145\text{ km} = 1\ DU_* = 1.031357\ DU_\oplus$

$a_{higher} = 6.610521\ R_\oplus = 6.610521\ DU_\oplus$

$a^*_{lower} = 1.0\ DU_*$

$a^*_{higher} = \frac{a_H}{a_L} = 6.4095\ DU_*$

Now, Finding TU_*: $1\ TU_* = \sqrt{\frac{a_L^3}{\mu}} = \sqrt{\frac{(6578.145\text{ km})^3}{3.986 \times 10^5\text{ km}^3/\text{s}^2}}$

$= \sqrt{714123.02\text{ s}^2} = 845.0567$ sec

Now, using Figure 27:

$\tau = .75 \frac{DU_*}{TU_*}$ (τ is not transfer time here, but rather, time transformation)

$\lambda_i = -.54$

Now, converting to km/sec:

$\tau = .75 \frac{DU_*}{TU_*} * \left(6578.145 \frac{\text{km}}{DU_*}\right)\left(\frac{1}{845.0567}\frac{TU_*}{\text{sec}}\right)$

$\Delta V = \boxed{5.8382\ \text{km/sec}}$ Answer

Details for full usage and explanation of Fig. 27, found in Ref (1)

FIGURE 26. ORBIT TRANSFER CURVE CALCULATIONS

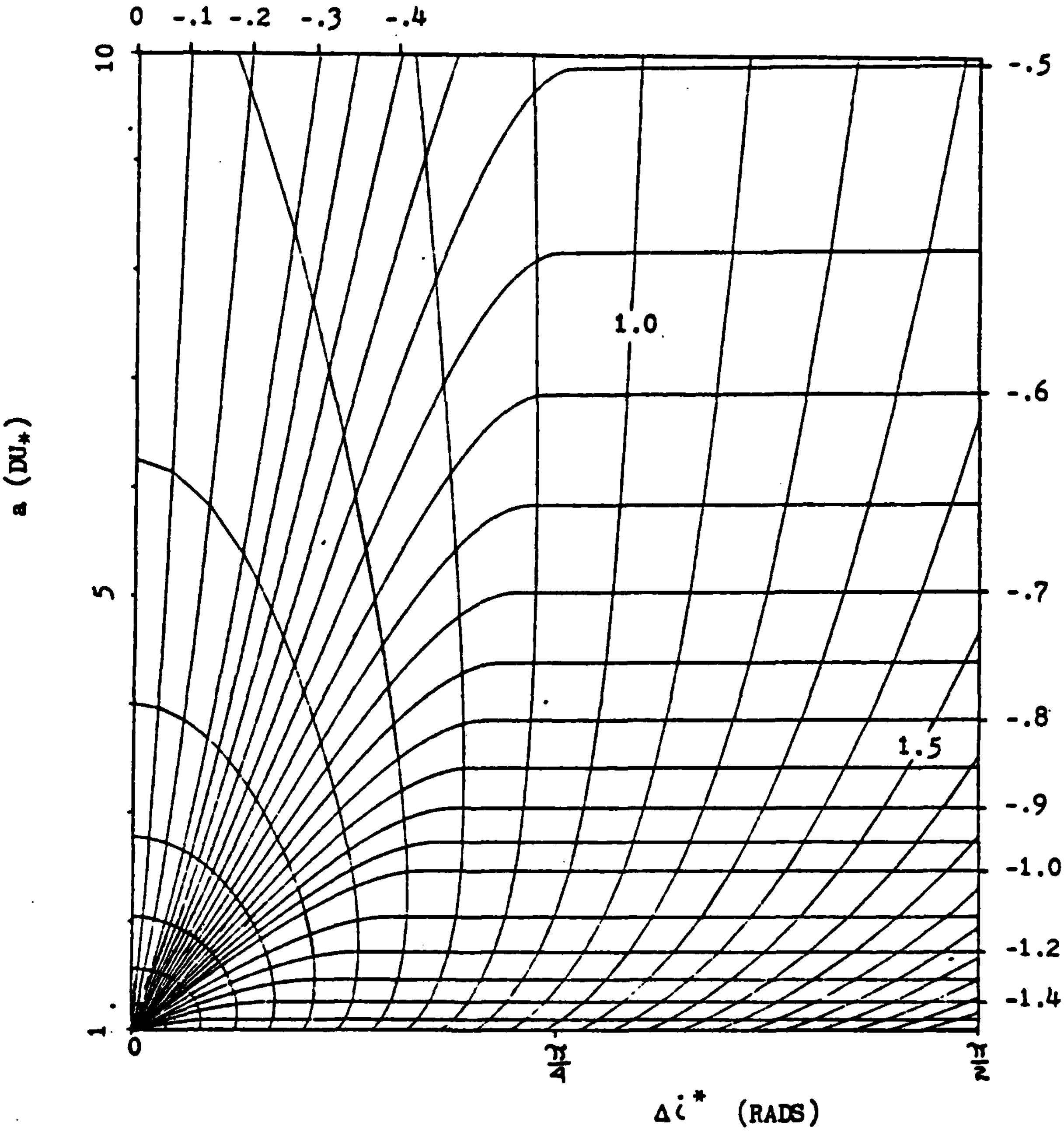

Figure 27. Universal chart for orbit transfer (1.)

APPENDIX III. SUMT Example Outputs

Included in this section are simply Xerox copies of some of the outputs that were obtained from the SUMT nonlinear optimization program runs for the EOTVs. The optimization program runs consisted of the five thruster technologies, each optimized for the GPS mission model. Thus, each EOTV and associated thruster technology was optimized for: a 908 kg payload; 1816 kg; 2724 kg; 3632 kg; 4540 kg; and 5448 kg payload. Additionally, a 1000 kg payload was used as a baseline. Thus the total initial number of runs was 35. To avoid bulk, the iterations which SUMT prints out between initial inputs and final values have not been included. For the same reason, only a few thrusters and payloads are represented in these copies.

```
SUBROUTINE RESTNT      74/74    OPT=1                          FTN 4.8+564        11/21/83  16.19.27        PAGE     1

         C     RESTRAINT PORTION
               SUBROUTINE RESTNT (IN,VAL)
               COMMON/SHARE/X(100),DEL(100),A(130,130),X(5),
              +P,PN,NFI,NPI
               IF (X(1) .LE. 1.0) X(1)=500.0
               IF (IN) 10,10,20
            10 VAL= P*X(2)+ X(3) + X(5)
               RETURN
            20 GO TO (21,22,23,24,25,26,27,28,29,30,31,32,33,34),IN
            21 VAL = X(1)-500.0
               RETURN
            22 VAL = 10000.0- X(1)
               RETURN
            23 VAL = X(2) - 10.0
               RETURN
            24 VAL = 10000.0 - X(2)
               RETURN
            25 VAL = X(3) - 10.0
               RETURN
            26 VAL = 10000.0 - X(3)
               RETURN
            27 VAL = X(4) - 0.5
               RETURN
            28 VAL = 20.0 - X(4)
               RETURN
            29 VAL = X(5) - 10.0
               RETURN
            30 VAL = 10000.0 - X(5)
               RETURN
            31 VAL = X(1) - 951.7656*X(4) - 72.6053
               RETURN
            32 VAL = X(2) - (X(4)/(0.0520))
               RETURN
            33 VAL = X(5) - (13.0 + 8*X(2))*(EXP(5.8382/(0.00981*X(1)))-1)
               RETURN
         C     PAYLOAD MASS IS: 4540 KG
            34 VAL=X(3)-(5540.+8*X(2)+X(5))*(EXP(5.8382/(0.00981*X(1)))-1)
               RETURN
               END

     SYMBOLIC REFERENCE MAP (R=1)

ENTRY POINTS
    3  RESTNT

VARIABLES       SN   TYPE           RELOCATION
  317   A            REAL     ARRAY    SHARE          144  DEL       REAL      ARRAY    SHARE
    0   IN           INTEGER           F.P.         23735  P         INTEGER            SHARE
23736   NI           INTEGER           SHARE        23737  N         INTEGER   ARRAY    SHARE
23740   NNI          INTEGER           SHARE        23737  NPI       INTEGER            SHARE
    0   VAL          REAL              F.P.                X         REAL      ARRAY    SHARE
```

FIGURE 28.

SUMT INPUT

RING - CUSP

4540 KG PAYLOAD

```
F =    .18485318E+04    F =    .18485435E+04    G =    .18489559E+04

VALUES OF X VECTOR

X(  1) =    .69641366E-12  X(  2) =    .34941910E-10  X(  3) =    .47884611E-11
X(  4) =    .67195975E-15  X(  5) =    .17084647E-10  X(

VALUES OF THE CONSTRAINTS

NOT INCLUDING THE NON-NEGATIVE CONSTRAINTS

G(  1) =    .76722000E-12  G(  2) =    .60100838E-12  G(  3) =    .32558568E-10
G(  4) =    .37654355E-12  G(  5) =    .48508131E-11  G(  6) =    .40395566E-12
G(  7) =    .73657067E-15  G(  8) =    .25765710E-09  G(  9) =    .17505031E-10
G( 10) =    .30F33066E-12  G( 11) =    .69281250E+02  G( 12) =   -.27918049E+04
G( 13) =   -.59657598E+03  G( 14) =   -.19973105E+04  G(

* * * * * * * * * * * * * * * * * * * * * * * * * * * * * * * * * * * * * * *
FINAL VALUE OF F =    1.84693184E+03

FINAL X VALUES

X(  1) =    5.34[illegible]E+02  X(  2) =    1.06613813E+02  X(  3) =    7.77572337E+02
X(  4) =    5.54391654E+01  X(  5) =    2.18049001E+02  X(

FINAL CONSTRAINT VALUES

G(  1) =    4.84324532E+03  G(  2) =    4.45075069E+03  G(  3) =    9.66138129E+01
G(  4) =    [illegible]E+03  G(  5) =    7.67572337E+02  G(  6) =    5.22202766E+03
G(  7) =    5.04351654E+0[illegible]  G(  8) =    1.4456[illegible]615E+01  G(  9) =    2.08049001E+02
G( 10) =    [illegible]E+02  G( 11) =    1.29046364E-07  G( 12) =   -5.2[illegible]014151E-06
G( 13) =   -1.1154[illegible]43E-[illegible]6  G( 14) =   -3.7222[illegible]08CE-06  G(
```

FIGURE 29. *SUMT OUTPUT*
RING CUSP, 4540 Kg P/L

```
SUBROUTINE RESTAT        74/74   OPT=1                    FTN 4.6+564        11/16/83  14.03.12        PAGE    1

      C      REAL ALL FUNCTION
             SUBROUTINE RESTAT (I,VAL)
             COMMON/SHARE/X(  ),DEL(  ),A(  ),I  ,Y(5),
            *P,N,NP1,NM1
             IF (X(1) .LE. 1. ) X(1)=
             IF (I.NE. 1) GO TO 20
        10   VAL= 10*X(2)+ X(3) + X(5)
             RETURN
        20   GO TO (21,22,23,24,25,26,27,28,29,30,31,32,33,34),IA
        21   VAL = X(1)-
             RETURN
        22   VAL = 10.  . - X(1)
             RETURN
        23   VAL = X(2) - 10.0
             RETURN
        24   VAL = 10.   . - X(2)
             RETURN
        25   VAL = X(3) - 10.0
             RETURN
        26   VAL = 10000.  - X(3)
             RETURN
        27   VAL = X(4) - 2.0
             RETURN
        28   VAL = 20.0 - X(4)
             RETURN
        29   VAL = X(5) - 10.0
             RETURN
        30   VAL = 10000.  - X(5)
             RETURN
        31   VAL = X(1) - 526.46*X(4) - 1648.643
             RETURN
        32   VAL = X(2) - (X(4)/(0.  52))
             RETURN
        33   VAL = X(5) - ((1000 + 10*X(2))*(EXP(5.0392/(0.00961*X(1)))-1)
             RETURN
      C      PAYLOAD MASS IS 4540KG
        34   VAL=X(3)-(4540.0+10*X(2)+X(5))*(EXP(5.0362/(0.00981*X(1)))-1)
             RETURN
             END

   SYMBOLIC REFERENCE MAP (R=1)

ENTRY POINTS
    3  RESTAT

VARIABLES     SN  TYPE          RELOCATION
  310  A          REAL     ARRAY    SHARE           144  DEL       REAL      ARRAY    SHARE
    4  IA         INTEGER           F.P.          23735  P         INTEGER            SHARE
23736  NM         INTEGER           SHARE         23734  N         INTEGER   ARRAY    SHARE
2374   NM1        INTEGER           SHARE         23737  NP1       INTEGER            SHARE
       VAL        REAL              F.P.              0  X         REAL      ARRAY    SHARE
```

FIGURE 30.

SUMT INPUT

BASELINE THRUSTER

4540 KG PAYLOAD

```
X( 4) = [illegible]      X( 5) = .312[illegible]+3     X(

VALUES OF THE CONSTRAINTS

NOT INCLUDING THE NON-NEGATIVE CONSTRAINTS

G( 1) =  .26978[illegible]E+14  G( 2) =  [illegible]            G( 3) =  .5[illegible]362[illegible]+0[illegible]
G( 4) =  .[illegible]E+[illegible]4        G( 5) =  .[illegible]        G( 6) =  .[illegible]75710[illegible]62E+04
G( 7) =  .1[illegible]375475E+[illegible]1     G( 8) =  .16676[illegible]24[illegible]+[illegible]2    G( 9) =  .3[illegible]377543E+03
G( 10) =  .96[illegible]6224[illegible]E+[illegible]4     G( 11) = -.4[illegible]E-[illegible]7     G( 12) =  .12392436E-05
G( 13) =  .323[illegible]E-[illegible]7      G( 14) = -.716[illegible]E-[illegible]6    G(

SOLUTION OF THE SUBPROBLEM

F =   .[illegible]195[illegible]52 E+04     P =   .2195[illegible]534E+04     G =   .21955539E+04

VALUES OF X VECTOR

X( 1) =  .1[illegible]563[illegible]E-11    X( 2) =  .5[illegible]2[illegible]1936E-11   X( 3) =  .29572735E-11
X( 4) =  .112[illegible]6665E-08    X( 5) =  .11872475E-10   X(

VALUES OF THE CONSTRAINTS

NOT INCLUDING THE NON-NEGATIVE CONSTRAINTS

G( 1) =  .12865275E-1[illegible]    G( 2) =  .56425574E-12    G( 3) =  .69091213E-10
G( 4) =  .374[illegible]2550E-12    G( 5) =  .30215844E-11    G( 6) =  .42540194E-12
G( 7) =  .28141762E-08    G( 8) =  .2233[illegible]9[illegible]5E-09    G( 9) =  .12263306E-10
G( 10) =  .38459673E-12    G( 11) = -.2581[illegible]5[illegible]E+02   G( 12) =  .66531482E+03
G( 13) =  .18[illegible]92773E+02    G( 14) = -.37657266E+03   G(

. . . . . . . . . . . . . . . . . . . . . . . . . . . . . . . . . . . . . . . . . . . . . . . . . .
FINAL VALUE OF F =  2.19585277E+03

FINAL X VALUES

X( 1) =  3.39726901E+03   X( 2) =  6.391F437EE+01   X( 3) =  1.24289303E+03
X( 4) =  3.32375870E+00   X( 5) =  3.13775366E+02   X(

FINAL CONSTRAINT VALUES

G( 1) =  2.[illegible]97[illegible]6901E+03   G( 2) =  6.6[illegible]213[illegible]9[illegible]E+03   G( 3) =  5.39184378E+01
G( 4) =  [illegible].930[illegible]615[illegible]E+03   G( 5) =  1.232[illegible]303F+03   G( 6) =  8.75710697E+03
G( 7) =  1.3237567[illegible]E+[illegible]   G( 8) =  1.6676[illegible]413F+01   G( 9) =  3.03775368E+02
G( 10) =  [illegible].5[illegible]622463E+13   G( 11) = -4.[illegible]E-0[illegible]   G( 12) =  1.23924542E-06
G( 13) =  3.37[illegible]4167E-[illegible]8   G( 14) = -7.[illegible]21662[illegible]E-07   G(
```

FIGURE 31.

SUMT OUTPUT
BASELINE, 4540 Kg P/L

```
SUBROUTINE RESIST      74/74    OPT=1                              FTN 4.?+564        11/16/?3  14.51.35        PAGE     1

      C     RESTRAINT FUNCTION
            SUBROUTINE RESIST (IN,VAL)
            COMMON/ZHARG/X(1? ),DEL(10 ),A(10),1 ?),?(5),
           *P,MN,NF?,NM)
            IF (X(1) .LE. 1.?) X(1)=?0?.?
            IF (IN) 1?,1 ,?
         10 VAL= 12*X(2)+ X(3) + X(5)
            RETURN
         20 GO TO (21,22,23,24,25,26,27,28,29,30,31,32,33,34),IN
         21 VAL = X(1)-??.?
            RETURN
         22 VAL = 1????. - X(1)
            RETURN
         23 VAL = X(2) - 10.?
            RETURN
         24 VAL = 10?00.? - X(2)
            RETURN
         25 VAL = X(3) - 10.0
            RETURN
         26 VAL = 10?00.? - X(3)
            RETURN
         27 VAL = X(4) - 2.0
            RETURN
         28 VAL = 20.0 - X(4)
            RETURN
         29 VAL = X(5) - 10.0
            RETURN
         30 VAL = 1??00.0 - X(5)
            RETURN
         31 VAL = X(1) - 367.93*X(4) - 973.72
            RETURN
         32 VAL = X(2) - (X(4)/(0.052))
            RETURN
         33 VAL = X(5) - (1000 + 12*X(2))*(EXP(5.8382/(0.00981*X(1)))-1)
            RETURN
      C     PAYLOAD MASS IS: 544?KG
         34 VAL=X(3)-(6448.0+12*X(2)+X(5))*(EXP(5.8382/(0.00981*X(1)))-1)
            RETURN
            END
```

FIGURE 32. *Sumt Input Printout*
3-Grid Ion optics, 5448 Kg P/L

```
G(  1) =   [illegible]          G(  2) =   [illegible]          G(  3) =   [illegible]E+02
G(  4) =   [illegible]          G(  5) =   [illegible]          G(  6) =   [illegible]
G(  7) =   [illegible]          G(  8) =   [illegible]          G(  9) =   [illegible]E+03
G( 10) =   [illegible]          G( 11) =   [illegible]          G( 12) =   .1[illegible]54493E-05
G( 13) =   [illegible]          G( 14) =   [illegible]          G(

SOLUTION OF THE SUBPROBLEM

F =   [illegible]   P =   [illegible]   R =   [illegible]

VALUES OF X VECTOR

X(  1) =   .12[illegible]5315[illegible]E-11   X(  2) =   [illegible]   X(  3) =   .2[illegible]33367E-11
X(  4) =   .71[illegible]162[illegible]2E-0[illegible]   X(  5) =   .740[illegible]E-11   X(

VALUES OF THE CONSTRAINTS

NOT INCLUDING THE NON-NEGATIVE CONSTRAINTS

G(  1) =   .1[illegible]32743E-11   G(  2) =   .52456[illegible]3E-12   G(  3) =   .41120[illegible]98E-10
G(  4) =   .3763145[illegible]E-12   G(  5) =   .[illegible]01417[illegible]E-11   G(  6) =   .45762656E-12
G(  7) =   .11529983E-08   G(  8) =   .25223[illegible]E-0[illegible]   G(  9) =   .7555[illegible]03E-11
G( 10) =   .39226317E-12   G( 11) =   -.339[illegible]E+02   G( 12) =   .6632724[illegible]E+03
G( 13) =   .21163[illegible]E+02   G( 14) =   -.247[illegible]63E+03   G(

* * * * * * * * * * * * * * * * * * * * * * * * * * * * * * * * * * * * * * * * * * * *
FINAL VALUE OF F =   3.56976[illegible]49E+03

FINAL X VALUES

X(  1) =   2.85834672E+03   X(  2) =   1.00595365E+02   X(  3) =   1.85954096E+03
X(  4) =   5.23095894E+00   X(  5) =   5.03084141E+02   X(

FINAL CONSTRAINT VALUES

G(  1) =   2.35[illegible]34672E+03   G(  2) =   7.1016532[illegible]E+03   G(  3) =   9.05953655E+01
G(  4) =   9.89940463E+03   G(  5) =   1.64054[illegible]6E+03   G(  6) =   8.14045904E+03
G(  7) =   3.23095694E+00   G(  8) =   1.4765[illegible]411E+01   G(  9) =   4.93084141E+02
G( 10) =   5.4969158[illegible]E+03   G( 11) =   -6.31553121E-0[illegible]   G( 12) =   1.23544123E-06
G( 13) =   3.94193194E-08   G( 14) =   -4.6173227[illegible]E-07   G(
```

FIGURE 33. SUMT OUTPUT PRINTOUT – FINAL VALUES, 3-GRID Hg, 5448 Kg P/L

APPENDIX IV. QGERT Example Outputs / Card Listings

The following figures contain examples of the output that can be expected from QGERT simulation programs. In the case of "flyoff" runs, only the summary printout was desired. But, for verification and validation, other printout options were selected. For the reader not familiar with QGERT, most of the output is automatically set up for the user, and for all four models, this methodology required that the User Function (UF) be employed to print some additional data on transactions at nodes. The only use of the UF for determining transfer time was in the EOTV model. Therefore, this is the only UF card listing included. However, main program card listings for all four vehicles are included.

```
*** INPUT CARDS ***

GEN,MADDOX,IUSVEH,12,10,1983,12,0,,7300,50,S,0,2*
SOU,1,0,1,D,M*
REG,2,1,1,D,M*
REG,3,1,1,D,M*
STA,4,1,1,P,R,90,4*
STA,5/LB2500,1,1,D,A*
STA,6/LB5000,1,1,D,A*
STA,7/LB10000,1,1,D,A*
STA,8/SATFAIL,1,1,D,A*
STA,9,1,1,P,A*
QUE,10/IUSQ,0,1,D,F,,0,0,1*
STA,12/GEO-A,1,1,D,A,,,6/1*
STA,14/IUSFAIL,1,1,D,A*
STA,15/GEO-B,1,1,D,B,40,3*
STA,16/GEO-I,1,1,D,I,50,15*
STA,20/LEOPAM,1,1,D,B*
ACT,1,1,NO,1,1*
ACT,1,4,,,2*
ACT,4,20,,,30,,0.65*
ACT,4,5,,,7,,0.10*
ACT,4,6,,,8,,0.20*
ACT,4,7,,,9,,0.05*
ACT,5,9,,,11*
ACT,6,9,,,12*
ACT,9,10,,,14,,0.965*
ACT,9,14,,,15,,0.035*
ACT,10,12,CO,0.5,16/IUSXFER,1*
ACT,12,15,,,22*
ACT,12,16,,,23*
ACT,16,18,,,24*
QUE,18/ENDBALK,0,0,D,F,19*
STA,19/FINALSTA,1,1,D,1,50,15*
VAS,5,1,CO,908*
VAS,6,1,CO,2724*
VAS,7,1,CO,5448*
PAR,1,20,27,10,0,120,0,5,0*
FIN*

*** NO ERRORS DETECTED IN INPUT DATA ***

*** EXECUTION WILL BE ATTEMPTED ***
  359   0   0 359  27  65  18   0  92  87   0  87   0   5  87  87   0   0  87 249

  352   0   0 352  34  80  16   0 114 110   0 110   0   4 110 110   0   0 110 222
```

FIGURE 34. INPUT CARDS – IUS MODEL

GERT SIMULATION PROJECT IUSVEH BY MADDOX
DATE 12/ 10/ 1983

FINAL RESULTS FOR 50 SIMULATIONS

AVERAGE NODE STATISTICS

NODE	LABEL	PROBABILITY	AVE.	STD.DEV.	SD OF AVE	NO OF OBS.	MIN.	MAX.	STAT TYPE
19	FINALSTA	1.0000	0.5000	0.0000	0.0000	50.	0.5000	0.5000	I
20	LEOPAW	1.0000	31.2458	1.0697	0.1513	50.	28.9551	33.6540	B
16	GEO-I	1.0000	0.5000	0.0000	0.0000	50.	0.5000	0.5000	I
15	GEO-B	1.0000	69.4864	5.6062	0.7928	50.	59.2974	90.1327	B
14	IUSFAIL	1.0000	3708.4764	1325.8957	187.5100	50.	923.6545	7202.6114	A
12	GEO-A	1.0000	3639.9960	161.2473	22.8038	50.	3273.0590	4041.4440	A
9		1.0000	3637.4319	164.2474	23.2281	50.	3281.2304	4050.3606	A
8	SATFAIL		NO VALUES RECORDED						
7	LB10000	1.0000	3566.9522	543.8803	76.9163	50.	2442.6479	4856.6492	A
6	LB5000	1.0000	3665.5566	216.5856	30.6298	50.	3202.5952	4222.2660	A
5	LB2500	1.0000	3560.1262	349.5960	49.4403	50.	2659.0735	4444.3379	A
4		1.0000	20.3045	0.2758	0.0390	50.	19.5413	20.9392	B

AVERAGE NUMBER IN Q-NODE / **AVERAGE WAITING TIME** / **NUMBER IN Q-NODE**

NODE	LABEL	AVE.	STD.DEV.	SD OF AVE	MIN.	MAX.	AVE.	STD.DEV.	SD OF AVE	MAX.
10	IUSQ	0.0000	0.0000	0.0000	0.0000	0.0000	0.0000	0.0000	0.0000	0.0000

AVERAGE SERVER UTILIZATION / **EXTREME VALUES**

SERVER	LABEL	NO. PARALLEL SERVERS	AVE.	STD.DEV.	SD OF AVE	NO. OF OBS.	MIN.	MAX.	MAX. IDLE (TIME OR SERVERS)	MAX. BUS
16	IUSXFER	1	0.0072	0.0005	0.0001	50.	0.0055	0.0082	593.6016	0.5000
0		0	0.0000	0.0000	0.0000	50.	0.0000	0.0000	7300.0000	0.0000

AVERAGE NO. BALKING PER UNIT TIME

NODE	LABEL	AVE.	STD.DEV.	SD OF AVE	NO. OF OBS.	MIN.	MAX.
10	IUSQ	0.0000	0.0000	0.0000	50.	0.0000	0.0000
18	ENDBALK	0.0144	0.0011	0.0002	50.	0.0111	0.0164

FIGURE 35.

IUS MODEL.
QGERT SUMMARY
OUTPUT.

```
*** INPUT CARDS ***

GEN,MADDUX,CENTAR,12,10,1983,12,0,,7300,50,S,0,2*
SOU,1,0,1,D,M*
REG,2,1,1,D,M*
REG,3,1,1,D,M*
STA,4,1,1,P,B,90,4*
STA,5/LB2500,1,1,D,A*
STA,6/LB5000,1,1,D,A*
STA,7/LB10000,1,1,D,A*
STA,8/SATFAIL,1,1,D,A*
STA,9,1,1,P,A*
QUE,10/IUSQ,0,1,0,F,,0,0,1*
STA,12/GEO-A,1,1,D,A,,,8/1*
STA,14/IUSFAIL,1,1,D,A*
STA,15/GEO-B,1,1,D,B,40,3*
STA,16/GEO-I,1,1,D,I,50,15*
STA,20/LEOPAM,1,1,D,8*
ACT,1,1,NO,1,1*
ACT,1,4,,,2*
ACT,4,20,,,30,,0.65*
ACT,4,5,,,7,,0.10*
ACT,4,6,,,8,,0.20*
ACT,4,7,,,9,,0.05*
ACT,6,9,,,12*
ACT,7,9,,,13*
ACT,9,10,,,14,,0.985*
ACT,9,14,,,15,,0.015*
ACT,10,12,CO,0.5,16/CNTSFER,1*
ACT,12,15,,,22*
ACT,12,16,,,23*
ACT,16,18,,,24*
QUE,18/ENDBALK,0,0,D,F,19*
STA,19/FINALSTA,1,1,D,1,50,15*
VAS,5,1,CO,908*
VAS,6,1,CO,2724*
VAS,7,1,CO,5448*
PAR,1,20,27,10,0,120,0,5,0*
FIN*

*** NO ERRORS DETECTED IN INPUT DATA ***

*** EXECUTION WILL BE ATTEMPTED ***

  358    0    0 358  28  59  17    0  76  73    0  75    0    3  73  73    0    0  73 254

  352    0    0 352  37  65  18    0  83  81    0  81    0    2  81  81    0    0  81 232
```

FIGURE 36. INPUT CARDS – CENTAUR MODEL

FINAL RESULTS FOR 50 SIMULATIONS

AVERAGE NODE STATISTICS

NODE	LABEL	PROBABILITY	AVE.	STD.DEV.	SD OF AVE	NO OF OBS.	MIN.	MAX.	STAT TYPE
19	FINALSTA	1.0000	0.5000	0.0000	0.0000	50.	0.5000	0.5000	I
20	LEOPAW	1.0000	31.2101	1.3606	0.1924	50.	28.7970	35.6752	B
16	GEO-I	1.0000	0.5000	0.0000	0.0000	50.	0.5000	0.5000	I
15	GEO-B	1.0000	83.2270	8.3108	1.1753	50.	61.5767	99.5335	B
14	IUSFAIL	0.8200	3519.9367	1619.8108	252.9095	41.	72.1721	6343.8721	A
12	GEO-A	1.0000	3609.6935	217.5160	30.7614	50.	2993.2768	4246.0663	A
9		1.0000	3606.7114	212.9154	30.1108	50.	2992.7766	4161.5093	A
8	SATFAIL		NO VALUES RECORDED						
7	LB10000	1.0000	3630.3997	398.7023	56.3850	50.	2942.9758	4581.3296	A
6	LB5000	1.0000	3607.5565	235.9212	33.3643	50.	2689.3860	4081.7556	A
5	LB2500	1.0000	3628.9495	397.5700	56.2249	50.	2613.7364	4623.4114	A
4		1.0000	20.3131	0.2357	0.0333	50.	19.7188	20.8267	B

AVERAGE NUMBER IN Q-NODE / **AVERAGE WAITING TIME** / **NUMBER IN Q-NODE**

NODE	LABEL	AVE.	STD.DEV.	SD OF AVE	MIN.	MAX.	AVE.	STD.DEV.	SD OF AVE	MAX.
10	IUSQ	0.0000	0.0000	0.0000	0.0000	0.0000	0.0000	0.0000	0.0000	0.0000

AVERAGE SERVER UTILIZATION / **EXTREME VALUES**

SERVER	LABEL	NO. PARALLEL SERVERS	AVE.	STD.DEV.	SD OF AVE	NO. OF OBS.	MIN.	MAX.	MAX. IDLE (TIME OR SERVERS)	MAX. ELS
16	CNTSFER	1	0.0060	0.0006	0.0001	50.	0.0050	0.0081	552.9892	0.5000
0		0	0.0000	0.0000	0.0000	50.	0.0000	0.0000	7300.0000	0.0000

AVERAGE NO. BALKING PER UNIT TIME

NODE	LABEL	AVE.	STD.DEV.	SD OF AVE	NO. OF OBS.	MIN.	MAX.

FIGURE 37. SUMMARY OUTPUT — CENTAUR MODEL

```
*** INPUT CARDS ***

GEN,MADDOX,ELCOTV,5,25,1983,13,0,,7300,50,8,0,2*
SOU,1,0,1,D,M*
REG,2,1,1,D,M*
REG,3,1,1,D,M*
STA,4,1,1,P,B,90,4*
STA,5/LB2500,1,1,D,A*
STA,6/LB5000,1,1,D,A*
STA,7/LB10000,1,1,D,A*
STA,8/SATFAIL,1,1,D,A*
QUE,9/OTVQ,11,11,D,F,,0,0.2,11*
QUE,10/SATQ,0,7,D,F,17,0,0.3,11*
SEL,11/LINKUP,ASM,CYC,B/1,,9,10*
STA,12/GEO-A,1,1,D,A,,,B/1*
STA,13/RETURN,1,1,P,A*
STA,14/OTVFAIL,1,1,D,A*
STA,15/GEO-B,1,1,D,B,48,3*
STA,16/GEO-I,1,1,D,I,50,15*
STA,17/SATQFULL,1,1,D,A*
STA,20/LEOPAM,1,1,D,B*
ACT,1,1,NO,1,1*
ACT,1,4,,,2*
ACT,4,20,,,30,,0.65*
ACT,4,5,,,7,,0.10*
ACT,4,6,,,8,,0.20*
ACT,4,7,,,9,,0.05*
ACT,5,10,CO,1,11*
ACT,6,10,CO,1,13*
ACT,6,10,CO,1,14*
ACT,7,10,CO,2,15*
ACT,11,12,UF,1,16/OTV1XFER*
ACT,11,12,UF,1,17/OTV2XFER*
ACT,11,12,UF,1,18/OTV3XFER*
ACT,11,12,UF,1,31/CTV4XFER*
ACT,11,12,UF,1,32/OTV5XFER*
ACT,11,12,UF,1,33/OTV6XFER*
ACT,11,12,UF,1,34/OTV7XFER*
ACT,11,12,UF,1,35/OTV8XFER*
ACT,11,12,UF,1,36/OTV9XFER*
ACT,11,12,UF,1,37/OTV10FER*
ACT,11,12,UF,1,38/OTV11FER*
ACT,12,13,UF,2,19*
ACT,13,14,,,21,,0.010*
ACT,13,9,,,20,,0.990*
ACT,12,15,,,22*
ACT,12,16,,,23*
ACT,16,18,,,24*
QUE,18/ENDWALK,0,0,D,F,19*
STA,19/FINALSTA,1,1,D,I,50,15*
PAR,1,20.27,10.0,120.0,5.0*
VAS,5,1,CO,908*
VAS,6,1,CO,2724*
VAS,7,1,CO,5448*
VAS,13,1,CO,0*
FIN*

*** NO ERRORS DETECTED IN INPUT DATA ***

*** EXECUTION WILL BE ATTEMPTED ***

359  0  0 359  42  66  20  0 194 194 194 197 186  0 197 197  0  0 197 231
```

FIGURE 38. *Input Cards – EOTV Model*

GERT SIMULATION PROJECT ELCOTV   BY MADDOX
DATE 5/ 25/ 1983

FIGURE 39.

SUMMARY OUTPUT
EOTV MODEL

FINAL RESULTS FOR 50 SIMULATIONS

AVERAGE NODE STATISTICS

NODE	LABEL	PROBABILITY	AVE.	STD.DEV.	SD OF AVE	NO OF OBS.	MIN.	MAX.	STAT TYPE
19	FINALSTA	1.0000	114.3183	2.8007	0.3961	50.	109.6476	123.5665	I
20	LEOPAN	1.0000	31.2550	1.2782	0.1808	50.	29.0049	34.3478	B
17	SATOFULL		NO VALUES RECORDED						
16	GEO-I	1.0000	114.3183	2.8007	0.3961	50.	109.6476	123.5665	I
15	GEO-B	1.0000	37.2694	2.7515	0.3891	50.	31.3145	43.5024	B
14	OTVFAIL	0.8200	3814.6672	1321.0469	206.3129	41.	1316.1802	6024.3266	A
13	RETURN	1.0000	3727.3152	163.9370	23.1842	50.	3400.8300	4046.6667	A
12	GEO-A	1.0000	3703.8993	162.6390	23.0289	50.	3355.8300	4005.6501	A
8	SATFAIL		NO VALUES RECORDED						
7	LB10000	1.0000	3732.5141	505.8314	71.5354	50.	2615.5958	5063.9031	A
6	LB5000	1.0000	3624.4194	229.3535	32.4355	50.	3165.1488	4013.4171	A
5	LB2500	1.0000	3694.6664	321.7873	45.5076	50.	2942.2280	4509.0182	A
4		1.0000	20.3113	0.2264	0.0320	50.	19.9068	20.7618	B

AVERAGE NUMBER IN Q-NODE / **AVERAGE WAITING TIME** / **NUMBER IN Q-NODE**

NODE	LABEL	AVE.	STD.DEV.	SD OF AVE	MIN.	MAX.	AVE.	STD.DEV.	SD OF AVE	MAX.
9	OTVQ	5.8751	0.9017	0.1275	3.6340	7.4606	215.2036	40.1795	5.6822	11.0000
10	SATQ	0.0278	0.0540	0.0076	0.0000	0.2794	1.0039	1.9370	0.2739	5.0000

AVERAGE SERVER UTILIZATION / **EXTREME VALUES**

SERVER	LABEL	NO. PARALLEL SERVERS	AVE.	STD.DEV.	SD OF AVE	NO. OF OBS.	MIN.	MAX.	MAX. IDLE (TIME OR SERVERS)	MAX. BUSY
0		0	0.0000	0.0000	0.0000	50.	0.0000	0.0000	7300.0000	0.0000
16	OTV1XFER	1	0.2701	0.0271	0.0038	50.	0.2126	0.3340	1093.7738	178.8000
17	OTV2XFER	1	0.2730	0.0253	0.0036	50.	0.2242	0.3291	819.7211	178.8000
18	OTV3XFER	1	0.2753	0.0281	0.0040	50.	0.2262	0.3281	850.7525	178.8000
31	OTV4XFER	1	0.2728	0.0312	0.0044	50.	0.2056	0.3252	903.6620	178.6000
32	OTV5XFER	1	0.2709	0.0252	0.0036	50.	0.2056	0.3222	906.0867	178.8000
33	OTV6XFER	1	0.2720	0.0257	0.0036	50.	0.2233	0.3428	918.8805	178.8000
34	OTV7XFER	1	0.2740	0.0293	0.0041	50.	0.2095	0.3311	1007.4423	178.8000
35	OTV8XFER	1	0.2721	0.0263	0.0037	50.	0.2301	0.3322	968.2383	178.8000
36	OTV9XFER	1	0.2718	0.0289	0.0041	50.	0.2170	0.3272	883.7188	178.8000
37	OTV10FER	1	0.2695	0.0265	0.0037	50.	0.2036	0.3281	892.1422	178.8000
38	OTV11FER	1	0.2721	0.0267	0.0038	50.	0.2277	0.3487	852.9960	178.8000

```
26 NOV 83 23:12:39   HARRIS FORTRAN 77 SAU OPTIMIZING COMPILER     01414-00       REV   VOS 2.3  PAGE     1
 MODULE NAME:  *MAIN*

      SUBROUTINE UI
      COMMON/QVAR/ NDE,NFTBU(100),NRFL(100),NRELP(100),NREL2(100),
     + NRUN,NRUNS,NTC(100),PARAM(100,4),TRFG,TNOW
      COMMON/MINE/AT1,X1,X2,X3,X4,X5,X6,X7,X8,T1,T2
      REAL X1,X2,X3,X4,X5,X6,X7,X8,T1,T2
      X1=2340.0
      X2=71.42
      X3=849.7
      X4=3.7139
      X5=455.0
      X6=0.2023
      X7=100.0
      X8=50.0
      T1=0.0
      T2=0.0
      RETURN
      END
```

FIGURE 40. EOTV MODEL – SUBROUTINE UI

```
26 NOV 83 23:12:39   HARRIS FORTRAN 77 SAU OPTIMIZING COMPILER     01414-00       REV   VOS 2.3  PAGE      3
 MODULE NAME:  *MAIN*

          SUBROUTINE UO
          COMMON/QVAR/ NDE,NFTRU(100),NREL(100),NRFLP(100),NREL2(100),
         + NRUN,NRUNS,NTC(100),PARAM(100,4),TREG,TNOW
          COMMON/PINE/AT1,X1,X2,X3,X4,X5,X6,X7,X8,T1,T2
          REAL X1,X2,X3,X4,X5,X6,X7,X8,T1,T2
          IF(TNOW.EQ.7300) THEN
          WRITE(6,300)NTC(1),NTC(2),NTC(3),NTC(4),NTC(5),NTC(6),NTC(7),
         +NTC(8),NTC(9),NTC(10),NTC(11),NTC(12),NTC(13),NTC(14),NTC(15),
         +NTC(16),NTC(17),NTC(18),NTC(19),NTC(20)
      300 FORMAT(/2X,I4,I4,I4,I4,I4,I4,I4,I4,I4,I4,I4,I4,
         +I4,I4,I4,I4,I4,I4,I4,I4)
          PRINT"(/3X,F14.5,2X,F14.5)",T1,T2
          END IF
          RETURN
          END
```

FIGURE 41. EOTV MODEL - SUBROUTINE UO

```
26 NOV 83 23:12:39   HARRIS FORTRAN 77 SAU OPTIMIZING COMPILER    01414-00       REV   VOS 2.3  PAGE    5
 MODULE NAME:  *MAIN*

          FUNCTION UF (IFN)
          COMMON/QVAR/ NDE,NFTRU(100),NREL(100),NRFLP(100),NREL2(100),
         + NRUN,NRUNS,NTC(100),PARAM(100,4),TRFG,TNOW
          COMMON/MINE/AT1,X1,X2,X3,X4,X5,X6,X7,X8,T1,T2
          REAL X1,X2,X3,X4,X5,X6,X7,X8,T1,T2
          GO TO ( 1,2 ), IFN
    1     IF(GATRB(1).EQ.908) THEN
          T1=71.4
          UF=T1
          ELSE IF(GATRB(1).EQ.2724) THEN
          T1=114.4
          UF=T1
          ELSE IF(GATRB(1).EQ.5448) THEN
          T1=178.8
          UF=T1
          END IF
          RETURN
    2     T2=45.0
          UF=T2
          RETURN
          END
```

FIGURE 42. *EOTV MODEL – SUBROUTINE UF*

```
*** INPUT CARDS ***

GEN,MADDOX,RBPV,11,19,1983,15,0,,7300,50,5,0,2*
SOU,1,0,1,D,M*
REG,2,1,1,D,M*
REG,3,1,1,D,M*
STA,4,1,1,P,R,90,4*
STA,5/LB2500,1,1,D,A*
STA,6/LB5000,1,1,D,A*
STA,7/LB10000,1,1,D,A*
STA,8/SATFAIL,1,1,D,A*
QUE,9/OTVQ,6,6,D,F,,0,0.2,11*
QUE,10/SATQ,0,7,D,F,17,0,0.3,11*
SEL,11/LINKUP,ASM,CYC,R/1,,9,10*
STA,12/GEO-A,1,1,D,A,,,B/1*
STA,13/RETURN,1,1,P,A*
STA,14/OTVFAIL,1,1,D,A*
STA,15/GEO-B,1,1,D,B,40,3*
STA,16/GEO-I,1,1,D,I,50,15*
STA,17/SATNFULL,1,1,D,A*
STA,20/LEOPAM,1,1,D,R*
STA,21/REFUEL1,1,1,D,B*
STA,22/REFUEL2,1,1,D,B*
ACT,1,4,,,2*
ACT,4,20,,,30,,0.65*
ACT,4,5,,,7,,0.10*
ACT,4,6,,,8,,0.20*
ACT,4,7,,,9,,0.05*
ACT,20,1,NO,1,50*
ACT,5,1,NO,1,51*
ACT,6,21,NO,1,52*
ACT,7,21,NO,1,53*
ACT,21,22,NO,1,54*
ACT,22,1,NO,1,55*
ACT,6,10,CO,1,13*
ACT,7,10,CO,2,15*
ACT,11,12,CO,0.5,16/ROTV1XF*
ACT,11,12,CO,0.5,17/ROTV2XF*
ACT,11,12,CO,0.5,18/ROTV3XF*
ACT,11,12,UF,1,31/OTV4XFER*
ACT,11,12,UF,1,32/OTV5XFER*
ACT,11,12,UF,1,33/OTV6XFER*
ACT,12,13,CO,0.5,19*
ACT,13,14,,,21,,0.025*
ACT,13,9,,,20,,0.975*
ACT,12,15,,,22*
ACT,12,16,,,23*
ACT,16,18,,,24*
QUE,18/ENDWALK,0,0,D,F,19*
STA,19/FINALSTA,1,1,D,1,50,15*
PAR,1,20.27,10.0,120.0,5.0*
VAS,5,1,CO,908*
VAS,6,1,CO,2724*
VAS,7,1,CO,5448*
VAS,13,1,CO,0*
FIN*

*** NO ERRORS DETECTED IN INPUT DATA ***

*** EXECUTION WILL BE ATTEMPTED ***
   1    2   3  4     5    6
 237    0    0 237  24   51   11   0  62  62  62  62  62   2  62  62   0   0  62 151  62  62
```

FIGURE 43. INPUT CARDS – RBPV MODEL

FINAL RESULTS FOR 50 SIMULATIONS

AVERAGE NODE STATISTICS

NODE	LABEL	PROBABILITY	AVE.	STD.DEV.	SD OF AVE	NO. OF OBS.	MIN.	MAX.	STAT TYPE
19	FINALSTA	1.0000	16.4300	0.2994	0.0423	50.	15.7381	17.1270	I
22	REFUEL2	1.0000	121.7104	10.6021	1.4994	50.	103.8572	151.0520	B
21	REFUEL1	1.0000	121.8574	10.8071	1.5284	50.	103.9418	150.9498	B
20	LEOPAK	1.0000	46.7046	4.5198	0.6392	50.	36.9375	58.3165	B
17	SATQFULL		NO VALUES RECORDED						
16	GEO-I	1.0000	16.4300	0.2994	0.0423	50.	15.7381	17.1270	I
15	GEO-B	1.0000	121.9173	10.8734	1.5377	50.	104.3088	151.0206	B
14	OTVFAIL	0.8000	3607.4903	1888.6774	298.6261	40.	351.8861	7028.4999	A
13	RETURN	1.0000	3640.5437	187.7344	26.5497	50.	3271.7672	4137.7110	A
12	GEO-A	1.0000	3640.0437	187.7344	26.5497	50.	3271.2672	4137.2110	A
8	SATFAIL		NO VALUES RECORDED						
7	LB10000	1.0000	3623.3992	658.7138	93.1562	50.	1988.8103	5105.9377	A
6	LB5000	1.0000	3627.9127	225.1549	31.8417	50.	3004.1619	4170.3262	A
5	LB2500	1.0000	3650.2036	437.1735	61.8257	50.	2782.6384	4639.8669	A
4		1.0000	30.5126	1.5043	0.2127	50.	27.4545	34.0634	B

		AVERAGE NUMBER IN Q-NODE					**AVERAGE WAITING TIME**			**NUMBER IN Q-NODE**
NODE	LABEL	AVE.	STD.DEV.	SD OF AVE	MIN.	MAX.	AVE.	STD.DEV.	SD OF AVE	MAX.
9	OTVQ	5.2330	0.5864	0.0829	1.4506	5.8921	591.1086	78.7886	11.1418	6.0000
10	SATQ	0.0000	0.0000	0.0000	0.0000	0.0000	0.0000	0.0000	0.0000	0.0000

			AVERAGE SERVER UTILIZATION						**EXTREME VALUES**	
SERVER	LABEL	NO. PARALLEL SERVERS	AVE.	STD.DEV.	SD OF AVE	NO. OF OBS.	MIN.	MAX.	MAX. IDLE (TIME OR SERVERS)	MAX. BUS
0		0	0.0000	0.0000	0.0000	50.	0.0000	0.0000	7300.0000	0.0000
16	ROTV1XF	1	0.0007	0.0001	0.0000	50.	0.0005	0.0008	1847.2362	0.5000
17	ROTV2XF	1	0.0007	0.0001	0.0000	50.	0.0005	0.0008	1490.1439	0.5000
18	ROTV3XF	1	0.0007	0.0001	0.0000	50.	0.0005	0.0008	1408.9201	0.5000
31	OTV4XFER	1	0.0411	0.0037	0.0005	50.	0.0329	0.0493	1566.0191	30.0000
32	OTV5XFER	1	0.0410	0.0037	0.0005	50.	0.0329	0.0493	1530.9970	30.0000
33	OTV6XFER	1	0.0410	0.0039	0.0005	50.	0.0329	0.0493	1776.1844	30.0000

AVERAGE NO. BALKING PER UNIT TIME

NODE	LABEL	AVE.	STD.DEV.	SD OF AVE	NO. OF OBS.	MIN.	MAX.
9	OTVQ	0.0000	0.0000	0.0000	50.	0.0000	0.0000
10	SATQ	0.0000	0.0000	0.0000	50.	0.0000	0.0000
18	ENDBALK	0.0082	0.0007	0.0001	50.	0.0067	0.0096

57.86 72.1 72.08

FIGURE 44.

SUMMARY OUTPUT
RBPV MODEL

APPENDIX V. Other Mission Possibilities / Sensitivities

The first two figures contain SUMT results for EOTVs including more realistic calculations of power available to the thrusters. End-Of-Life (EOL) rather than Beginning-Of-Life (BOL) sizing of the solar panels has been included. That is, the effect of Van-Allen radiation degradation has been incorporated such that the full power required is available at the end of the vehicle's lifetime. Provision has also been made for more avionics and housekeeping power requirements as well as some cabling losses. Further, transfer time calculations include 10% occultation during earth shadowing.

The next five figures show other mission possibilities which were discussed in Chapter 6, but with the earth shadow effects included. These missions can be thought of as representative of yet other rover, sensing, repair / rescue (satellite only) and visit type missions to enhance operational capabilities in near-earth space.

TABLE 17.

1000 KG Payload, EOL Sizing, Occultation Included

```
9340= * * * * * * * * * * * * * * * * * * * * * * * * * * * * * * * *
* * * * * * * * * * * * * * * * * * 
9350=  FINAL VALUE OF F =   4.22477465E+03
9360=
9370=
9380=  FINAL X VALUES
9390=
9400=  X(  1) =    3.03579551E+03  X(  2) =    2.97976855E+02  X(  3) =
1.10812166E+03
9410=  X(  4) =    3.11328282E+00  X(  5) =    7.32838151E+02  X(
9420=
9430=  FINAL CONSTRAINT VALUES
9440=
9450=  G(  1) =    2.53579551E+03  G(  2) =    6.96420449E+03  G(  3) =
2.87976855E+02
9460=  G(  4) =    9.70202315E+03  G(  5) =    1.09812166E+03  G(  6) =
8.89187834E+03
9470=  G(  7) =    2.61328282E+00  G(  8) =    1.68867172E+01  G(  9) =
7.22838151E+02
9480=  G( 10) =    9.26716185E+03  G( 11) =  -1.72876753E-08  G( 12) =
2.59544322E-07
9490=  G( 13) =  -2.15277396E-07  G( 14) =  -4.78692527E-07  G(
9500=*EOR
```

TABLE 18.

2724 KG Payload, EOL Sizing, Occultation Included

```
9490= * * * * * * * * * * * * * * * * * * * * * * * * * * * * * * * *
* * * * * * * * * * * * * * * * * *
9500=  FINAL VALUE OF F =   4.57638125E+03
9510=
9520=
9530=  FINAL X VALUES
9540=
9550=  X(  1) =   3.37846146E+03  X(  2) =   3.18957204E+02  X(  3) =
1.34059987E+03
9560=  X(  4) =   3.47330562E+00  X(  5) =   6.84123751E+02  X(
9570=
9580=  FINAL CONSTRAINT VALUES
9590=
9600=  G(  1) =   2.87846146E+03  G(  2) =   6.62153854E+03  G(  3) =
3.08957204E+02
9610=  G(  4) =   9.68104280E+03  G(  5) =   1.33059987E+03  G(  6) =
8.65940013E+03
9620=  G(  7) =   2.97330562E+00  G(  8) =   1.65266944E+01  G(  9) =
6.74123751E+02
9630=  G( 10) =   9.31587625E+03  G( 11) =   4.23460733E-09  G( 12) =
-3.75312084E-08
9640=  G( 13) =  -9.25061613E-07  G( 14) =  -2.66353163E-06  G(
9650=*EOR
```

TABLE 19

LSS 2, 20,000 KG Payload, 24 Ring-Cusp XE Thrusters, 12 BIMODs, with Occultation

```
10150= * * * * * * * * * * * * * * * * * * * * * * * * * * * * * * * *
* * * * * * * * * * * * * * * * * *
10160=  FINAL VALUE OF F =    6.24838310E+03
10170=
10180=
10190=  FINAL X VALUES
10200=
10210=  X(   1) =    6.06485577E+03  X(   2) =    1.21072537E+02  X(   3) =
2.73374196E+03
10220=  X(   4) =    6.29577216E+00  X(   5) =    6.08900253E+02  X(
10230=
10240=  FINAL CONSTRAINT VALUES
10250=
10260=  G(   1) =    5.56485577E+03  G(   2) =    3.93514423E+03  G(   3) =
1.11072537E+02
10270=  G(   4) =    9.87892746E+03  G(   5) =    2.72374196E+03  G(   6) =
7.26625804E+03
10280=  G(   7) =    5.79577216E+00  G(   8) =    1.37042278E+01  G(   9) =
5.98900253E+02
10290=  G(  10) =    9.39109975E+03  G(  11) =    1.33033609E-07  G(  12) =
-4.57452325E-06
10300=  G(  13) =   -8.93935066E-07  G(  14) =   -5.78521576E-06  G(
10310=*EOR
```

TO GEO = 241.23 DAYS

RETURN = 53.50 DAYS

ROUND
TRIP   = 293.73 DAYS

TABLE 20

LSS 3, 29,480 KG Payload, 32 Ring-Cusp XE Thrusters,
16 BIMODs, with Occultation

```
10300= * * * * * * * * * * * * * * * * * * * * * * * * * * * * * * * * *
* * * * * * * * * * * * * * * * * * 
10310=  FINAL VALUE OF F =   8.61602884E+03
10320=
10330=
10340=  FINAL X VALUES
10350=
10360=  X(  1) =    6.28088055E+03  X(  2) =    1.25437291E+02  X(  3) =
3.80555340E+03
10370=  X(  4) =    6.52273911E+00  X(  5) =    7.96482131E+02  X(
10380=
10390=  FINAL CONSTRAINT VALUES
10400=
10410=  G(  1) =    5.78088055E+03  G(  2) =    3.71911945E+03  G(  3) =
1.15437291E+02
10420=  G(  4) =    9.87456271E+03  G(  5) =    3.79555340E+03  G(  6) =
6.19444660E+03
10430=  G(  7) =    6.02273911E+00  G(  8) =    1.34772609E+01  G(  9) =
7.86482131E+02
10440=  G( 10) =    9.20351787E+03  G( 11) =    1.68802217E-09  G( 12) =
1.71096417E-07
10450=  G( 13) =  -3.55357770E-08  G( 14) =  -2.93657649E-07  G(
10460=*EOR
```

TO GEO = 250.81 DAYS

RETURN = 52.49 DAYS

ROUND
TRIP   = 303.30 DAYS

TABLE 21

Rover Vehicle, 8 Ring-Cusp XE Thrusters,
Interchangeable Sensors, 500 KG, Shadowing

```
9220= * * * * * * * * * * * * * * * * * * * * * * * * * * * * * * * * *
* * * * * * * * * * * * * * * * * *
9230=  FINAL VALUE OF F =    1.37461359E+03
9240=
9250=
9260=  FINAL X VALUES
9270=
9280=  X(   1) =    3.95768990E+03  X(   2) =    7.84975642E+01  X(   3) =
4.01332023E+02
9290=  X(   4) =    4.08187334E+00  X(   5) =    3.45301052E+02  X(
9300=
9310=  FINAL CONSTRAINT VALUES
9320=
9330=  G(   1) =    3.45768990E+03  G(   2) =    6.04231010E+03  G(   3) =
6.84975642E+01
9340=  G(   4) =    9.92150244E+03  G(   5) =    3.91332023E+02  G(   6) =
9.59866798E+03
9350=  G(   7) =    3.58187334E+00  G(   8) =    1.59181267E+01  G(   9) =
3.35301052E+02
9360=  G(  10) =    9.65469895E+03  G(  11) =  -2.61934474E-10  G(  12) =
-4.79021764E-08
9370=  G(  13) =  -6.05959940E-08  G(  14) =  -8.06412572E-08  G(
9380=*EOR
```

TO GEO = 105.67 DAYS

RETURN = 90.92 DAYS

ROUND
TRIP   = 196.59 DAYS

TABLE 22

Repair/Refurbish Vehicle, 8 Ring-Cusp XE Thrusters,
Interchangeable Repair Modules, 1000 KG, Shawdowing

```
9550= * * * * * * * * * * * * * * * * * * * * * * * * * * * * * * * *
* * * * * * * * * * * * * * * * * * 
9560=  FINAL VALUE OF F =    1.53783936E+03
9570=
9580=
9590=  FINAL X VALUES
9600=
9610=  X(  1) =   4.46852564E+03  X(  2) =   8.88189255E+01  X(  3) =
4.41148314E+02
9620=  X(  4) =   4.61858412E+00  X(  5) =   3.86139645E+02  X(
9630=
9640=  FINAL CONSTRAINT VALUES
9650=
9660=  G(  1) =   3.96852564E+03  G(  2) =   5.53147436E+03  G(  3) =
7.88189255E+01
9670=  G(  4) =   9.91118107E+03  G(  5) =   4.31148314E+02  G(  6) =
9.55885169E+03
9680=  G(  7) =   4.11858412E+00  G(  8) =   1.53814159E+01  G(  9) =
3.76139645E+02
9690=  G( 10) =   9.61386035E+03  G( 11) =   4.33647074E-09  G( 12) =
6.66668711E-08
9700=  G( 13) =  -1.62508513E-08  G( 14) =  -2.47455318E-08  G(
9710=*EOR
```

TO GEO = 116.22 DAYS

RETURN = 101.73 DAYS

ROUND
TRIP   = 217.95 DAYS

TABLE 23

Free Rover, 500 KG Payload, 8 Ring-Cusp XE Thrusters,
Interchangeable Sensors/Modules,
1600 KG Extra Propellant, Shadowing

```
9130= * * * * * * * * * * * * * * * * * * * * * * * * * * * * * * * *
* * * * * * * * * * * * * * * * * *
9140=  FINAL VALUE OF F =   1.61174152E+03
9150=
9160=
9170=  FINAL X VALUES
9180=
9190=  X(  1) =    4.65776684E+03  X(  2) =    9.26425162E+01  X(  3) =
5.65150266E+02
9200=  X(  4) =    4.31741084E+00  X(  5) =    3.05451120E+02  X(
9210=
9220=  FINAL CONSTRAINT VALUES
9230=
9240=  G(  1) =    4.15776684E+03  G(  2) =    5.34223316E+03  G(  3) =
8.26425162E+01
9250=  G(  4) =    9.90735748E+03  G(  5) =    5.55150266E+02  G(  6) =
9.43484973E+03
9260=  G(  7) =    4.31741084E+00  G(  8) =    1.51825892E+01  G(  9) =
2.95451120E+02
9270=  G( 10) =    9.69454888E+03  G( 11) =    2.03726813E-08  G( 12) =
3.20460458E-09
9280=  G( 13) =   -2.83522240E-07  G( 14) =   -6.70475856E-07  G(
9290=*EOR
```

TO GEO = 148.92 DAYS

RETURN = 80.39 DAYS

ROUND
TRIP = 229.31 DAYS

BIBLIOGRAPHY

1. Alfano, Salvatore. Low Thrust Orbit Transfer. MS Thesis AFIT/GA/AA/82D-2. School of Engineering, Air Force Institute of Technology (AU), Wright-Patterson AFB OH, Air Force Institute of Technology, December 1982.

2. Bate, Roger R., Donald D. Mueller, Jerry E. White. Fundamentals of Astrodynamics. New York: Dover Publications, Inc., 1971.

3. Brewer, George R. Ion Propulsion, Technology and Applications. New York: Gordon and Breach, Science Publishers, Inc., 1970.

4. Budnick, Frank S., Richard Mojena, Thomas E. Vollmann. Principles of Operations Research for Management. Homewood, Illinois: Richard D. Irwin, Inc., 1977.

5. Byers, David C. Characteristics of Primary Electric Propulsion Systems. AIAA Paper 79-2041, Princeton/AIAA/DGLR 14th International Electric Propulsion Conference, Princeton, N.J., Oct 30 - Nov. 1, 1979.

6. Byers, David C. Upper Stages Utilizing Electric Propulsion. NASA Technical Memorandum 81412. Cleveland, Ohio: NASA Lewis Research Center, March 1980.

7. Byers, David C., and Raymond S. DiEsposti. Geocentric Mission Sensitivity to Ion Thruster System Technology - Hg SOA. Data compilation from computer runs. NASA Lewis Research Center, Cleveland, OH, July 1, 1982.

8. Byers, David C., and Vincent K. Rawlin. "Critical Elements of Electron-Bombardment Propulsion for Large Space Systems," Journal of Spacecraft and Rockets, 14: 648-653 (November 1977).

9. Byers, David C., Fred F. Terdan, and Ira T. Myers. Primary Electric Propulsion for Future Space Missions. NASA Technical Memorandum 79141. Cleveland, Ohio: NASA Lewis Research Center, May 1979.

10. Cake, J.E., G.R. Sharp, J.C. Oglebay, F.J. Shaker, R.J. Zavesky. Modular Thrust Subsystem Approaches to Solar Electric Propulsion Module Design. Cleveland, Ohio: NASA Lewis Research Center, November 1976. (AIAA Report #76-1062)

11. Centaur G Technical Description -- A High-Performance Upper Stage for Use in the Space Transportation System. Report CGTD-3. General Dynamics, Convair Division Product Report. San Diego, CA, February 1983.

12. 30-Centimeter Ion Thrust Subsystem Design Manual. NASA Technical Memorandum 79191. Cleveland, Ohio: NASA Lewis Research Center, June 1979.

13. Challita, Antonios, Timothy J. McCormick, and John P. Barber. Advanced Energy Storage System - Phase 3 Review. Prepared for Air Force Rocket Propulsion Laboratory by IAP Research, Inc. Dayton, OH. 4 August 1983.

14. Cox, James E. "Electromagnetic Propulsion Without Ionization," Journal of Spacecraft and Rockets, 18: 449-456 (September - October 1981).

15. Davis, Eldon E. Future Orbital Transfer Vehicle Technology Study, I, II. Boeing Aerospace Company. NASA Contract Report 3535. May 1982.

16. Fearn, D. G. A Review of Future Orbit Transfer Technology. Technical Report # 81080. Farnbourough, England: Royal Aircraft Establishment, June 1981.

17. Fearn, D. G. "Electric Propulsion of Spacecraft," Journal of the British Interplanetary Society, 35: 156-166 (1982).

18. Fearn D. G. The Use of Ion Thrusters for Orbit Raising. Technical Report # 78068. Farnbourough, England: Royal Aircraft Establishment, June 1978. (AD A061792)

19. Finke, Robert C., ed. "Electric Propulsion and Its Applications to Space Missions," Progress in Astronautics and Aeronautics, vol 79. New York: American Institute of Aeronautics and Astronautics, 1981.

20. Floyd, R. M., Capt. Description of SUMT Library. AFIT Handout for CDC Cyber computer. Air Force Institute of Technology, Wright Patterson AFB OH, February 1982.

21. Hazard, Hap. U. S. Space Launch Systems (Second Revision). Los Angeles, California: Navy Space Systems Activity. Report # NSSA-R-20-72-2. July 1977.

22. Hill, Philip G., and Carl R. Peterson. Mechanics and Thermodynamics of Propulsion (Third Printing). Reading, Massachusetts: Addison-Wesley Publishing Co., Inc., 1970.

23. Ion Propulsion for Spacecraft. NASA brochure. Cleveland, Ohio: NASA Lewis Research Center, 1977.

24. Jahn, Robert G. Physics of Electric Propulsion. New York: McGraw Hill Book Company, 1968.

25. Kaplan, Marshall H. Modern Spacecraft Dynamics and Control. New York: John Wiley & Sons, 1976.

26. Kaufman, Harold R. "Origin of the Electron-Bombardment Ion Thruster," Journal of Spacecraft and Rockets, 18: 289-292 (July-August 1981).

27. Kaufman, H. R., and Raymond S. Robinson. Electric Propulsion for Upper Stage/Transfer Vehicle. NASA-CR-168022. Dept. of Physics, Colorado State University, Fort Collins, Colorado, for NASA Lewis Research Center, Cleveland, OH, September 1982.

28. Kaufman, H. R., and Raymond S. Robinson. Electric Thruster Performance for Orbit Raising and Maneuvering. AIAA Reprint. Physics Dept., Colorado State University, Fort Collins, Colorado.

29. Kerslake, William R. Sert II Thrusters--Still Ticking After Eleven Years. NASA Technical Memorandum 81774. Cleveland, Ohio: NASA Lewis Research Center, July 1981.

30. Kilmer, Charles R., Methods of On-Orbit Maintenance for Geosynchronous Satellites. MS Thesis. Mechanical Engineering Department, Colorado State University, Fort Collins, CO. Fall, 1977.

31. Maloy, Joseph E., Carl R. Dulgeroff, and Robert L. Poeschel. Electric Propulsion - Characteristics, Applications, and Status. AIAA Reprint. 1979.

32. Masek, T. D., et al. Advanced Electrostatic Ion Thruster for Space Propulsion. Final Report. Ion Physics Department, Hughes Research Laboratories. NASA CR-159406. NASA Lewis Research Center, Cleveland, OH. 21 May 1976 - 21 Jan 1978.

33. Mylander, Charles W., Raymond L. Holmes, Garth P. McCormick. A Guide to SUMT-Version 4. Paper RAC-P-63. Research Analysis Corporation, McLean, Virginia, October 1971 (AD-731391).

34. Perkins, David R. Preliminary Analysis and Comparison of Recoverable Space Based Orbit Transfer Vehicles for LEO to GEO Missions. Air Force Rocket Propulsion Lab. This document is undergoing publication, 1983.

35. Pipes, William E., III. Advanced Spacecraft Deployment System Study, vols I, III. AFRPL Report # AFRPL-7R-80-43 vols I, III. Edwards AFB, CA: Air Force Rocket Propulsion Laboratory, September 1980.

36. Poeschel, R. L. Development of Advanced Inert-Gas Ion Thrusters. NASA CR-168206. Final Report by Hughes Research Laboratories for NASA Lewis Research Center, Cleveland, OH, July 1983.

37. Pritsker, A. Alan B. Modeling and Analysis Using Q-GERT Networks (Second Edition). New York: John Wiley & Sons, 1979.

38. Ramsey, William D. Inert Gas Ion Thruster Program. NASA-CR-165521. Final report by Xerox Electro-Optical Systems, Pasadena, CA, for NASA Lewis Research Center, Cleveland, OH, December 1980.

39. Rawlin, Vincent K. Extended Operating Range of the 30-cm Ion Thruster with Simplified Power Processor Requirements. NASA Technical Memorandum 81729. NASA Lewis Research Center, Cleveland, OH, April 1981.

40. Rawlin, Vincent K. Operation of the J-Series Thruster Using Inert Gas. NASA Technical Memorandum 82977. NASA Lewis Research Center, Cleveland, OH, November 1982.

41. Rawlin, Vincent K., and Charles E. Hawkins. Increased Capabilities of the 30-cm Diameter Hg Ion Thruster. NASA Technical Memrandum 79142. NASA Lewis Research Center, Cleveland, OH, May 1979.

42. Regetz, John D., and C. H. Terwilliger, Jr. Cost-Effective Technology Advancement Directions for Electric Propulsion Transportation Systems in Earth-Orbital Missions. NASA Technical Memorandum 79289. NASA-Lewis Research Center, Cleveland, OH, October 1979.

43. Rehder, John J., and Kathryn E. Wurster. "Electric vs Chemical Propulsion for a Large-Cargo Orbit Transfer Vehicle," Journal of Spacecraft and Rockets, 16: 129-134 (May-June 1979).

44. Rudolph, L. K. and K. M. Hamlyn. A Comparison Between Advanced Chemical and MPD Propulsion for Geocentric Missions. Martin Marietta Denver Aerospace. AIAA Paper 83-1391, AIAA/SAE/ASME 19th Joint Propulsion Conference, Seattle, Washington, June 27-29, 1983.

45. Sovey, J. S. Improved Ion Containment Using a Ring-Cusp Ion Thruster. NASA Technical Memorandum 82990. NASA Lewis Research Center, November, 1982.

46. Sovey, J. S. "Performance of a Magnetic Multipole Line-cusp Argon Ion Thruster," Journal of Spacecraft and Rockets, 19: 257-269 (May-June 1982).

47. Space Flight with Electric Propulsion. NASA brochure.

Cleveland, Ohio: NASA Lewis Research Center, 1969.

48. "Space Station Design." Unpublished class report for M.C. 6.76, Air Force Institute of Technology, Wright Patterson AFB OH, 10 Dec 1982.

49. "Space Tug." Unpublished class report for S.E. 5.31, Air Force Institute of Technology, Wright Patterson AFB OH, September 1983.

50. Sponable, Jess M. Optimizing the Space Transportation System. MS Thesis AFIT/GA/AA/82D-10. School of Engineering, Air Force Institute of Technology (AU), Wright-Patterson AFB OH, December 1982.

51. Stuhlinger, Ernst. "Electric Propulsion Ready for Space Missions," Astronautics and Aeronautics: 66-77 (April 1978).

52. Stuhlinger, Ernst. Ion Propulsion for Space Flight. New York: McGraw Hill Book Co., 1964.

53. Tapley, B. D., H. Hagar. Estimates of Unmodeled Forces on a Low-Thrust Space Vehicle. Contract # AFOSR 72-2233. Austin, Texas: The University of Texas at Austin, Report for the Air Force Office of Scientific Research (September 1972) (AD-765 233).

54. Terwilliger, C. H., and W. W. Smith. Electric Propulsion for Near-Earth Space Missions. NASA CR-159735. Final Report prepared by Boeing Aerospace Company for NASA Lewis Research Center, Cleveland, OH, Feb 1978 - Apr 1979.

55. Thruster Endurance Test by Ion Physics Department of Hughes Research Laboratories. Final Report for NASA Lewis Research Center, May 1976. (NASA CR-135011)

56. Vondra, Robert J. One Millipound Pulsed Plasma Thruster Development. AIAA Paper 82-1877, AIAA/JSASS/DGLR 16th International Electric Propulsion Conference, New Orleans, LA, Nov. 17 - 19, 1982.

57. Wismer, David A., and R. Chattergy. Introduction to Nonlinear Optimization - A Problem Solving Approach. New York: Elsevier North Holland, Inc, 1978.

58. Zelany, Milan. Multiple Criteria Decision Making. New York: McGraw Hill Book Company, 1982.

VITA

Lee W. Maddox was born in Andrews, Texas on 30 October 1950. He graduated from College High School, Bartlesville, Oklahoma in 1969. In June of 1973, he graduated from the University of Tulsa, Oklahoma, with a B.S. in Aerospace / Mechanical Engineering and was commissioned in the U.S. Air Force through the ROTC program. He worked in the Structural Engineering Dept. of North American Rockwell, Tulsa Division, while awaiting active duty. After entering active duty, he completed Undergraduate Navigator Training, Electronic Warfare Officer Training, and B52-G Combat Crew Training. Subsequently he was assigned to B-52 bombers at Barksdale AFB, LA, where he served in positions including Instructor Electronic Warfare Officer, Simulator Supervisor, and Wing Staff Officer, Defensive Systems. During night school at Barksdale, he completed a masters degree from the University of Southern California. This was the Master of Science in Systems Management. He entered the Air Force Institute of Technology in May 1982, and completed the Master of Science in Space Operations in December, 1983. His next assignment will be to intelligence Systems, Space Command, Colorado Springs, CO.

Permanent Address:

404 Oak Park Rd.

Bartlesville, OK 74003

6c. ADDRESS *(City, State and ZIP Code)*
Air Force Institute of Technology
Wright-Patterson AFB, Ohio 45433

7b. ADDRESS *(City, State and ZIP Code)*

8a. NAME OF FUNDING/SPONSORING ORGANIZATION

8b. OFFICE SYMBOL *(If applicable)*

9. PROCUREMENT INSTRUMENT IDENTIFICATION NUMBER

8c. ADDRESS *(City, State and ZIP Code)*

10. SOURCE OF FUNDING NOS.

PROGRAM ELEMENT NO.	PROJECT NO.	TASK NO.	WORK UNIT NO.

11. TITLE *(Include Security Classification)*
See Box 19

12. PERSONAL AUTHOR(S)
Lee W. Maddox, B.S., M.S., Capt, USAF

13a. TYPE OF REPORT
MS Thesis

13b. TIME COVERED
FROM ________ TO ________

14. DATE OF REPORT *(Yr., Mo., Day)*
1983 December

15. PAGE COUNT
162

16. SUPPLEMENTARY NOTATION

Approved for public release: IAW AFR 190-17.
Lynn Wolaver 7 May 84
LYNN E. WOLAVER
Dean for Research and Professional Development
Air Force Institute of Technology (ATC)
Wright-Patterson AFB OH 45433

17. COSATI CODES

FIELD	GROUP	SUB. GR.
21	03	
22	01	

18. SUBJECT TERMS *(Continue on reverse if necessary and identify by block number)*
Electric Propulsion, Ion Propulsion, Orbit Transfer Vehicles, Primary Electric Propulsion, Space Tug

19. ABSTRACT *(Continue on reverse if necessary and identify by block number)*

Title: Analysis of Electric Propulsion Orbit Transfer Vehicles vs IUS, Centaur-G, and a Reuseable Bipropellant System.

Thesis Chairman: Mark M. Mekaru, LTC, USAF

Abstract: See Reverse.

20. DISTRIBUTION/AVAILABILITY OF ABSTRACT
UNCLASSIFIED/UNLIMITED ☒ SAME AS RPT. ☐ DTIC USERS ☐

21. ABSTRACT SECURITY CLASSIFICATION
UNCLASSIFIED

22a. NAME OF RESPONSIBLE INDIVIDUAL
Mark M. Mekaru, LTC, USAF

22b. TELEPHONE NUMBER *(Include Area Code)*
513-255-2549

22c. OFFICE SYMBOL
AFIT/ENS

This study began with the need for enhancing the Shuttle (STS) with a reuseable Orbit Transfer Vehicle (OTV) or tug. Electric OTVs (EOTVs) were optimized for NavStar GPS payloads in this initial analysis. The optimized EOTV was then modeled in a QGERT simulation "flyoff" against IUS, CENTAUR-G, and a non-aerobraking reuseable bipropellant OTV.

To accomplish the nonlinear optimization, data points from electric thruster tests performed by NASA-Lewis Research Center were linearized for specific impulse and thrust vs input power to the thruster. These two relationships included thruster efficiencies and propellant losses such that results would reflect actual lab-prototype thruster operation. A nonlinear optimization program (SUMT) found the minimum combination of power supply mass and propellant mass for BIMOD-based EOTVs deploying payloads from LEO to GEO. Of five thruster technologies optimized, the Ring-Cusp 3-Grid Ion Thruster operating on Xenon emerged as the best choice for the simulation. The results of the subsequent simulation "flyoff" over a 20-year period indicated that CENTAUR-G would have the lowest total Life-Cycle Cost (LCC), but the EOTV would have the lowest LCC / KG of mass delivered to orbit. The reuseability and efficient propellant usage of the EOTV suggested other mission possibilities. These included a roving intelligence / sensor platform, a repair/refurbish/return vehicle, and a LSS component delivery vehicle. The overall methodology developed can be used by decisionmakers / analysts to optimize other electric thrusters / vehicles and compare with the same or other chemical systems.

END

FILMED

6-84

DTIC